UNIVERSITÀ DELLA CALABRIA

UNIVERSITA' DELLA CALABRIA

Dipartimento di Farmacia e Scienze della Salute e della Nutrizione

Dottorato di Ricerca in

MEDICINA TRASLAZIONALE

CICLO

XXXI

Benefits of advanced techniques and data processing for the analysis of complex biological and food matrices

Settore Scientifico Disciplinare CHIM/08

Coordinatore: Ch.mo Prof. Sebastiano Andò

Supervisore/Tutor: Ch.mo Prof. Gaetano Ragno

Dottoranda: Dott.ssa Claudia Spatari

Benefits of advanced techniques and data processing for the analysis of complex biological and food matrices

Index

Vantaggi nell'uso di tecniche e elaborazione dati avanzate nell'analisi di matrici biologiche e alimentari complesse

RIASSUNTO DELLA RICERCA

Durante i tre anni di dottorato in Medicina Traslazionale, il mio lavoro di ricerca si è concentrato sull'applicazione di tecniche analitiche avanzate e sull'elaborazione dei dati per lo studio di matrici complesse biologiche e alimentari.

Recenti studi hanno dimostrato che in circa il 10% dei campioni di latte materno acquistato online è presente DNA bovino che dimostra adulterazione intenzionale. I rischi associati al consumo da parte del neonato di latte umano adulterato con contaminanti animali o altro sono molti e gravi, tra cui carenza di ferro, disidratazione, aumento del potenziale di carico di soluto renale (PRSL) e reazioni allergiche, motivo per il quale risulta fondamentale la ricerca di eventuali adulteranti nel latte materno.

L'applicazione di tecniche chemiometriche sullo spettro IR del latte materno si è dimostrata molto efficace nel tracciare anche minime variazioni nella composizione e nelle caratteristiche del latte umano, essendo in grado di sfruttare le informazioni non specifiche memorizzate nello spettro IR. In questo caso, l'elaborazione delle impronte digitali spettrali ATR-FTIR mediante regressione PCA e PLS, è stata in grado di rilevare l'aggiunta fraudolenta di acqua o latte di mucca. In particolare, la tecnica PLS-DA è risultata essenziale per riconoscere il latte materno puro dal latte adulterato. Un'ulteriore definizione di quattro modelli PLS1 ha consentito inoltre la determinazione della quantità di adulteranti specifici aggiunti.

La ricerca sulle matrici alimentari è stata estesa a una serie di oli commestibili al fine di verificare la loro fotostabilità. Tecniche di irradiazione forzata, in combinazione con analisi spettroscopica UV-vis, FTIR-ATR e cromatografica HPLC-DAD, hanno mostrato cambiamenti quantitativi e qualitativi dei principali acidi grassi.

La ricerca si è concentrata in seguito sull'olio di lino, data la sua grande importanza come alimento funzionale. Anche in questo caso, la spettroscopia UV e l'HPLC hanno

rivelato cambiamenti significativi nella concentrazione di acidi grassi, ridotti al 35% dopo 48 ore di esposizione alla luce. La quantità di lignani, altri importanti componenti nutraceutici, ha invece mostrato una significativa stabilità. La fotoprotezione dell'olio di lino è stata in seguito dimostrata dall'uso di contenitori di vetro ambrato associato all'aggiunta di ascorbil palmitato quale agente antiossidante. I risultati ottenuti sono importanti per aumentare la durata di conservazione dell'olio di semi di lino o di altri oli commestibili, mediante l'adozione di formulazioni appropriate e accurata protezione fisica.

Il monitoraggio dei farmaci nei fluidi biologici ha rappresentato un altro argomento importante del mio lavoro di tesi. Particolare attenzione è stata rivolta allo sviluppo di un metodo analitico per il monitoraggio della quantità dell'anestetico bupivacaina nel sangue del cordone ombelicale. La determinazione del farmaco è stata definita mediante un metodo di estrazione SPE seguito da analisi HPLC e GC-MS. Questo studio sta procedendo con l'analisi di un gran numero di campioni reali, al fine di valutare la sicurezza degli anestetici somministrati durante il parto naturale e nel contempo ottimizzare il protocollo terapeutico attualmente utilizzato in partoanalgesia.

Un'esperienza fondamentale durante il dottorato è rappresentata dal periodo trascorso presso un laboratorio di ricerca dell'Università di Utrecht in Olanda. Qui ho avuto l'opportunità di studiare per un semestre (dal 26 settembre 2016 al 27 Marzo2017) presso il laboratorio di ricerca guidato dal prof. Rolf Sparidans. In tale occasione ho approfondito le mie conoscenze sull'uso della cromatografia LC-MS/MS applicata allo studio della farmacocinetica di nuovi farmaci antitumorali. In particolare ho partecipato allo studio di un saggio bioanalitico del farmaco lorlatinib, un inibitore ALK di terza generazione. La preparazione del campione e l'ottimizzazione delle condizioni cromatografiche sono state le fasi più impegnative del lavoro essendo stato il primo test sviluppato e validato per questo prodotto. Una procedura LC-MS / MS è stata ottimizzata e validata sul sangue di topi al fine di stabilirne le proprietà farmacocinetiche.

Ancora presso il gruppo di ricerca dell'Unical, parte dell'attività di ricerca è stata svolta su matrici farmaceutiche. In particolare si è studiata la stabilità in soluzione acquosa e alla luce di una 1,4-diidropiridina (siglata M3) di nuova sintesi, data la nota scarsa solubilità e fotolabilità di questa classe di farmaci. Una serie di tensioattivi, tra questi i tween, è stata testata per promuovere la solubilità in acqua, ottenendo risultati incoraggianti con l'uso del tensioattivo non ionico Tween20. Successivamente, la fotostabilità del complesso M3-Tween20 è stata studiata vagliando la capacità fotoprotettiva del materiale di diversi contenitori: quarzo, PET blu, PET ambrato, vetro scuro rivestito. La migliore fotoprotezione è stata garantita dal PET ambrato e dal contenitore in vetro scuro. I risultati ottenuti dimostrano che l'uso combinato di tensioattivi e contenitori specifici rappresenta una strategia interessante da applicare ai farmaci fotolabili e a carattere prevalentemente lipofilo.

Benefits of advanced techniques and data processing for the analysis of complex biological and food matrices

INTRODUCTION

The issue of quality assurance in the analytical chemistry laboratory has become of great importance in recent years. Several analytical approaches have been developed for the study and analysis of complex chemical systems and most of them aim at the determination of different contaminants in organic, pharmaceutical and food matrices. The analytical techniques applied to these chemical systems, in particular the chemical-physical methodologies, have shown an impressive evolution, being able to perform a large number of determinations from a single sample, simultaneously and rapidly. In this context, an important support has been given by chemometry, a branch of analytical chemistry that uses mathematical-statistical methods for the resolution of analytical problems.

During my three-year PhD, advanced analytical methods have been applied for these aims:

1. To determine enviromental or pharmaceutical contaminants in **breast milk** and **human blood** samples;
2. To evaluate the photostability of **edible oils** and **drugs** through stressing irradiation test.

Breast milk is the most important and complete food for a newborn because is rich of protein, fats and carbohydrates. Thanks to its composition, human milk results healthy, species-specific, preventive against allergies, intolerances and diseases [1-2]. If a mother provides a low amount of milk or the composition of her milk results unable to satisfy newborn's necessity, the use of donated milk is very important [3-4]. Commercial infant-formula is an alternative but human milk is often preferred by mothers [5].

Because of the vigorous screening and multi-step strict processing of Human Donated Milk Banks present all over the world, the milk is mainly available by a physician's prescription and for high-risk infants (typically premature or ill) residing in the Neonatal Intensive Care Unit (NICU). So, the lack of availability of breast milk forces individuals to search to the community for donor human milk (DHM) [6-7]. However, the phenomenon of milk sharing is very dangerous [8] because purchased human milk may be subjected to milk adulteration (i.e., diluted with another form of milk). Recent studies showed that there was cow DNA in 10% of the breast milk samples bought through online community, in amounts (~10% contamination) that would reveal intentional adulteration [9]. The risks associated with infant consumption of plant or animal adulterated human milk are many and serious including iron deficiency, dehydration, increased potential renal solute load (PRSL), and allergic reactions [10-15].

Another important area of research on biological fluids is the monitoring of drugs in the cord blood. Many studies report damages in children caused by anesthesia such as respiratory depression, poor fetal positioning and increased fetal heart rate variability. So, the evaluation of the amount of drug in the cord blood acquires a significant value [16]. At the same time, the development of bioanalytical assay for the quantification of drugs in plasma results fundamental to test novel drugs [17].

The study of the effect of light on food matrices, in particular vegetable oils, is also of considerable importance. Our study focused mainly on the thermal and photo stability of different seed oils and in particular of the linseed oil.

Regarding the pharmaceutical matrices, our focus has been on the dihydropyridine compounds, the most commonly used as antihypertensive drugs but characterized by significant photoinstability. The oxidation to the pyridine derivative represents the first, and in many cases the only, step of the degradation mechanism. Photodegradation process leads to a loss of pharmacological activity and formation of toxic products. For this reason, several analytical techniques have been proposed for DHP determination in the presence of their photoproducts. According to their instability to light, DHPs are all marketed in solid formulations, especially tablets,

because photodegradation is particularly fast in solution [18]. For this reason, the evaluation of new strategies to realize stable-liquid oral formulation of novel DHPs was the object of one section of my research work.

During my three-year PhD course, I had the opportunity to study for a semester at the research laboratory led by prof. Sparidans, at the University of Utrecht, the Netherlands, where I deepened my knowledge on the use of chromatography LC-MS/MS applied to the pharmacokinetic study of new anticancer drugs.

Universiteit Utrecht

In the following figure the main topics studied are schematized.

- Evaluation of breast milk sophistication and adulteration;
- Identification and quantification of drugs in cord blood;
- Development of a bioanalytic assay to quantify antitumoral drugs in plasma;
- Photodegradation processes of food and pharmaceutical matrices.

Benefits of advanced techniques and data processing for the analysis of complex biological and food matrices

FOOD MATRICES

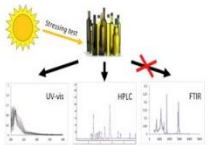

C. Spatari, M. De Luca, G. Ioele, G. Ragno. A critical evaluation of the analytical techniques in the photodegradation monitoring of edible oils. *LWT - Food Science and Technology 76, 147-155, 2017*

C. Spatari, G. Ioele, G. Ragno, F. Grande, M. De Luca. Photo and thermal stress of linseed oil and stabilization strategies. *(J Food Sc Technol, submitted)*

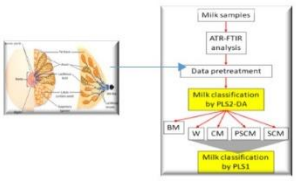

M. De Luca, G. Ioele, C. Spatari, L. Caruso, M.P. Galasso, G. Ragno. Assessment of adulteration in breast milk by combining FTIR spectroscopy and chemometric analysis. *LWT - Food Science and Technology (submitted)*

C. Spatari, M. De Luca, G. Ioele, M.P. Galasso, G. Ragno. Assessment of adulteration of breast milk by coupling FTIR spectroscopy and chemometric analysis. *EFMC-YMCS Young Medicinal Chemist Symposium. Lubiana 6-7 Settembre 2018.*

BIOLOGICAL MATRICES

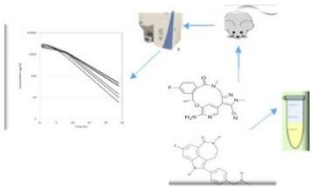

C. Spatari, W. Li, A.H. Schinkel, G. Ragno, J.H.M. Schellens, J.H. Beijnen, R.W. Sparidans. Bioanalytical assay for the quantification of the ALK inhibitor lorlatinib in mouse plasma using liquid chromatography-tandem mass spectrometry. *Journal of Chromatography B, 1083 (2018) 204–208*

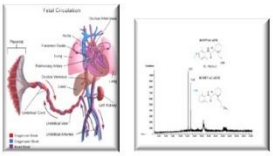

C. Spatari, G. Ioele, A. Leggio, M.De Luca, E. Belsito, G. Pucci, A. Mancuso, A. Liguori, G. Ragno G. Monitoring of anesthetic drugs in the cord blood during labor analgesia. *XXIV National Meeting in Medicinal Chemistry / 10th Youngest Medicinal Chemist's Symposium. Perugia 11,14 Settembre 2016*

DRUG SYSTEMS

M. De Luca, G. Ioele, C. Spatari,G. Ragno. Photostabilization studies of antihypertensive 1,4-dihydropyridines using polymeric containers. *International Journal of Pharmaceutics. 505, 1–2, 376–382*

M. De Luca, G. Ioele, C. Spatari, G. Ragno. Photodegradation of 1, 4-dihydropyridine antihypertensive drugs: an updated review. *International Journal of Pharmacy and Pharmaceutical Sciences, 10 (1), 8-18, 2018*

M. De Luca, G. Ioele, C. Spatari, G. Ragno. A single mcr-als model for drug analysis in different formulations: application on diazepam commercial preparations. *Journal of Pharmaceutical and Biomedical Analysis. 134, 346-351, 2017*

M. De Luca, G. Ioele, C. Spatari, G. Ragno. Optimization of wavelength range and data interval in chemometric analysis of complex pharmaceutical mixtures. *J. Pharmaceutical Analysis, 6 (2016) 64-69*

1. ANALYTICAL METHODOLOGIES

Instrumental analysis is a field of analytical chemistry that investigates analytes using scientific instruments. The most used techniques are based on spectroscopy, mass spectrometry and chromatography. In the last decades, instrumental analysis has been coupled with the multivariate analysis of experimental data. Chemometric methods are versatile and can be applied to data obtained from the use of most modern analytical techniques. In the following paragraphs, the analytical and chemometrics techniques used in my work are illustrate in detail.

1.1Liquid chromatography

HPLC-DAD

The liquid chromatography of high performance (HPLC), is an effective and versatile technique and represents the natural instrumental evolution of low-pressure column chromatography. Its peculiarity is that in a few minutes it can separate very complex mixtures and determine the quantitative composition together with information on the chemical nature of the substances. It is one of the most widely used chromatographic techniques in both industrial and medical -scientific research. (Fig. 1)

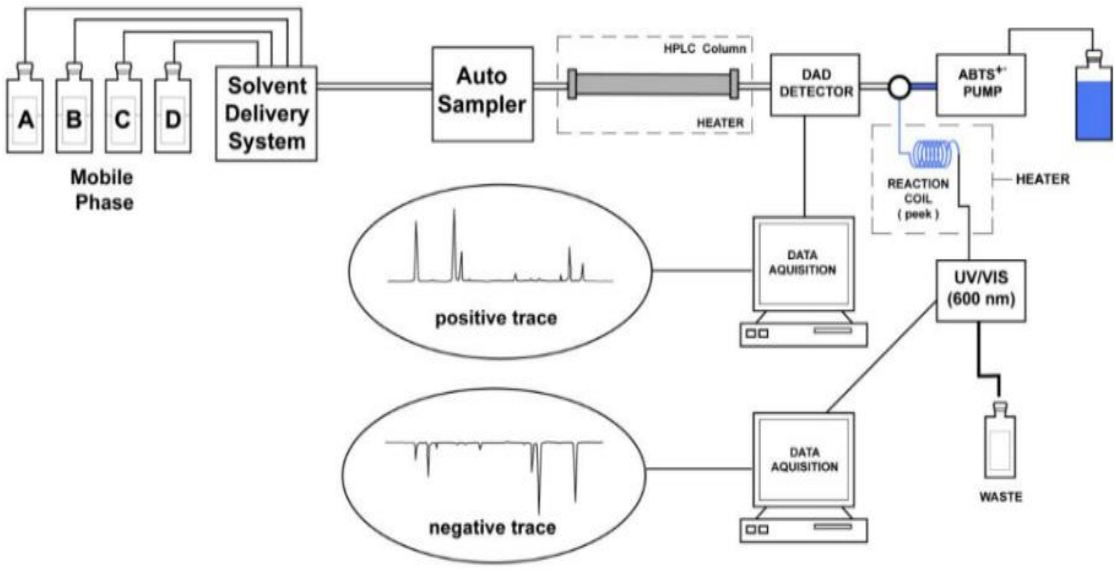

Figure 1. Scheme of HPLC

Among different kind of detectors, the diode array detector (DAD) is one of the most useful in analytical chemistry. DAD has two light sources: a tungsten lamp which is the source of visible light and a deuterium lamp which is the source of ultraviolet (UV) light. The UV lamp is in the light path of the visible lamp. The flow cell is positioned before the grating so by time light arrives at the grating, the intensity of the light at certain wavelenghts has been attenuated. The amount of attenuation is dependent on the type and amount of compound eluting through the cell as well as the lenght on the cell (typically about 10 mm). (Fig. 2)

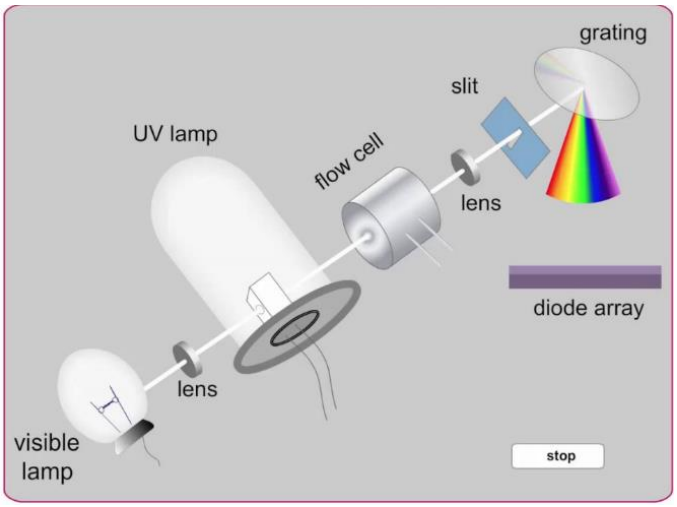

Figure 2. Scheme of diode array detector (DAD)

In my lab, HPLC analysis of food and drug samples was carried out by using a HP 1100 pump fitted with a diode array detector G1315B (Agilent Technologies) and a Rheodyne 7725 manual injector. The LC column was a C18 Gemini (Phenomenex), 250 4.6 mm x 5 mm.

LC-MS

Liquid Chromatography - Mass Spectrometry (LC/MS) is an analytical technique for identification, quantitation and mass analysis of a wide variety of non-volatile or semi-volatile organic or inorganic compounds in a mixture.

The principle of LC-MS/MS is based on the fragmentation of charged ions and the detection of the resulting fragment. This method usually is a reverse phase chromatography, where the metabolite binds to the column by hydrophobic interactions in the presence of a hydrophilic solvent and is eluted off by a more hydrophobic solvent. As the metabolites appear from the end of the column they enter the mass detector, where the solvent is removed and the metabolites are ionized.

The metabolites must be ionized because the detector can only work with ions, not neutral molecules. And ions only fly through a vacuum, so removal of the solvent is the first step. The mass detector then scans the molecules it sees by mass and produces a full high-resolution spectrum, separating all ions that have different masses. (Fig.3)

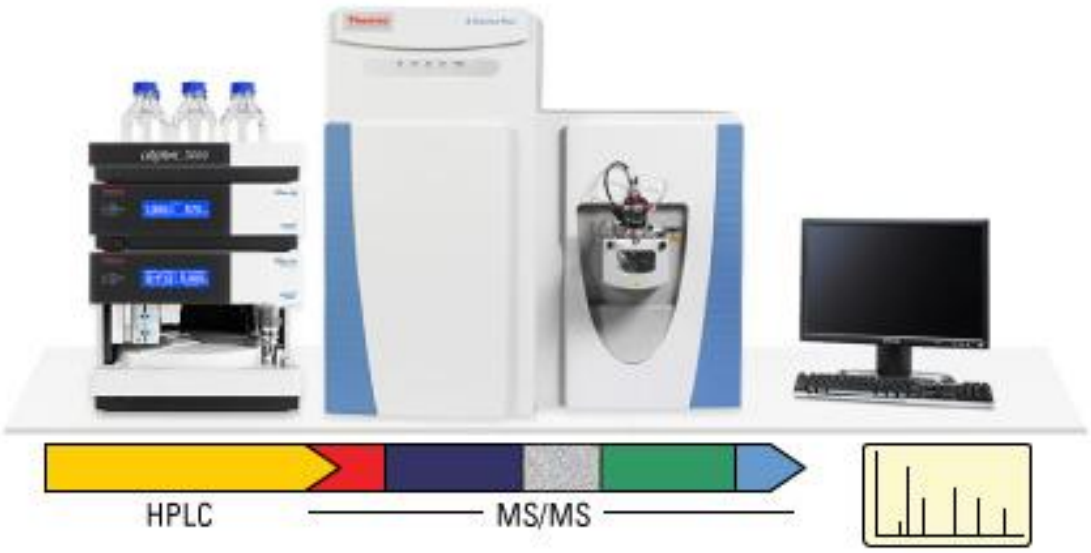

Figure 3. Scheme of LC-MS

Even if this tecnique has very highly sensitivity and selectivity, the major limit is represented by the **matrix effects**, that can be an issue and it also need a strict investigation to optimize method validation.

In order to develop the bioanalytical assay here described, the Shimadzu (Kyoto, Japan) chromatographic system charactherized by a DGU-14A degasser, two LC10-

ADvp-µ pumps, a Sil-HTc autosampler and a CTO-10Avp column oven was used. Plasma samples were injected (5 µL) on a Varian Polaris C18-A (50×2.0 mm, 3 µm, Varian, Middelburg, The Netherlands), protected by an Agilent Polaris C18-A Chromsep guard cartridge (10×2.0 mm, 3 µm, Agilent, Santa Clara, USA).

1.2 Spectroscopy

FTIR-ATR

For the analysis of breast milk and oil samples, FTIR analysis was performed with FTIR spectrophotometer (Perkin Elmer Spectrum-two) characterized by ATR sampler (attenuated total reflectance). The ATR sampler allows direct analysis of the sample without any pretreatment. This is an emerging analytical technique that has good sensitivity and repeatability. The sample is placed in close contact with an optical element consisting of a crystal with a high index of refraction. The IR beam passes through this element, originating a reflected ray that can penetrate up to a thickness of 2 µm in the sample. As a result of the radiation absorption from the sample, an attenuated radius is generated which is recorded as an ATR spectrum rich in analytical signals typical of the sample. (Fig. 4)

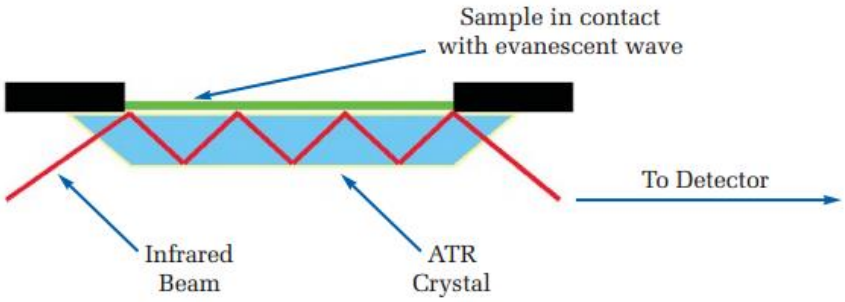

Figure 4. Scheme of FTIR-ATR

UV-VIS

Ultraviolet-visible spectroscopy (UV-Vis) refers to absorption spectroscopy in the ultraviolet-visible spectral region. Precisely it uses light in the visible and adjacent (near-UV and near-infrared (NIR)) ranges. UV/Vis spectrophotometer is used in the quantitative determination of concentrations of the absorber in the solutions of

transition metal ions and highly conjugated organic compounds. The Beer-Lambert law states that the absorbance of a solution is directly proportional to the concentration of the absorbing species in the solution and the path length. Thus, for a fixed path length, UV/Vis spectroscopy is a perfect tool to determine the concentration of the absorber in a solution. The absorbance changes with concentration. This can be taken from references (tables of molar extinction coefficients), or more accurately, determined through building a calibration curve. (Fig.5)

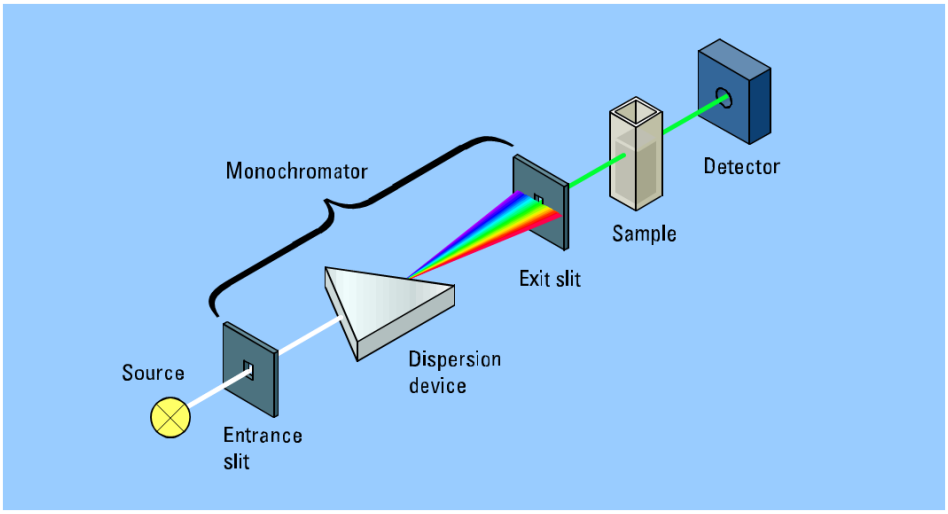

Figure 5. Scheme of Uv-vis spectrophotometer

The degradation process of both oils and drug was monitored by UV-vis spectrophotometric analysis, carried out on an UV spectrophotometer Agilent 8453 with diode array detector (Agilent Technologies, CA, USA).

1.3 Photodegradation testing

The stressing irradiation tests were conducted by using an irradiation device that respects the ICH directives about the nature of the light source.

The Suntest CPS + (Fig. 6) provides information about the long-term response of the product exposed to light, particularly solar radiation. The instrument is the ideal

equipment for routine tests during production phases or for simulating the display of new materials. The device is equipped with an electronic system (CPS, Controlled Power System) that offers constant control over irradiation, allowing a good reliability in providing a reproducible test. The microprocessor controls the whole unit, in particular the sensor for irradiation, the temperature and the internal standard for its measurement, and allows to program and check each step of the test through pre-established programs.

The radiation system consists of a Xenon arc lamp and a quartz filter that permits the emission of a light spectrum with distribution of wavelengths very similar to sunlight. A series of glass filters of various kinds are available for the selection of certain spectral zones. The great advantage of this equipment is to produce faster results, suitable for carrying out accelerated stability and, above all, reproducible, regardless of variations in sunlight depending on the season, time and place. The unit is equipped with a cooling unit which reduces the temperature of the test chamber under conditions of maximum irradiation to approximately 20 °C.

Figure 6. Suntest CPS+

Instrumental parameters:

- Radiation range between 300 and 800 nm
- Radiation power between 250 and 765 W /m^2
- Temperature range between 10 and 100 °C

Filters:

- Special UV glass for outdoor light simulation (> 290 nm)
- Window glass (> 310 nm)
- Solar ID 65 glass, in combination with window glass (ICH standards).

The following diagram shows the spectrum of sunlight and the one produced by the Xenon lamp mounted on the instrument.

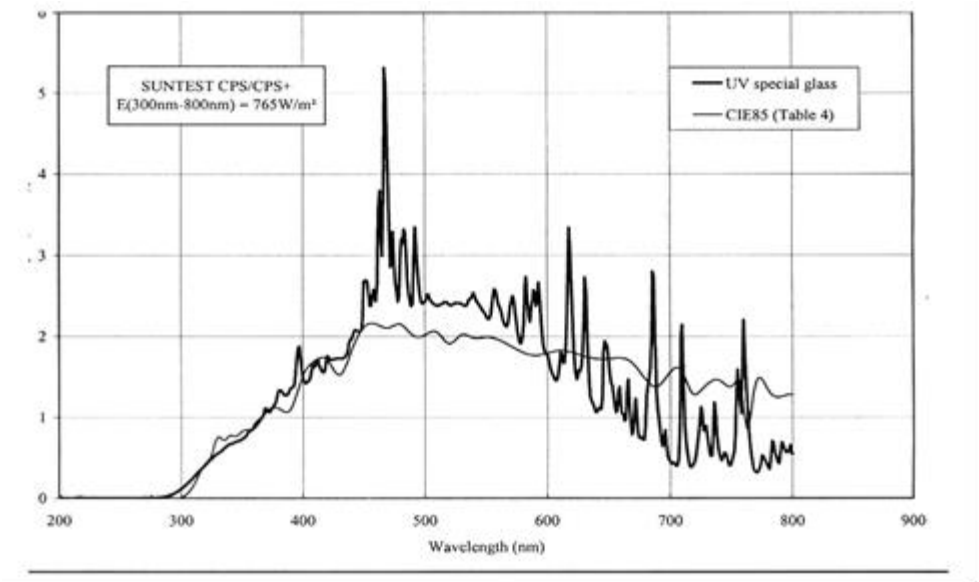

In the following diagram, instead, the spectral region is reported in detail between 250 and 450 nm, with the comparison between the radiations obtained through the filters that cut the spectrum below 290 nm (UV glass) and 310 nm (Window glass).

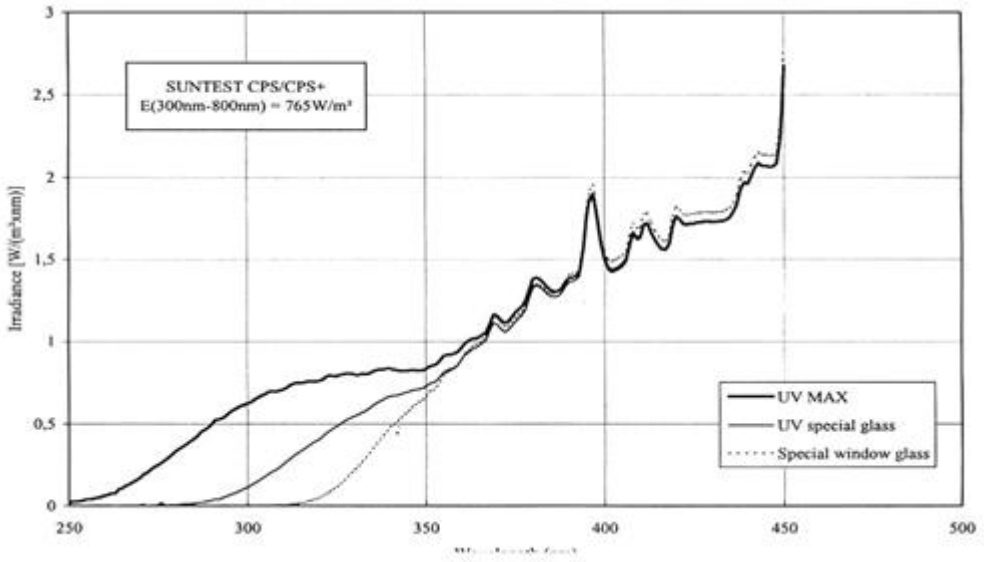

1.4 Chemometrics

The complexity of the spectra and the high number of variables involved in the complex analytical systems require chemometric procedures to ensure the validity of the results.

Chemometrics allows a multivariate approach to the process to be studied by taking into account all the variables involved, allowing to make the most of all the information contained in the data to be analyzed. The variables potentially involved are numerous, they are not all controllable with the desired precision and many are not exactly aware of the relevance for the problem under examination. Moreover, in most cases, the correlations between the variables and their non-linear effects or non-predictive non-linearities, which make the analytical approach even more difficult, are not known. Chemometrics is very useful for the possibility to monitor and study the effect of the process variables, making them vary together. This allows the maximum information to be extracted from any data set.

According to this concept and considering the amount of data obtained from complex systems, it is essential to distinguish the useful information in the experimental data and exclude all information useless for our analysis, such as the presence of

experimental noise, redundant information due to correlation between variables, good information not directly useful for the problem analysed.

Among the existing chemometric techniques, those mainly used in this thesis work were:

- experimental design (Design of Experiments, DoE),
- exploratory analysis (Principal Component Analysis, PCA),
- multivariate regression (Partial Least Squares, PLS);
- classification methods (Partial Least Squares-Discriminant Analysis, PLS-DA).
- Multivariate Curve Resolution-Alternating Least Squares (MCR-ALS).

Principal component analysis (PCA) provides to extract the main information from a data matrix and express this information by projection of the samples on a set of new orthogonal variables called principal components (PCs). When PCA is run, the amount of original variables is reduced to a few PCs that contain the main information stored in the original data. The PCs are built such that the first one carries most information, followed by the second one carrying less information, and so on. When the number of PCs increases, the variance contained by the new PCs can belong to the instrumental noise. The algorithm NIPALS (Non-linear IterativePartial Least Squares) was used to calculate the PCs.

PLS regression is a factor analysis method, very useful in the processing of spectroscopic data for the calibration analysis of complex mixtures [19,20].

In applying PLS procedure, the spectroscopic data (descriptor variables) are arranged in a matrix X (n, m) while a second matrix Y contains the concentration data (response variables). The algorithm PLS1 is adopted in presence of one vector y, while PLS2 regression is applied for a matrix Y (n, k) in which the components or classes are more than one (k > 1). X and Y are mean-centered and then decomposed in factors. Consecutive orthogonal factors are selected with the aim to maximize the covariance

between descriptors and responses. PLS modelling is achieved when the factors that explain most of the covariation between both data sets are found.

In PLS-DA, Y-variable takes on value 1 for the samples belonging to the class and 0 for those not belonging to the class. In calibration, the Y values correspond to the sample composition [21,22], and specifically to the amount of milk adulteration in this study. A PLS model can be validated by internal and/or external validation procedure. Full cross-validation (FCV), a well-known internal procedure, provided a direct estimate of the error rate incurred by the model. The number of factors was chosen by evaluating the parameters root mean square error of cross validation (RMSECV) and correlation coefficient R^2. The prediction performance of the PLS models was evaluated by an external validation by using new samples (not enclosed in the calibration step). The obtained results were discussed by comparing the figures of merit root mean square error of prediction (RMSEP) and percentage error in predicted concentrations (RE%), calculated as follows:

$$\text{RMSECV or RMSEP} = \sqrt{\frac{\sum_{i=1}^{n} (c_i - \hat{c}_i)^2}{n}}$$

$$\text{RE}(\%) = 100 \sqrt{\frac{\sum_{i=1}^{n} (c_i - \hat{c}_i)^2}{\sum_{i=1}^{n} c_i^2}}$$

where, c_i and $\hat{c}_i$ are, respectively, the known and calculated percentage of milk adulteration in sample i and n is the total number of samples in the validation step.

The photodegradation processes of drugs was monitored by spectrophotometric analysis and the data were processed by MCR techinique to estimate spectra and concentration profiles of the components envolved. The first step in this procedure is to construct a data matrix **D**. The samples (individual spectra) are defined in the rows of this matrix, while in each column we find the UV-Vis absorption values measured at a length of spectrum wave. A D_K data matrix is so obtained that can be

represented assuming a binary model based on the distribution of several wavelengths, applicable with the Lambert-Beer law:

$$D_K = C_K S^T + E_K$$

where the rows of the D_K matrix are the spectra collected at different reaction times and the columns are the kinetic signals recorded at various wavelengths. $\mathbf{C_K}$ is the matrix of the concentration profile of the compounds involved in the kinetic process, while S^T is the matrix of the relative pure spectra, finally, $\mathbf{E_K}$ represents the matrix of the non-modeled residual data or variance not explained by the model:

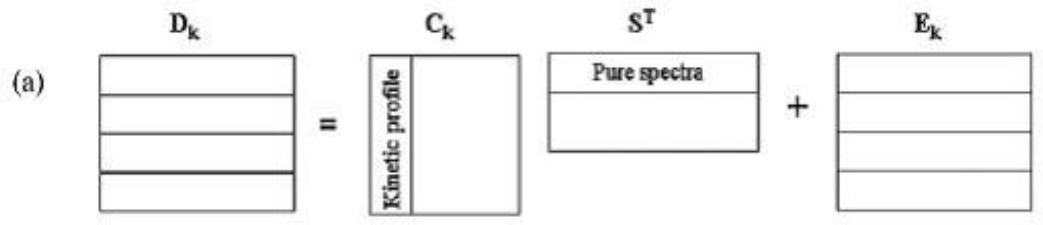

In the MCR analytical approach, a first phase evaluates the number of components that appear within the data of the DK matrix. This step is performed by a rank analysis of the DK matrix, through the Singular Value Decomposition (SVD) technique., an effective algebraic tool that, calculates the highest singular values associated with the most relevant compounds.

Subsequently, the initial estimates of ST or CK can be obtained by using two chemometric techniques based on the identification of the respective variables of spectra or concentrations, SIMPLISMA and Evolving factor analysis (EFA).

Regardless of which technique is used to obtain an estimate of ST or C, these are iteratively optimized, according to a regressive constraint procedure, called Alternating Least Squares (ALS). At each iteration, new values of the matrix of the ST spectra and of the matrix of the CK concentrations are obtained, alternatively solving the following two least-squares equations:

$$CK = DK\,(ST) + ST = (CK) + DK \text{ where } (S^T)^+ + e\,(C_K)^+$$

they are the pseudo-inverse respectively of the ST and CK matrices. After each iterative cycle, a new reproduction of the DK matrix is produced, starting from ST and

CK. Finally, when the convergence practice is finished, the optimization process can also be defined as concluded. The convergence criterion can be established by a pre-established number of iterative cycles or, more often, can be deduced from the numerical finding of the lack of fit (LOF), obtained in two consecutive iterations. The LOF, ie the lack of adaptation, is calculated according to the expression:

$$\%\mathrm{LOF} = 100 \times \sqrt{\frac{\sum_{ij}(d_{ij} - d_{ij}^{*})^2}{\sum_{ij} d_{ij}^2}}$$

where dij is the experimental absorbance at reaction time i and at the wavelength j and d * ij is the absorbance obtained with the MCR-ALS model. When the differences between numerous fit obtained from consecutive iterations are below a threshold value, the optimization is completed. Another parameter used to indicate the quality of the adaptation obtained from the MCR-ALS is the percentage of explained variance or percentage of variation explained, indicated with r^2 and calculated according to the following equation:

$$r^2(\%) = 100 \times \frac{\sum_{ij} d_{ij}^{2*}}{\sum_{ij} d_{ij}^2}$$

The software used is MATLAB, a high-performance language for technical computation that integrates calculation, visualization and programming in an easy-to-use environment where problems and solutions are expressed in familiar mathematical notation. MATLAB is an interactive system in which the basic element allows the resolution of technical calculation problems, in particular those with vector and matrix formulations, through much simpler and leaner algorithms than those that would be necessary in a scalar language program not interactive. It features a family of application-specific solutions called toolboxes, which provide the foundation for applying sophisticated technology and for solving particular categories of problems.

2. ANALYSIS OF FOOD MATRICES

2.1 Assessment of adulteration of breast milk by coupling FTIR spectroscopy and chemometric analysis.

Breast milk (BM) is the best food for the newborn as it provides a unique combination of proteins, carbohydrates, lipids, minerals, vitamins and particular bioactive components. It is considered a biological system, a living tissue, able to satisfy not only nutritional but also psycho-emotional needs of the infant.

Lactation develops in two phases:

1. Initial phase of limited secretion towards the end of pregnancy

2. Induction phase towards 32-40 hours after delivery.

The continuous evolution of the milk composition not only guarantees the maintenance of the nutritional needs of the newborn but above all guarantees optimal values of pH and osmolarity that regulate the intestinal functions of the child. Breast milk goes through three main phases: colostrum, transitional milk and mature milk. Colostrum is perfect as a baby's first food: it is low in fat and rich in carbohydrates, proteins, vitamin A and antibodies. It has a high digestibility and at the same time a high nutritional power.

Colostrum is produced in small quantities, adapted to the size of the infant's stomach and to the function of the kidneys, which, immature, are not able to handle large volumes of liquids. Colostrum can be considered a concentrate of antioxidants. The antioxidant capacity of colostrum-milk is particularly important for children born preterm in which the antioxidant defense system is immature and therefore is not able to defend the body from oxidative stress. From the 3rd / 14th day the colostrum become "transition milk" in which the content of immunoglobulins and proteins decreases while that of sugars and fats increases. It is produced during what is commonly called "whipped milk", ie a more abundant production. The evolution times from colostrum to mature milk are however subject to great inter-individual

variability. Mature milk is produced after the 10th day of lactation and appears less viscous and more liquid. However, this milk contains all the nutrients necessary for the healthy development of the baby. The milk flowing at the beginning of the feed is low in fat and high in lactose, sugar, proteins, vitamins, minerals and water. During feeding, the fat content increases and the sugar content decreases (table 1).

Table 1. Breast milk composition in three stages of breastfeeding

Content (g/L)	Colostrum	Transition Breast Milk	Breast Milk Mature
Proteins	23	16	10
Sugars	57	64	70
Lipids	30	35	42
Minerals	3.1	2.6	2.4
Calories	5800	635	700

2.1.1 The Human Milk Bank

The Human Milk Bank (HMB) refers to a collection point for milk donated by different mothers, distributed, after appropriate treatment, to the infants who are in absolute need of it. In general, HMB carries out activities to promote breastfeeding, donation of human milk, information on the usefulness of human milk and research to improve the nutritional aspects of the premature baby. Donated human milk can be considered like an essential drug, when breast milk is not available, especially in the early postpartum period or for premature babies, especially those more critical and with a birth weight of less than 1,500 g admitted to Neonatal Intensive Care.

The reality of the Human Milk Banks (HMB) (Fig. 7) is already present in our country and is constantly evolving: these facilities offer a service that aims to select, collect, store and distribute the donated human milk, to be used for specific medical needs. HBMs are essential to meet the needs of pre-term infants, but they are also useful

when newborns suffering from pathology as they promote an adequate growth, provide multiple benefits both in the short and medium-long term and promote a better neurocognitive development than commercial formula milk.

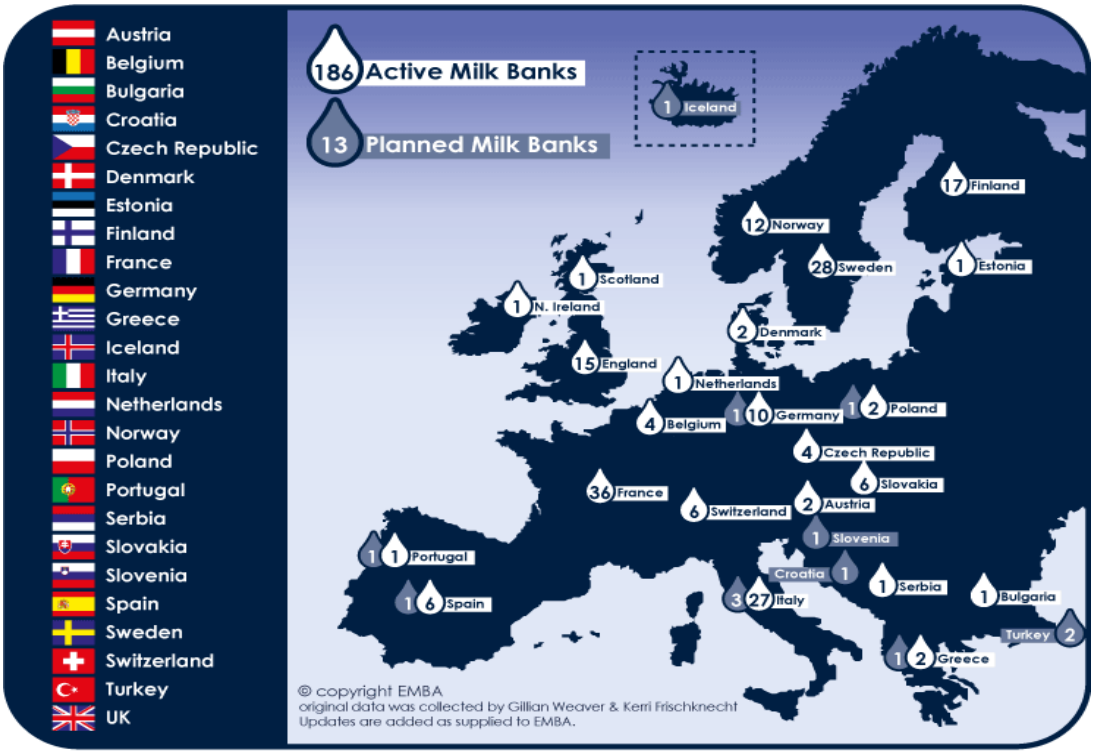

Figure 7. Active Milk Banks in Europe

Our country is currently one of the most active in Europe; the activity and the quality of the procedures of the existing banks in Italy is coordinated by the Italian Association of Donated Milk Banks (AIBLUD) established in 2005, which promotes the importance and benefits of woman's milk and her donation in order to increase public awareness.

In Calabria, in Cosenza, there is the bank of human milk donated "Galatea", unique in Calabria, founded in 2007, the bank is in operation at the U.O.C. of Neonatology and Neonatal Intensive Therapy of the Hospital Presidium of Cosenza. (Fig. 8)

Figure 8. Human Milk Bank Galatea in Cosenza

2.1.2 Experimental

BM samples were collected from the Milk Bank in Cosenza Hospital (Calabria, Italy). The milk is donated by voluntary mothers who respect all the characteristics included in the Bank protocol: health status certification and traceability of donated milk. The cow milk samples were purchased from local dairy-product company in Cosenza (Italy).

A set of 220 samples for analysis, consisting of pure BM and adulterated BM, was prepared. For this aim, 60 BM samples (BM set) were made available by the Milk Bank, coming from different mothers donating at different times. These samples were divided into 5 different aliquots. A first set of 20 pure BM was analyzed without any adulteration (set BM). 50 samples were prepared from each of the other four aliquots by adding respectively water (set W), whole cow milk (set CM), semi-skimmed cow milk (set SSCM) and skimmed cow milk (SCM set). The amount of water or cow milk was added in the range 5 - 50%. Applying the Kennard-Stone sampling method [23] from each set were selected 40 samples for the modeling procedures and 10 samples to validate the models.

Chemometric methods. A PCA study of the data patterns was performed to highlight the differences between samples of pure BM and adulterated BM. The unsupervised data analysis on the milk fingerprints aimed to extract the useful information from the data matrix by projecting samples and variables on a set of new orthogonal variables, called principal components (PCs) [24,25].

Classification and assessment of adulteration involved the use of various PLS models: a preliminary PLS2 discriminant analysis (PLS2-DA) model designed to detect the possible addition of water or different types of cow milk and subsequent four PLS1 calibration models able of determining the amount of adulterant added. Figure 9 shows the scheme of the analytical procedure.

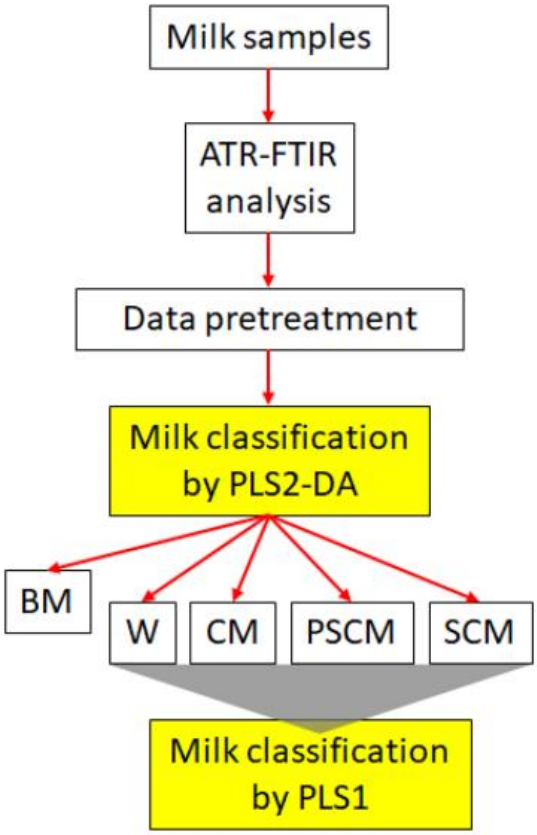

Figure 9. Scheme of multivariate analysis procedure.

2.1.3 Results and Discussion

Exploratory analysis of atr-ftir fingerprints of milk samples. The FTIR spectra of pure BM and the various types of cow milk included in this study are shown in Fig. 10. The absorption bands in the ranges 1630-1680 cm^{-1} and 1510-1570 cm^{-1} may be associated with C=O stretching or N-H and C-H bending vibration of the milk proteins [26,27]. The bands 2920, 2850, and 1743 cm^{-1} may be due to the antisymmetric and symmetric stretching of CH_2 and C=O groups, respectively, from the fatty milk components [28]. The absorption bands in the ranges 3200-3700, 1030-1200 and 900-450 cm^{-1} have been associated with carbohydrate structures [29].

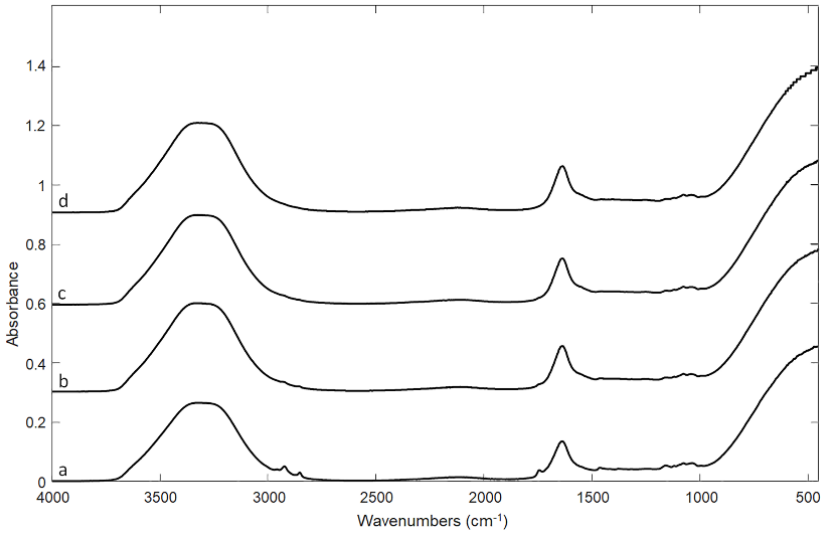

Figure 10. FT-IR spectra for pure BM (a), CM (b), PSCM (c) and SCM (d) samples.

A very strong overlap between the spectral signals of human milk and pasteurized cow milk is evident throughout the full recorded spectral region, suggesting a high similarity in the composition of the matrices. No characteristic signal was identified to be used as a differentiation marker, thus making it impossible to detect milk adulteration by a simple visual analysis. Therefore, it seemed necessary to perform a multivariate data study, with the aim of interpreting the data matrices, taking into account the full information from the FTIR fingerprints of the samples. Therefore, it seemed necessary to perform a multivariate data study, with the aim of interpreting the data matrices defined on the information obtained from FTIR fingerprints.

Raw FTIR spectra were pre-treated to select the information more useful for the chemometric modelling. First of all, only the wavelength range between 3000 and 1000 cm^{-1} were considered, discarding the terminal regions because considered rich in instrumental noise and useless information carriers [30]. After that, a mathematical pre-treatment of the data seemed necessary to minimize instrumental problems as baseline fluctuation or noise. Derivatization by Savitzky–Golay algorithm, standard normal variate (SNV) and multiple scatter correction (MSC), described in several papers [31,32], were applied on the FTIR recorded data. A

significant enrichment in the data variance was reached when the raw data were transformed in derivative signals. Different mathematical parameters were tested in applying the derivative elaboration reaching the best results when the following parameters were set: 1st order, number of smoothing points 7, polynomial order 2.

A PCA multivariate explorative analysis of the milk samples was performed on all the FTIR fingerprint spectra previously transformed in derivative data. PCA modelling gave 95,74% of explained variance, considering the first four PCs. The evaluation of the information available in the PC score plot showed that PC2 (6.66%) and PC4 (3.12%) were the richest principal components in useful information for our purposes.

Figure 11 shows the score plot PC2 vs PC4. The grouping of the samples was clear making it possible to distinguish the pure BM samples and the BM samples adulterated with water or cow milk. However, this PCA modelling identified only one cluster of BM samples adulterated with cow milk but was unable to distinguish the type of cow milk added.

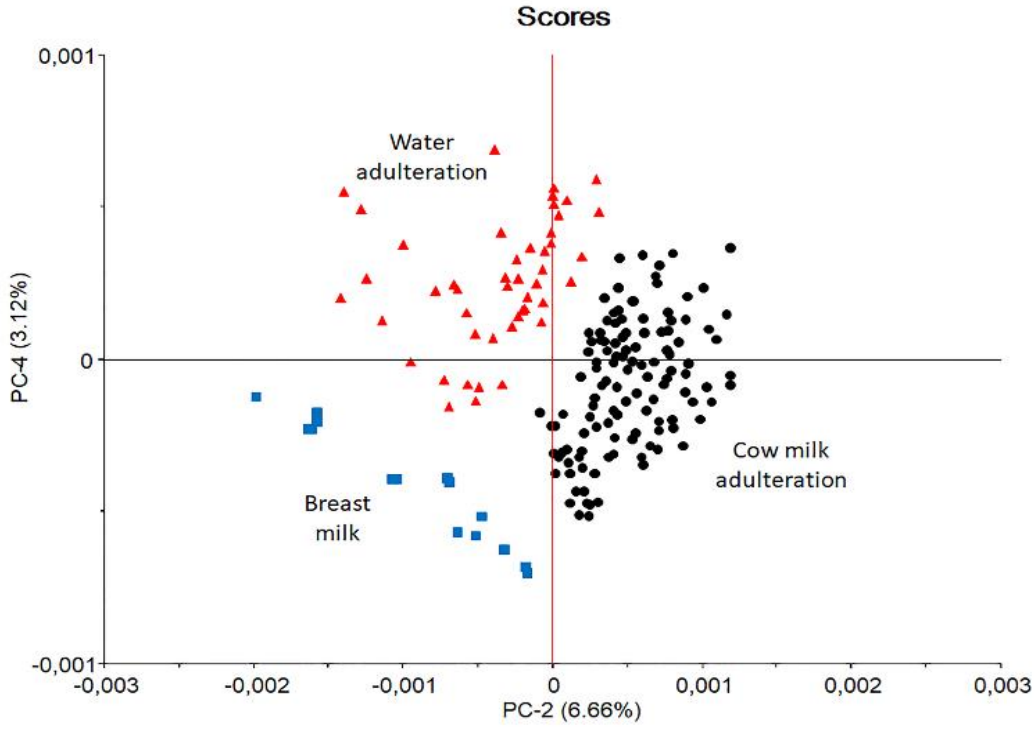

Figure 11. Score plot (PC2 vs PC4) by PCA analysis.

Classification of milk samples by pls-da modelling. A PLS2-DA modelling was developed with the aim to classify the milk samples as pure BM or adulterated with water (W), whole cow milk (CM), partially skimmed (PSCM) and skimmed (SCM). PLS2 algorithm required the setting of more than one Y variable. In this study, five Y variables/classes (Y_{BM}, Y_W, Y_{CM}, Y_{PSCM} and Y_{SCM}) were set in modelling, assigning the value 1 to the samples belonging to each class and 0 to those belonging to other classes.

The PLS2-DA classification model was validated by full cross validation and its performance evaluated in terms of correlation coefficient R^2 and RMSECV. The figures of merit, shown in Table 2, were statistically acceptable by considering 6 factors, with RMSECV values between 0.122 and 0.145 and R^2 in the range 0.857 - 0.944. Figure 12 shows the score plot PC2 vs PC4 by PLS-DA modelling, in which the discrimination across all classes is greatly improved.

Table 2. Statistical parameters of PLS-DA and PLS models from FCV and external validation procedures

PLS-DA		**Full cross validation**				
Class Y_n	Factors	R^2	RMSECV			
BM	6	0.9446	0.1221			
W	6	0.9274	0.1379			
CM	6	0.8574	0.1432			
PSCM	6	0.8718	0.1449			
SCM	6	0.9263	0.1231			
PLS		**Full cross validation**		**External validation**		
Model	Factors	R^2	RMSECV	R^2	RMSEP	RE%
PLS_W	2	0.9884	0.9841	0.9723	1.1718	2.8054
PLS_{CM}	3	0.9465	1.3539	0.9267	1.3812	3.3124
PLS_{SCM}	4	0.9628	1.3217	0.9616	1.3351	3.1124
PLS_{PSCM}	3	0.9822	1.5375	0.9778	1.2155	2.9134

This model was applied to an external prediction set consisting of 60 samples: 10 samples of pure BM and 10 samples from each subset of adulterated samples. According with the PLS-DA procedure, a sample was considered belonging to a class n when the predicted value of Y_n was higher than 0.5 [33]. The classification results obtained are listed in Table 3 through a confusion matrix. 100% of BM and W samples were well classified while some difficulties were found in classifying the samples adulterated with cow milk. To be precise, the PLS2-DA model was able to identify 100% of the samples adulterated with cow milk but the exact type of cow milk added was only identified for 90% of the samples. No samples were detected as suspect origin.

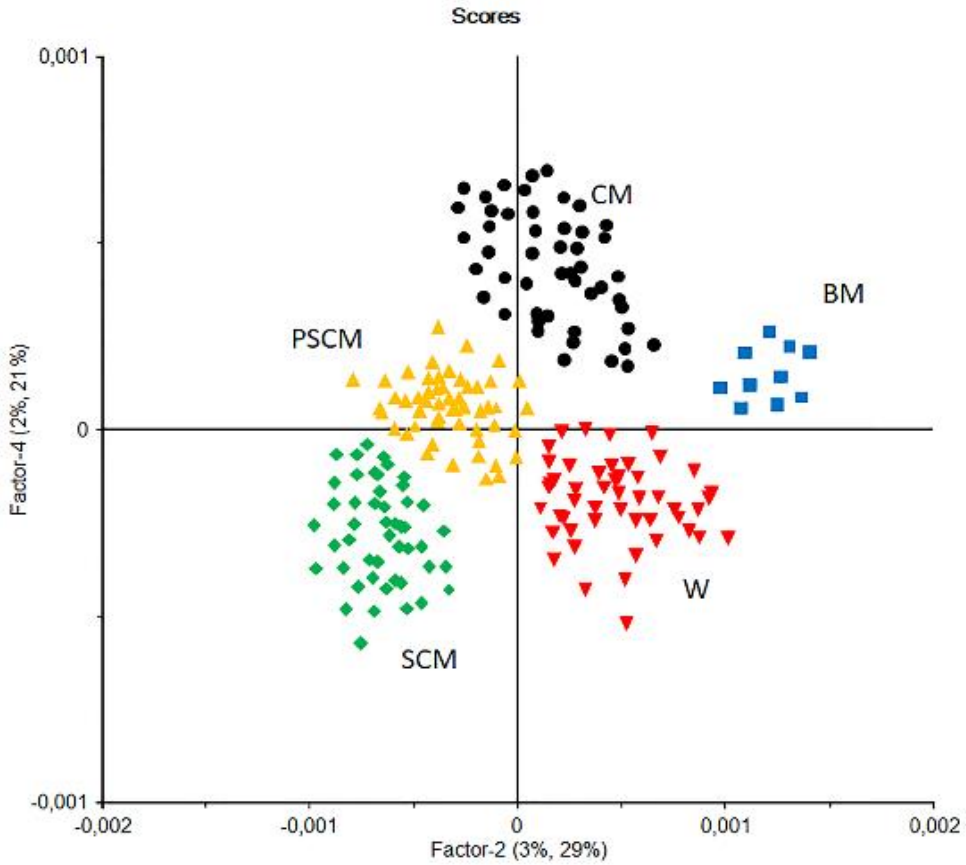

Figure 12. Score plot (PC2 vs PC4) by PLS-DA regression.

. Table 3. Confusion matrix from PLS2-DA external validation

	Real					
Predicted	Y_n	BM	W	CM	PSCM	SCM
	BM	10				
	W		10			
	CM			10		
	PSCM				8	1
	SCM				2	9

Estimate of adulteration by PLS1 approach. In order to quantify the amount of adulterant added to BM, four PLS1 calibration models were built by using the sets W, CM, PSCM and SCM, respectively. Full cross validation permitted to select the optimal number of factors for all the models by evaluating the parameters R^2 and RMSECV. The obtained values of the parameters for all the data sets are listed in Table 2.

The calibration report of PLS_W described a robust model, since only 2 factors were enough to explain 98.84% of Y variance. Full cross validation showed high prediction ability in determining the amount of water added, providing RMSECV and R^2 values of 0.988 and 0.9841, respectively. The three models dedicated to the assay of the different types of added cow milk required three factors for the models PLS_{CM} and PLS_{SCM} and four factors for the PLS_{PSCM} model. The statistical parameters were however satisfactory with R^2 above 0.947 and RMSECV below 1.54.

The prediction power of the PLS models was tested by performing validation on the external sample set prepared for this aim. Table 2 summarizes the statistical results carried out from the external validation, in terms of R^2, RMSEP and percentage relative error (RE%). The prediction procedure showed satisfactory results for all the types of milk adulteration. The model PLSw highlighted the best results with RE% and RMSEP values of 2.81% and 1.172, respectively. The values of RMSEP were in the range 1.21 and 1.38 in applying the relative PLS models to the samples adulterated with cow milk.

ANALYSIS OF FOOD MATRICES

2.2 A critical evaluation of the analytical techniques in the photodegradation monitoring of edible oils

In recent years the strong interest in the study of vegetable oils has increased due to their versatility not only in food but also in the pharmaceutical, cosmetic and technological fields.

In this work the different analytical techniques currently used to monitor quality of food matrix were compared to evaluate the effects of light on a series of edible oils (peanut, sunflower, corn, olive, linseed and soy oils).

Olive oil is obtained from the fruit (drupe) of the olive tree, which contains Dicotiledonee, Olacee family, genus Olea, species Olea Europaea L. Olive oil is obtained by cold pressing of the olive pulp and, as we all know, it is a fluid-looking oil with a distinctive scent and a color ranging from golden yellow to green. It is one of the richest in oleic acid (about 62%), the most abundant of monounsaturated fatty acids with a long chain in our body, with great nourishing and emollient properties for the skin. In addition to oleic acid, olive oil contains about 15% linoleic acid, 15% palmitic acid and 2% stearic acid and an unsaponifiable fraction ranging from 1 to 2% which provides a fatty acid, chlorophyll, vitamin E, phytosterols with restorative and anti-inflammatory action and squalene, one of the main components of the skin's surface.

The oil is indispensable during childhood as it contributes to the body growth and also during adulthood because prevents artery and heart disorders and lowers the level of cholesterol in the blood. In addition to reducing the risk of heart disease, it has an anti-aging function for the skin and bones as it is rich in vitamin E, which protects against decalcification, osteoporosis and fractures, together with vitamin E, beta-carotene (provitamin A) and a whole series of antioxidant substances such as phenolic compounds. Olive oil is certainly the most famous for its organoleptic

characteristics and healthy ingredients that make it a major player in the Mediterranean Diet [34,35].

Linseed oil, extracted from the seeds of the flax plant *Linum usitatissimun*, is rich in omega 3 and omega 6, useful for the heart and against high cholesterol, and is widely used in the field of cosmetics.

The composition of linseed oil is 50% of omega 3 and 25% omega 6 which are essential fatty acids with a lot of benefits on human health but we must supplement with the diet. It also contains oleic acid (15-18%) and saturated fats (5-10%), vitamin E and vitamin B, lecithin, a large part of proteins and fibers and finally many minerals such as magnesium and zinc.

Peanut oil is obtained by squeezing under pressure or by means of solvents and refining of the seeds of the *Arachis hypogaea L.* plant. The composition of peanut oil is very similar to the composition of classic olive oil; in fact, it contains for more than one-half monounsaturated fat, which we remember to be those fats that give the highest quality to vegetable oil, 18% of saturated and 27% polyunsaturated. Despite of this, the oil does not contain proteins, carbohydrates and gluten so can also be used for the feeding of the ciliaci.

Peanut oil contains a good dose of vitamin E which is an excellent antioxidant, and in fact rancid less than other vegetable oils. Contains vitamin K and many tocopherols (207 mg) especially tocopherol gamma, associated with cardiovascular health. If it is used as a supplement, peanut oil is also a good bowel cleanser, helps hormone regularization and preventing rheumatism. The oil of peanut seeds, also thanks to its organoleptic properties, is more used than olive oil. It contains a considerable dose of vitamin E [36,37] which retards the process of rancidity than other oils, but is also more susceptible to contamination by aflatoxins [38].

Soybean oil is rich in polyunsaturated fatty acids, including linoleic and α linoic acids and also saturated acids, such as palmitic and stearic [39]. Soybean oil has good cholesterol-lowering properties beacuse it contains small doses of lecithin, which besides helping to fight bad cholesterol, is also useful in case of diseases or neurological dysfunction. It is used to flavor raw food or for producing margarine,

after hydrogenation. It is not suitable for frying, as it is unstable to oxidation and high temperature [40].

Sunflower oil is obtained by pressing the seeds of the *Helianthus annus plant*. It belongs to the Asteraceae family and in fact its large flower is actually an inflorescence composed of many small flowers each of which produces a fruit with a seed inside. The plant can grow up to 3 meters in height and the inflorescence can have a diameter of 85 cm.

The composition of sunflower oil is essentially of unsaturated fatty acids, about 32% of oleic acid and 52% of linoleic precursors of omega 3 and 6 fatty acids; these compounds are important for heart health, production of energy, transport of oxygen, creation of hemoglobin in the bloodstream and even for keeping the bodily hormonal system in balance. Sunflower oil is rich in vitamin E, known to be not only an antioxidant compound but also able to protect cell membranes fighting free radicals responsible for cellular aging. It is often used for frying because quite stable at high temperatures [41].

Corn oil is extracted from the germinating part (called germ) of the caryopsis of the seed of the Zea mays plant, commonly called corn or maize. This plant is native to the Americas and is currently widespread in the world until it became a common plant also cultivated in Italy. The oil extraction yield is not very high; in fact, it is only 15-20% on the whole of the whole part of the corn seed. Corn oil has a dark color, amber red and only after refining acquires a clear and limpid appearance.

It is rich in polyunsaturated fats of the omega-6 family (30%) and omega-9 (55-60%). On the contrary, it is omega-3 and this composition must be kept in mind as it is recommended to take a right ratio between omega 6 and 3 (4: 1 respectively). This parameter shows us that if we want to use corn oil in the diet we must integrate omega 3 with other foods such as linseed oil. [42]. In corn oil there are no proteins and this allows to use it for those who have problems with excess uric acid and high azotemia or even in cases of liver problems and intoxication. It also contains a good dose of vitamin E useful to improve some dermatoses and skin problems such as eczema and redness, even in children. Vitamin E is an excellent antioxidant to reduce

and counteract free radicals responsible among other things for cellular aging. In 10 g of oil, which corresponds to a cooking spoon, we can have 30% of RDA (recommended daily dose) of vitamin E. Corn oil can also contain provitamin A always if the extraction oil is raw and therefore can be considered a useful supplement to reinforce and balance the skin and hair.

The composition of the mineral salts sees the presence of iron and some other trace elements depending on the stage of transformation of the oil extraction process. The corn oil has a good laxative action thanks to the fact that intestinal lowers its absorption, this involves its elimination with the faecal mass that will be softer, favoring mechanical emptying and facilitating in cases of constipation. With corn oil it is possible to prepare the soap, in fact the saponifiable fraction is 2% and the oil contains sterols, phospholipids and gamma-tocopherol. It can be used for saponification with the creation of natural soaps also made by hand. The consistency of the soap obtained only from corn oil is softer than the common soap even if it carries with it the typical properties of this oil; it is also very stable. Corn oil soap gives skin moisture, delicacy and has good emollient properties. In the field of renewable energy, corn is used to produce bioethanol and biofuel depending on whether it is transformed or used as a biomass directly.

As can be deduced from the description of the properties of each oil, the study of stability is extremely important to guarantee consumers high quality products and to provide the correct information on their correct storage. Usually, oxidation represents the major cause of degradation and it occurs if the oil is exposed to air, heating, exposure to light, catalysts, etc. In particular, the protection of the oils from light appears so of great importance to ensure that the products maintain the full original nutritional and organoleptic characteristics.

This work aims to verify the performance of the widely used analytical techniques in assessing any alteration by light irradiation on a series of edible oils. The photodegradation tests were conducted in accordance with international rules (International Conference on Harmonization, 2003) [43] and the oil samples were

analyzed by FTIR and UV spectroscopy and HPLC, just before the experiments and at several time intervals up to 9 h of total irradiation.

2.2.1 Experimental

Corn, linseed, olive, peanut, soybean and sunflower oils were purchased commercially and stored in the dark at 25 C. N-hexane for UV-vis analysis, sodium hydroxide, hydrochloric acid, petroleum ether, formic acid 98% (lab grade); acetonitrile and methanol, both of chromatographic grade; linoleic, linolenic and oleic acids (standard grade), were all purchased from Sigma-Aldrich (Milan, Italy).

The samples for UV analysis were prepared by diluting 1.0 g of oil in hexane and then opportunely diluting this solution up to obtain a concentration of 0.8 mg/mL. FTIR analysis were made by placing a drop of the samples on the ATR surface and infrared spectra were recorded in the range 4000e450 cm^{-1}. Scan number and resolution were fixed at 8 scans and 4 cm^{-1}, respectively. The spectrum of the ATR element versus room air was used as background. Before each analysis, the ATR plate was cleaned by scrubbing it with hexane and ethanol.

HPLC analysis of linoleic, linolenic e oleic acids, stored at 4 °C before the use, were carried out. For this aim, the compounds were appropriately solubilized in methanol and the solutions filtered through a 0.22 mm Millipore filter (Billerica, MA, USA). Mixtures of the standards were also prepared at concentration ratios close tothose of the studied oils. Determination of the fatty acids in the oil samples was performed after appropriate extraction: 5 g of oil were hydrolyzed with 50 mL of 0.5 M NaOH at 25 °C for 3 h. The dispersion was extracted by adding 50 mL of petroleum ether two times, to remove the unsaponifiable fraction. The aqueous phase was acidified with 1 M HCl to pH 2.9 and then extracted with 50 mL of petroleum ether two times. The organic solvent was removed at 40 °C under pressure. Finally, the acids were recovered with 4 mL of methanol and filtered through 0.22 mmMillipore filters before HPLC injection. The chromatographic separation was achieved at room temperature by C18 column (250 mm x 4.6 mm x 5 mm Phenomenex), isocratic

mobile phase of acetonitrile/methanol (90:10 v/v) adjusted with formic acid to pH 5.5, flow rate 1 mL/min.

Photodegradation experiments. Oil samples were subdued to light irradiation without any treatment. Photodegradation experiments were conducted in the Xenon camera test fixing the irradiation power of 350 W/m^2, internal temperature at 25 °C; UV-filter glass >290 nm. The filter adopted mimicked the effect of the sunlight outside. Analysis was recorded at 30, 60, 90, 120, 180, 240, 360, 540 min. In order to minimize any interference of extraneous light in the experiments, all laboratory procedures were executed in a dark room equipped with a red lamp of 60Watt a distance of at least 2m.

Chemometric elaboration. Principal component analysis (PCA) provides to extract the main information from a data matrix and express this information by projection of the samples on a set of new orthogonal variables called principal components (PCs). When PCA is run, the amount of original variables is reduced to a few PCs that contain the main information stored in the original data. The PCs are built such that the first one carries most information, followed by the second one carrying less information, and so on. When the number of PCs increases, the variance contained by the new PCs can belong to the instrumental noise. Different validation procedures can be used to select the optimal number of PCs. In this work, cross validation procedure was adopted, in which the same samples are used both for modelling and testing. A selection of samples was kept out from the calibration and the model is built on the remaining samples. After that, the kept-out samples were predicted and the prediction residuals computed.

The process was repeated with another subset of the calibration set, and so on until every object was left out once. All prediction residuals were combined to compute the validation residual variance and to estimate the optimal number of PCs [44]. The Unscrambler X software version 10.3 from CAMO (Computer Aided Modelling, Trondheim, Norway) was used for the multivariate data elaboration.

2.2.2. Results and Discussion

FT-IR analysis. The IR spectra of the different oils are shown in figure 13. By observing the image, it is evident that all oils have characteristic bands, in particular between 2850 and 3000 due to CH strechting, 1740 due to the ester portion of triglycerides, a broad band between 1027 and 1112, due to the CO bond and to 721 due to CH out of the deformation plane [45].

Because of the strong similarity between the spectra of different oils, it is difficult to determine any differences through traditional methods.

In this case, multivariate analysis is a more appropriate investigation tool to explore all the signals along the entire wavelength range [46,47]. Chemometric elaboration is able to distinguish clearly between the different types of oil, with the exception of sunflower oil or corn. (Fig.14)

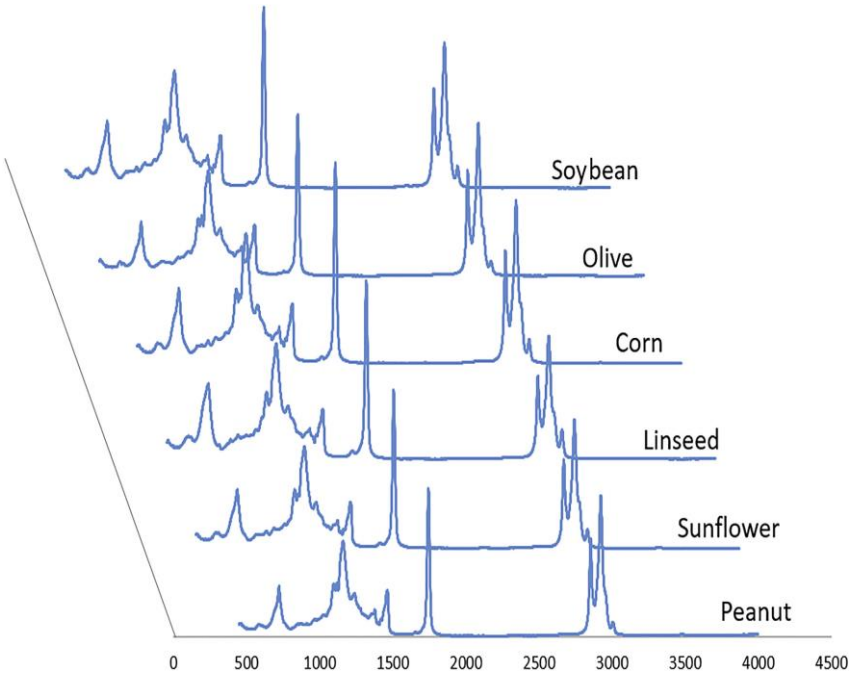

Figure 13. The IR spectra of all vegetable oils.

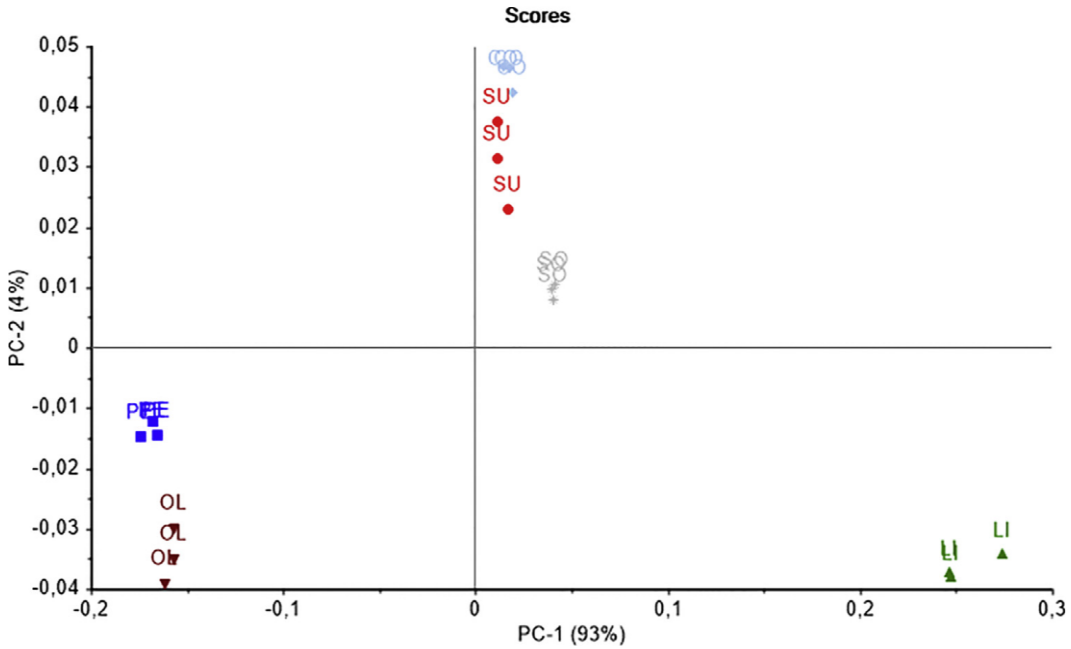

Figure 14. PC1/PC2 score plot by PCA analysis on the edible oils.

The oils were subjected to a suntest forced photodegradation experiment in accordance with the ICH standards, using the wavelength range over 290 nm to simulate the external light and at a temperature of 25 °C to avoid thermal degradation. The spectra registration was made at different time intervals, such as 30, 60, 90, 120, 180, 240, 360, 480, 540 min.

The simple "visual" analysis of the spectra suggests a complete overlap of the spectra and in addition application of the multivariate analysis, despite the well-known sensitivity, confirmed no significant change in the spectra during the stressing experiment.

UV analysis. In order to verify the photostability of oils, photodegradation was also monitored using UV-vis spectroscopy. Also in this case the spectra of the oil samples, suitable diluted, were recorded at different time intervals up to 540 min.

By observing the UV spectra of each oil at zero time (fig. 15), it's clear the presence of a major peak in the 210-220 nm region due to p/p*transitions of single ethylene chromophores and to n / s* transition sof carbonyl chromophores.

In soybean, peanut and flax oils, peaks around 230-280 nm are particularly evident due to the double and triple conjugate bonds, almost absent in the other oils.

The figure 16 summarizes the sequence of spectra for each oil recorded during the stress test. Unlike the IR spectra, UV analysis showed a continuous variation of the spectral trend, confirming the sensitivity of the oils to light.

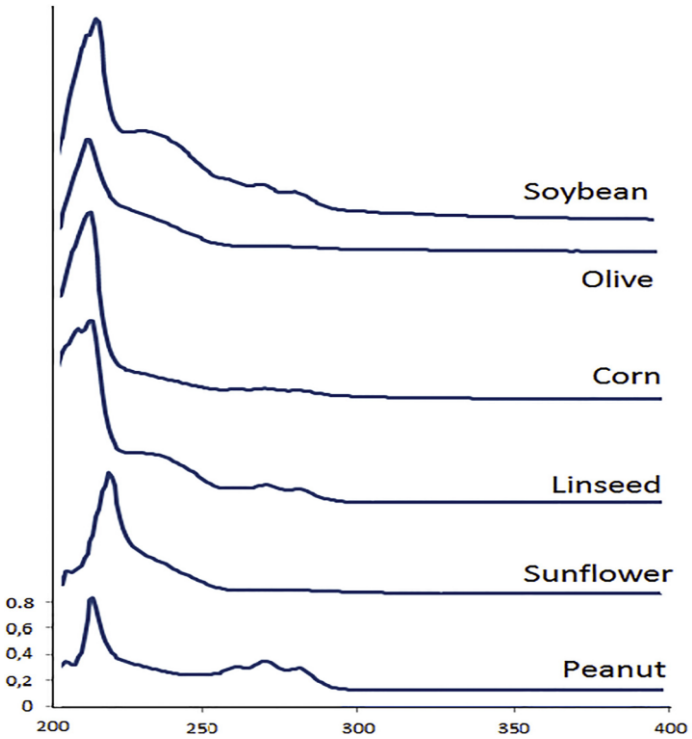

Figure 15. The UV-vis spectra of all edible oils.

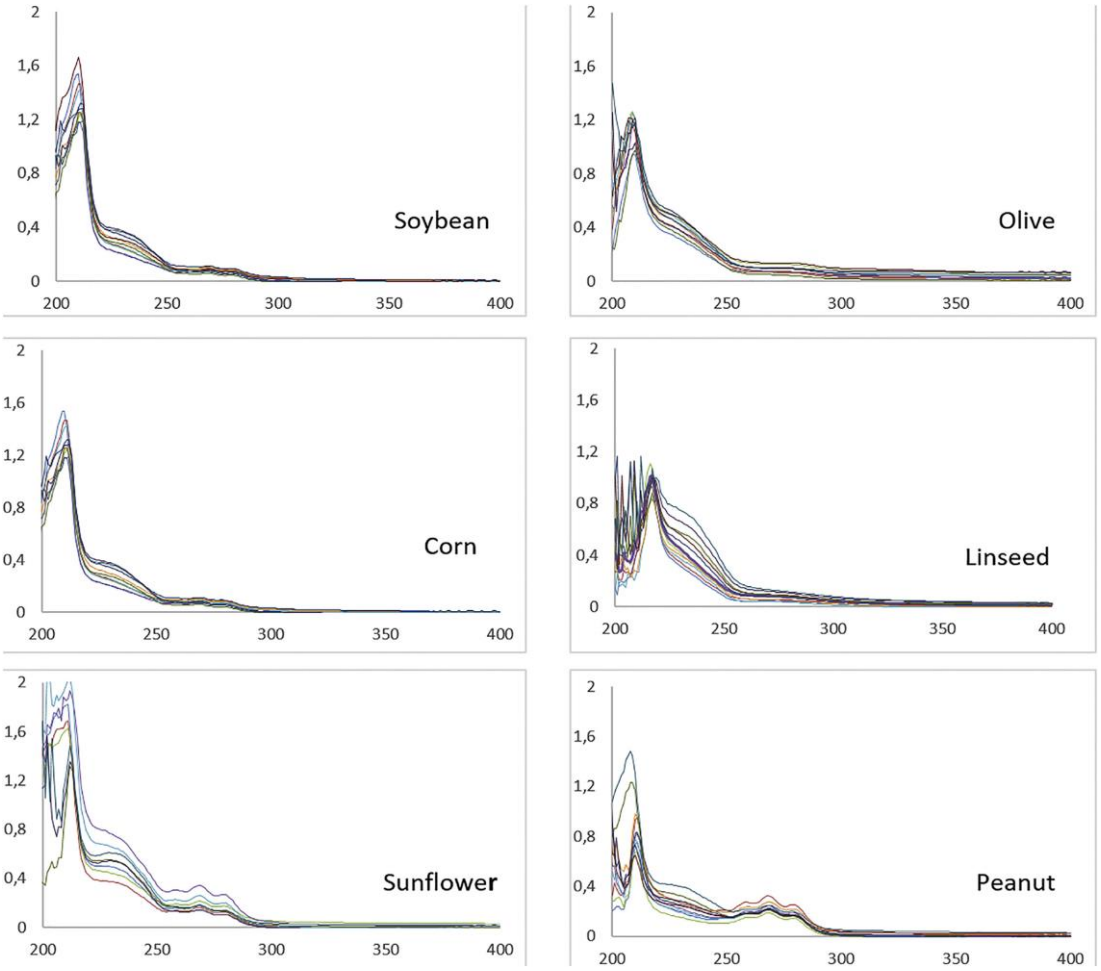

Figure 16. UV spectra of the oils recorded at different interval along photodegradation test.

Even if the spectral analysis shows the photostability of olive oil and corn, in general the oils undergo qualitative-quantitative alterations when exposed to light, alterations that, however, the IR is not able to detect. Probably degradation leads to the formation of a chromophore that absorbs in the UV range but does not alter the functional groups responsible for absorption in the IR range.

HPLC analysis. A further control of the consequences of the light exposure on the oils was performed by monitoring the content of the main fatty acids, linoleic, linolenic and oleic acids, present all studied oils. After the fatty acid extraction described in detail above [48], the chromatographic conditions were optimized by varying the ratios between the solvents and modulating the flow rate of the mobile phase

accordingly. Finally, the mixture which allowed a better separation of the peaks was revealed acetonitrile: methanol 90:10, acidified with formic acid pH 5.5.

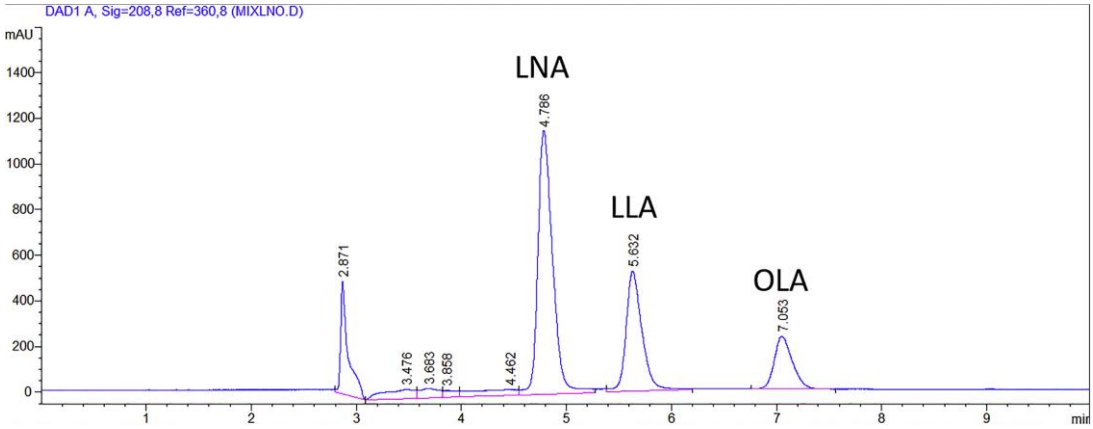

Figure 17. HPLC chromatogram of the standard linolenic (LNA), linoleic (LLA) and oleic (OLA) fatty acids

The quantity of the analytes was in agreement with that reported in the literature. The retention times (RT) were 4.7, 5.6 and 7.1 min for linolenic, linoleic and oleic acid, respectively, in accordance with the lipophilicity of the analytes. The calibration curves of the three analytes were calculated in the range 0.01-3.00 mg/mL for oleic and linolenic acid and 0.001-1.500 mg/ml for linoleic acid. These relationships were used to quantify the fatty acids before and after the photodegradation experiments. The figure 18 (a-d) shows the comparison between the chromatograms before and after the stress test.

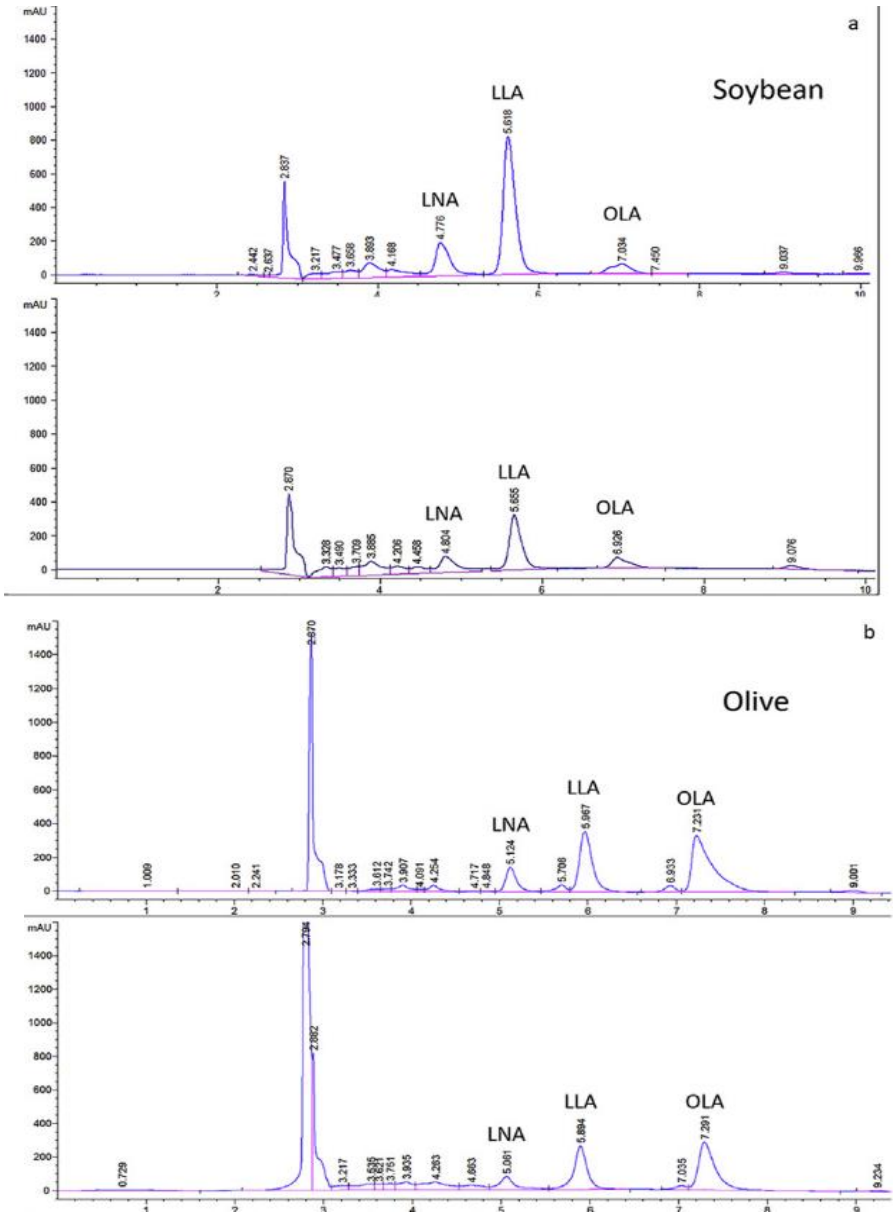
a
Soybean
LLA
LNA
OLA
b
Olive
LLA
LNA
OLA

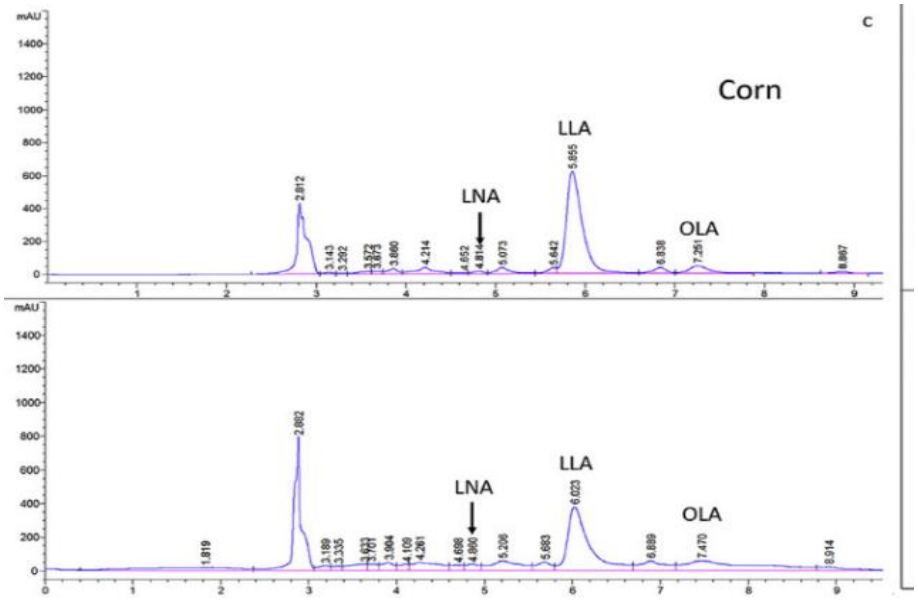
c
Corn
LLA
LNA
OLA
mAU
LNA
LLA
OLA

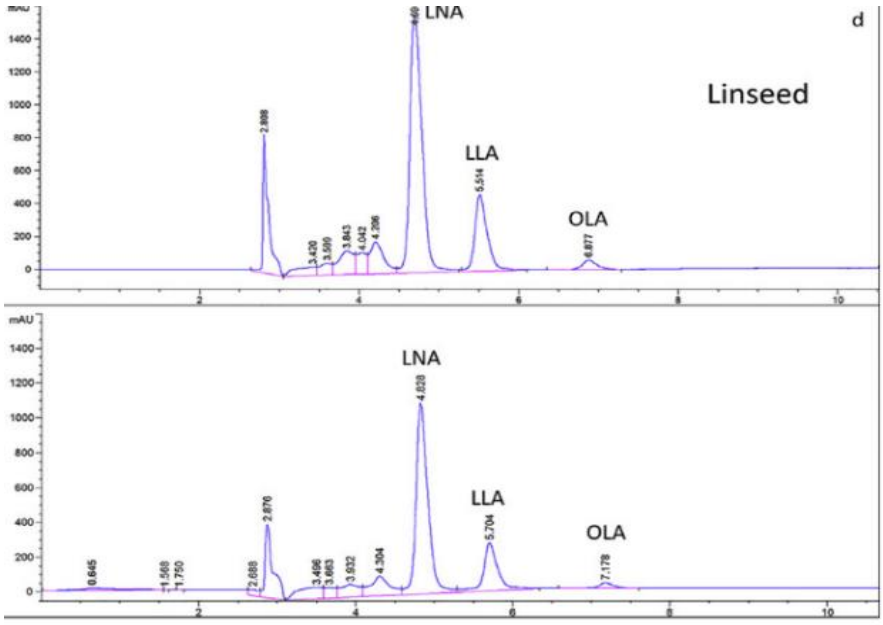
d
Linseed
LNA
LLA
OLA
mAU
LNA
LLA
OLA

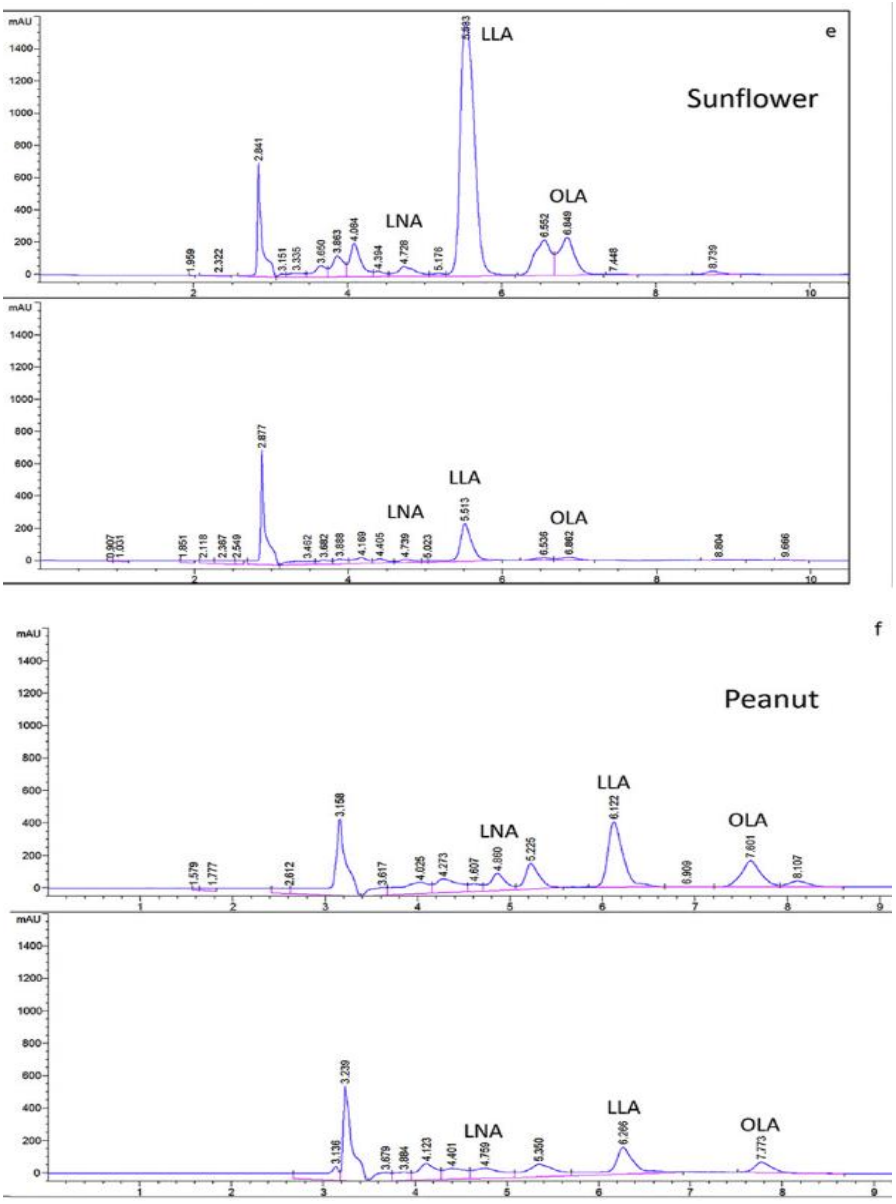

Figura 18 a-f. HPLC chromatograms of the fatty acids extracted by edible oils before and after light irradiation test

Except for olive oil, the fatty acid content decreased during the photodegradation experiment. The results obtained further confirm our hypothesis that IR is an inadequate tool for determining the effects of light on oils.

ANALYSIS OF FOOD MATRICES

2.3 Photo and thermal stress of linseed oil and stabilization strategies.

Nowadays, LO is considered a *functional food* because is a good source of omega-3 and -6 polyunsaturated fatty acids, dietary fiber and other minor nutrients. In particular, the ω-6 linoleic acid (LLA) and ω-3α-linolenic acid (LNA) are important as precursors of other fatty acids of both series. The polyunsaturated fatty acids, as well as being components of cell membranes, are important protective factors in heart disease, in the prevention and treatment of hypertension, in type II diabetes, in immune and inflammatory disorders [49 -51]. Furthermore, the presence of oleic acid (OLA) is important, since it has been shown that a high consumption of this fatty acid is associated with a lesser possibility to develop cardiovascular and tumor pathologies [52]. Linseed also contains polyphenolic compounds known as *lignans*, considered as phytoestrogen analogues [53] and studied for their potential pharmacological use in pathologies related to hormones [54]. In linseed, the main lignan is secoisolariciresinol (SEC), mainly in the form of diglucoside [55] toghether with discrete quantities of lariciresinol (LAR) and matairesinol (MAT). Determination of SEC in the flax seed has been performed by HPLC-DAD [56]. Consumption of lignans reduces cardiovascular risk and inhibits the growth of some types of diabetes [57-58].

Since functional foods contain bioactive components that provide health benefits, appropriate preservation of these bioactive components is therefore fundamental to guarantee their good properties. Recurrent episodes of failures in maintaining the quality of functional foods have been reported [59;60]. One of the main problems associated with the use of LO as a source of omega-3/6 fatty acids and lignans is the easy oxidation and rancidity process due to the high concentration of these components. In addition, potentially toxic secondary products for human health could also be formed [61]. The analysis through UV spectroscopy has allowed to follow any variation of the overall drug or food matrices and at the same time to monitor the main components during the photo- and thermal degradation

experiments [62;63]. On the contrary FTIR spectroscopy, even if is an efficient analytical technique capable of characterizing many food matrices, it it turned out to be not suitable to study the photolability of vegetable oils [64;65]. HPLC techniques have been used to determine the composition of fatty acids, especially omega-3 and -6. The fatty acids have been determined by HPLC after specific extraction [66] and the photodegradation tests performed in accordance with international rules [67;68].

The different types of formulation and packaging can also drastically affect the chemistry of bioactive components and their duration. Unfortunately, there are few documents on the packaging, but it would be helpful to have a complete overview of the requirements for proper food storage and therefore the right packaging standards. One of the most used strategy to reduce the oxidation of the omega fatty acids was the addition of antioxidants. The antioxidant properties of tocopherols and ascorbic acid in inhibiting the decomposition of hydroperoxides was demonstrated fundamental in preserving the quality of food by reducing the formation of aldehydes [61]. Another study uses phenolic compounds such as myricetin, (+) - catechins, genistein and caffeic acid as antioxidants. Their protective effect was assessed by monitoring the form of hydroperoxide and the residual concentration of antioxidants. Among these, myricetin has shown a significant reduction in the oxidation of linoleic acid [69].

This work aims to define any changes in LO when exposed to normal or stressed storage conditions of light and temperature. In addition to the photo-thermal stress study, some strategies are also proposed for minimizing LO photolability through physical and chemical approaches.

2.3.1 Experimental

LO was purchased commercially and stored in the dark at 4 °C. n-hexane for UV-vis analysis, sodium hydroxide, hydrochloric acid, petroleum ether, formic acid 98% were lab grade; acetonitrile and methanol of chromatographic grade; LLA, LNA, OLA, LAR, SEC, MAT and ascorbyl palmitate (AP) (standard grade), were purchased from Sigma-Aldrich (Milan, Italy).

Stressing photodegradation tests were conducted by the Suntest CPS+ camera (Heraeus, Italy), equipped with a Xenon lamp, whose radiant spectrum is largely overlapping with the spectrum of the solar radiation. The instrument allows to select specific spectral regions by interposing specific filters; the internal temperature can be adjusted by means of a refrigerant unit to avoid sample heating due to the lamp. UV analysis was performed by Agilent 8453 UV spectrophotometer equipped with diode array detector (Agilent Technologies, CA, USA). HPLC analysis was performed using an HP1100 pump equipped with a G1315B (Agilent Technologies) diode detector and a Rheodyne 7725 manual injector.

Standard solutions 500 mg of LO were diluted in 10 mL of hexane and the solution was further diluted 1:10 witH the same solvent. These samples (n=10) were used to record the UV spectra of LO before degradation tests. The standard solutions of LLA, LNA and OLA, stored at 4 °C before the use, were prepared by solubilizing 1.60, 3.02 and 5.76 mg, respectively, in 1 mL of methanol and further filtration through a 0.22 µm filter. Analogously, the standard solutions of MAT, LAR and SEC were prepared by weighing 1.02, 1.08 and 1.03 mg, respectively, and diluting in methanol up to obtain concentration ranges between 0.06 and 0.5 mg/mL. All the samples were analyzed by HPLC to carry out the regression equations of the analytes. These equations were then used to calculate the analytes concentration along the degradation tests.

The UV spectra of LO along the degradation tests were performed after dilution, following the procedure above described. Determination of the fatty acids in the LO samples was performed after appropriate extraction as follows: 5 g of LO were hydrolyzed with 50 mL of 0.5M NaOH at 25 °C for 3 h under stirring. 50 mL of petroleum ether were added twice to the dispersion, in order to remove the unsaponifiable fraction. The aqueous phase was acidified with 1M HCl to pH 2.9 and then extracted twice with 50 mL of petroleum ether. The organic solvent was removed at 40 °C under pressure. Finally, the analytes were recovered with 4 mL of methanol and filtered through 0.22 µm filters before HPLC injection.

The chromatographic separation of the fatty acids was achieved on a LC-C18 Gemini column (Phenomenex) 250 x 4.6 mm x 5 µm at room temperature in isocratic mode.

The mobile phase was a mixture acetonitrile/methanol (90:10 v/v) adjusted with formic acid to pH 5.5; flow rate was 1 mL/min; injection volume was 20 µL. Determination of the lignans was made by extracting 45 g of LO with methanol (3 x 20 mL). The methanol phase was then concentrated under pressure and diluted in acetonitrile 4 mL. This solution was treated with hexane (3 x 10 mL) and concentrated under pressure, diluted in methanol 1 mL and then filtered through a 0.45 µm PTFE filter. This sample was analyzed by HPLC [70]. HPLC separation of the lignans was obtained on the same column above reported at room temperature in isocratic mode. The mobile phase was a mixture methanol/water (70:30 v/v) adjusted with formic acid to pH 3.4; flow rate was 0.65 mL/min; injection volume was 20 µL.

Photodegradation experiments LO samples were subjected to light irradiation without any pretreatment. Photodegradation experiments were conducted in the Xenon camera test by setting the irradiation power to 350 W/m^2, corresponding to 21 kJ/m2 146 ·min, and the internal temperature at 25 °C. The UV-filter glass (>290 nm) was interposed between the lamp and the samples so to mimic the effect of the sunlight outside. UV and HPLC analyses were recorded at 6 h intervals up to 48 h, after specific treatment above described. In order to minimize any interference by the extraneous light, all laboratory procedures were executed in a dark room equipped with a red lamp of 60 W at a distance of at least 2 m.

Thermal degradation of LO was performed by placing the samples in a water bath maintained at 60 °C in the dark for 48 h and monitoring the samples by UV and HPLC, after specific treatment above reported, at 6 h intervals. Chemical and physical protection LO photostabilization experiments were carried out, under the same forced irradiation conditions reported above. The LO samples were placed in quartz and transparent glass and the results compared with those obtained from the adoption of amber glass. Moreover, the photoprotection experiments were performed by adding the antioxidant AP with concentrations in the range 0.01-0.20% w/v.

2.3.2 Results and Discussion

UV and HPLC Analysis. The oil samples, diluted up to a concentration of 5 mg/ml, were subjected to UV analysis and by observing the spectrum are evident absorption bands at 230 and 280 nm, typical of double and triple conjugated bonds, respectively. The high absorbance around 210-220 nm is due to n → σ* transitions of carbonyl chromophores and to π → π* transitions of single ethylene chromophores. HPLC analysis of the main fatty acids, LLA, LNA and OLA, was optimized by using the mixture of the relative standard solutions. The chromatographic parameters such as retention time and degree of resolution of the chromatogram were improved gradually changing the eluent mixture and finally the best result was reached by using a mixture 90:10 methanol: water pH 5.5 (formic acid). The retention times (RT) were 4.7, 5.4 and 6.5 min for LNA, LLA and OLA, respectively, as shown in Fig. 19a.

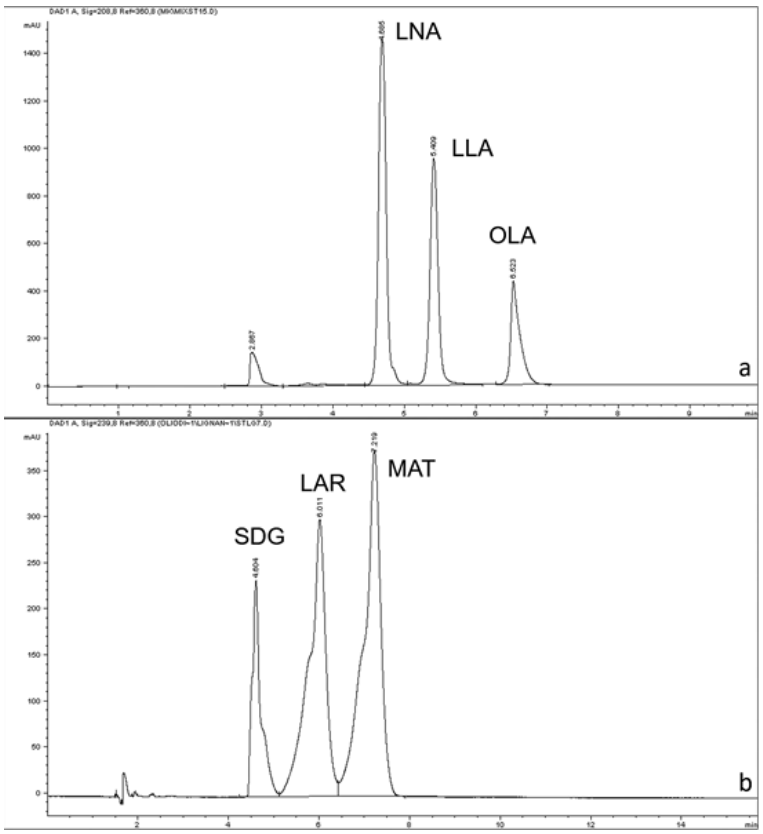

Figure 19 a-b. HPLC chromatogram of standard mixture samples: (a) fatty acids LNA (0.23 mg/mL), LA (0,37 mg/mL) and OLA (0.60 mg/mL); (b) lignans SEC (0.1 mg/mL), MAT (0.1 mg/mL) and LAR (0.25 mg/mL).

The amount of fatty acids in LO, before or along the degradation tests, was calculated through the respective calibration curves, built on the data from HPLC analysis of the standard samples in the range 0.015-0.909 mg/mL for LLA, 0.028-1.152 mg/mL for LNA and 0.016-0.800 mg/mL for OLA. The separation of the lignans in HPLC chromatography was also optimized, using a mixture of methanol: water acidified at pH 3.5 with acetic acid. The RT values were 4.6, 6.0 and 7.2 min for SEC, LAR and MAT, respectively, as shown in Fig. 19b. The regression data are listed in Table 4 and the curves are shown in Fig 20.

Table 4. Parameters of the regression curves for the fatty acids and lignans.

Analyte	Slope	Intercept	Correlation coefficient	Validation range (μg/mL)
LLA	37.541	-2664.8	0.9902	0.016-0.800
LNA	53.025	-395.2	0.9788	0.015-0.909
OLA	10.325	-104.61	0.9933	0.028-1.152
LAR	54.846	8498.3	0.9823	0.060 - 0.500
SEC	20.929	1569	0.9989	0.060 - 0.500
MAT	21.767	520.18	0.9956	0.060 - 0.500

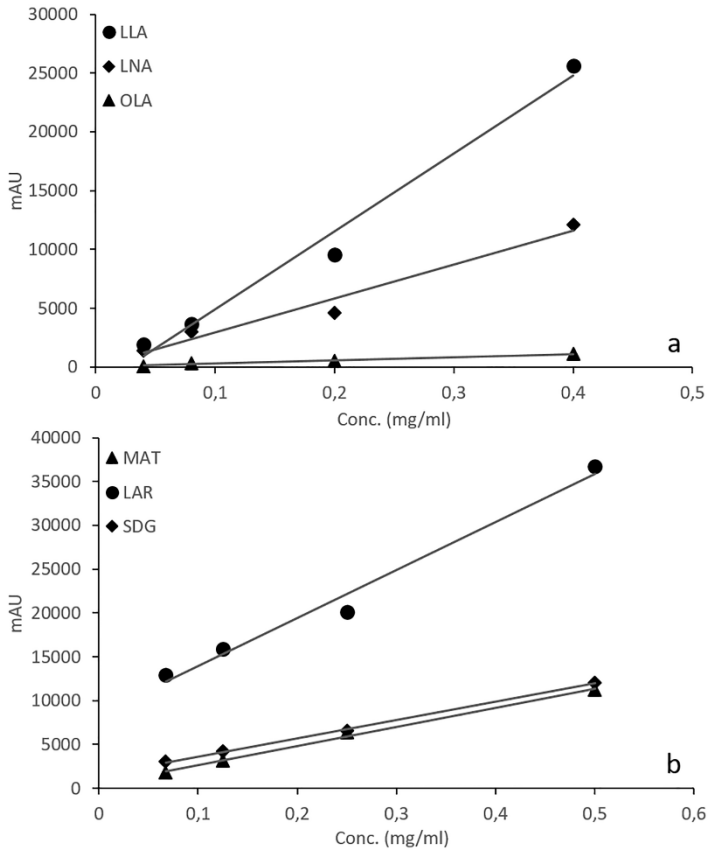

Figure 20. Regression curves obtained from HPLC data of the standard solutions of fatty acids

Photodegradation experiment. Three samples of LO were subjected to forced photodegradation in quartz flasks in order to investigate their behavior, avoiding any interference from the container. Exposure to the light of linseed oil in a container transparent to all radiation is important to distinguish its behavior from exposure to open air, widely covered in studies on its use in painting. The UV spectra, shown in Fig. 21, were recorded before and along the photodegradation experiments at the interval times before detailed. By observing spectra profile, both the characteristic bands around 230 nm and 280 nm have a growing trend. In the same way, the absorption band in the range 210-220 nm increased because the formation of carbonyl chromophores. Many authors have actually reported that the oils undergo a radical-type degradation that initially forms hydroperoxides which in turn are transformed into alcohols, acids, aldehydes, ketones and lactones [41; 71].

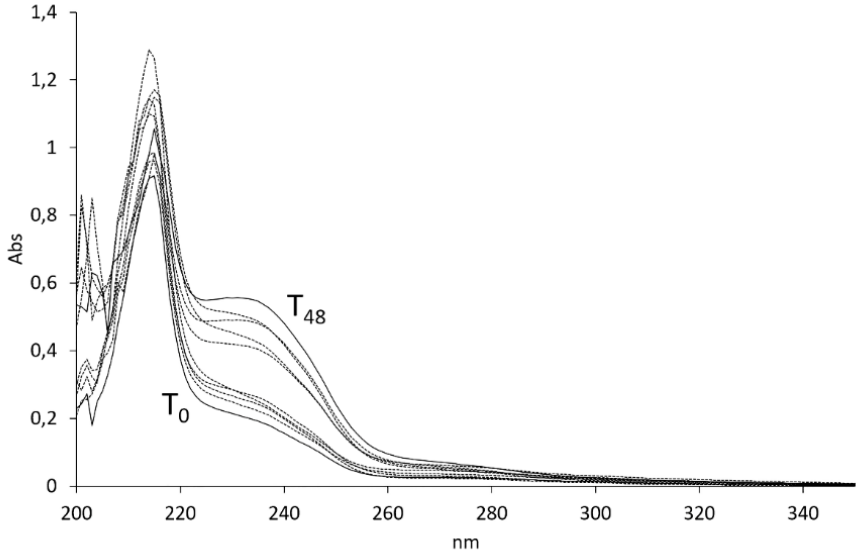

Figure 21. Sequential UV spectra of LO in quartz recorded at time intervals along forced irradiation

The amount of the studied fatty acids along the stressing irradiation test was monitored trough HPLC analysis of the samples at time steps of 6h up to 48 h. A clear decrease of all the analytes was demonstrated. Fig. 22 shows the chromatograms recorded at time 0 and after 18 h of the stressing photodegradation test.

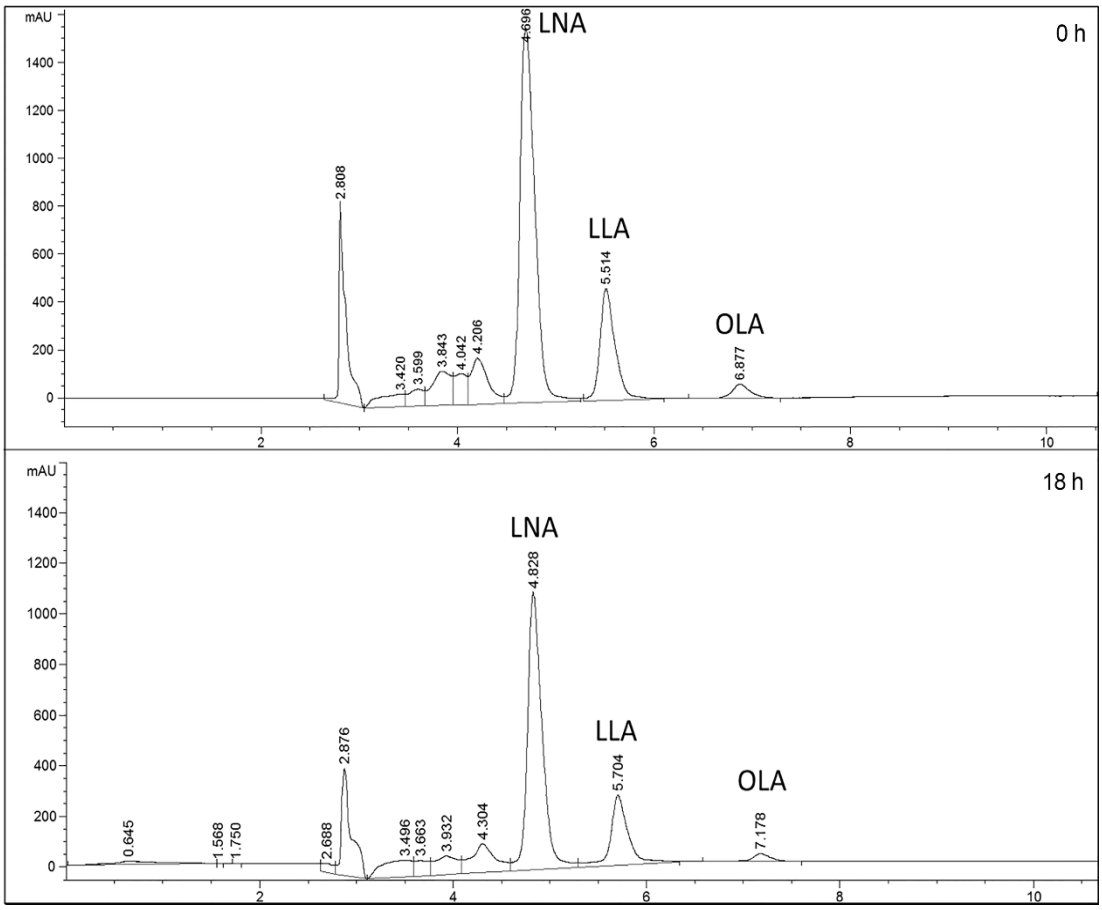

Figure 22. Sequential chromatograms of LO in quartz recorded at time 0 and after 18h of forced irradiation

Exposure of the oil to light causes a decrease of LLA and LNA of about 70% after only 6h. After that, the transformation proceeded more slowly up to a residual amount of about 35% at the end of the experiment (48 h of total exposure). In contrast, OLA showed a higher stability, with a residual percentage of 84% after 6 h and 43% after 48 h of irradiation. These results were calculated on the data collected from three samples tested. The photodegradation profiles of the single fatty acids are plotted in the graph of Fig. 22. On the contrary, the concentration of the lignans studied did not show a significant variation after the photodegradation tests. The residual concentration of all these analytes was in the range between 95 and 105%, values that cannot be attributed to a sure degradation but rather to a statistical variation of the results.

Thermodegradation testing. The thermal resistance of LO was investigated by placing the samples in a water bath fixed at 60 °C, maintained in the dark, up to 48 h. Aliquots of the samples were analysed by UV and HPLC at intervals of 6 h. The fatty acids remain stable if subjected at high temperature mantaining a residual concentration between 94-97% after 12 h and 87-95% after 48 h. Regarding lignans, only at higher temperatures, up to 250 °C, caused their degradation. However, the lignans contained in the linseed were the most stable at high temperatures, resisting even for a few minutes even at 250 °C [72].

2.3.3 Photoprotection strategies

In order to improve the photostability of LO, two different approaches, physical and chemical, were investigated.

Physical protection. The photodegradation experiments of the oil samples were initially conducted in transparent glass containers. The results obtained were very similar to those in which quartz containers were used, suggesting that the region of the spectrum responsible for degradation is that of the visible where both materials are transparent. Subsequently, the irradiation test was repeated while maintaining the same operating conditions using amber glass. Fortunately, the results have greatly improved after 12h of irradiation in fact the residual amount of LNA increased from a value slightly higher than 50%, for quartz and glass, to a value of 82% in amber glass. LLA value changed from 65% to over 90% while the values for OLA changed from 75% to 88%. Despite the amber glass has shown to have a greater photoprotective power, after 12 h the oil does not maintain its characteristics, confirming that after some time the degradation proceeds even if the sample is not exposed to light [73].

Chemical protection. The addition of an antioxidant substance to food matrices is one of the most common strategies to prevent the phenomenon of oxidation. In this work ascorbyl palmitate was added as an antioxidant agent, known for both water and oil

solubility. In the literature there are some works in which the antioxidant power of ascorbyl palmitate is increased by the addition of tocopherols [74].

The action of the AP was evaluated by subjecting the oil samples to a forced photodegradation experiment in quartz containers so as to eliminate the interference of the container. A concentration ranges from 0.01% to 0.02% it was initially added up to a concentration of 0.05% which gave the best results. In Fig. 23, the degradation profiles of fatty acids show a significant increase in stability with a residual percentage between 50-60% after 48 h, higher than the values recorded with the adoption of amber containers. However, it should be noted that the protective effect of colored glass in the first 12 h remained even higher for all analytes.

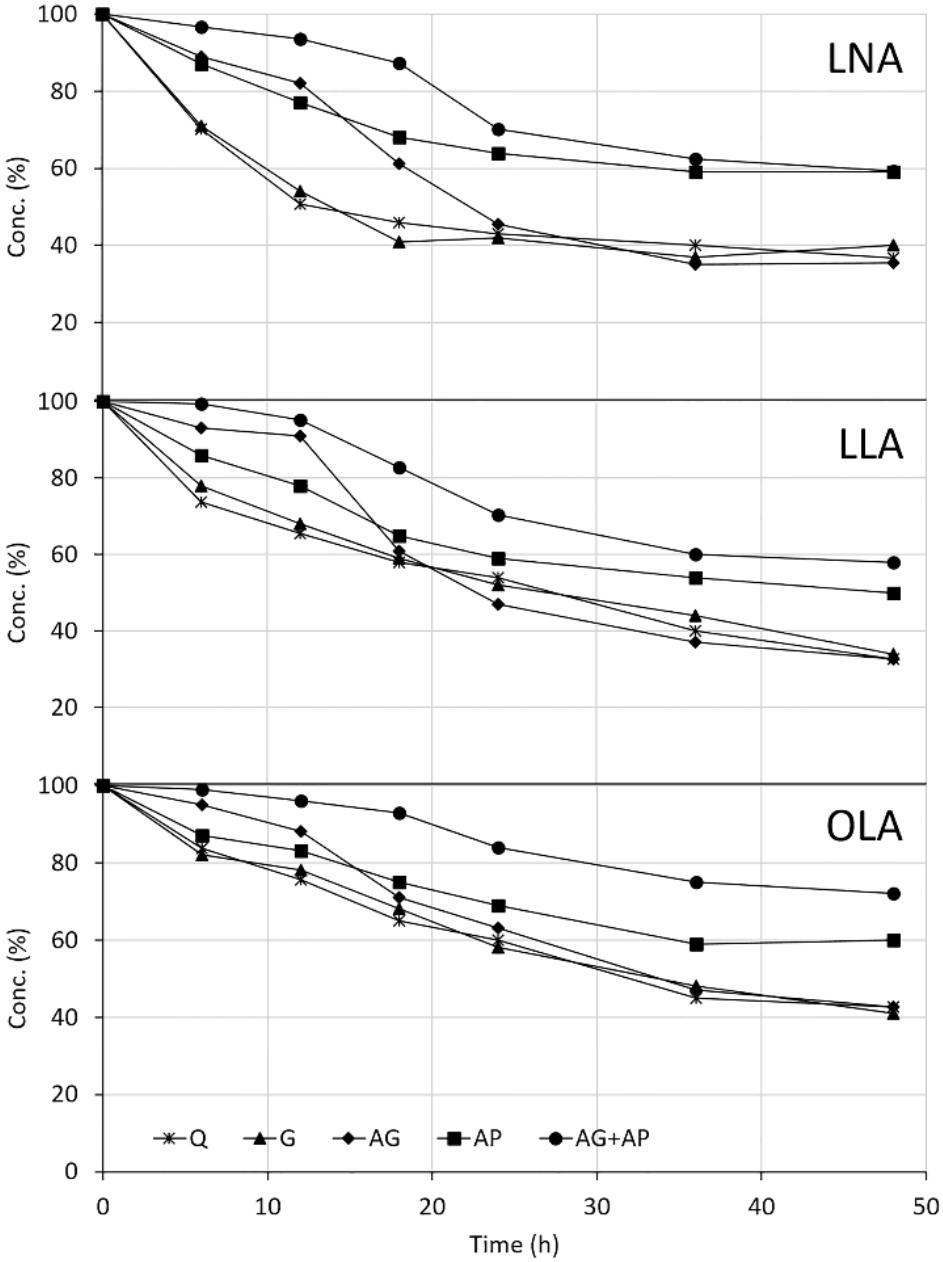

Figure 23. Kinetic study of fatty acids degradation LNA, LLA and OLA at different experiment conditions: quartz (Q), glass (G), amber glass (AG), ascorbate palmitate (AP) and amber glass + ascorbate palmitate (AG+AP)

Chemical-physical protection. Finally, the synergistic action of AP and amber glass was evaluated on oil samples subjected to forced irradiation tests. The concentration of the main fatty acids was monitored by HPLC analysis by using the same previous conditions. Concentration of AP was of 0.05% and power of irradiation was 350 W/m^2.

The results were satisfactory as the residual concentration remained at 95% after 12 hours of irradation and never dropped below 57% even after 48 hours.

This photoprotection technique turns out to be a good strategy as it prevents the radical oxidation process responsible for oil alteration.

3. ANALYSIS OF BIOLOGICAL MATRICES

3.1 Monitoring of anesthetic drugs in the cord blood during labor analgesia.

The umbilical cord (Fig. 24) represents the vital link between mother and child during the period of pregnancy as it provides the fetus with all the nutrients necessary for its development. Its presence allows the transfer of gas and other substances between mother and fetus, without there being any direct exchange between the blood of the two organisms. In this way, the so-called "placental barrier" can prevent the passage of many harmful substances, even if some can still cross it and damage the fetus.

Inside the umbilical cord there are three blood vessels: the umbilical vein on one side and the two umbilical arteries, wound in a spiral around it, on the other. The latter, unlike those of the systemic circulation, carry venous blood, while oxygen-rich blood and oxygen flow into the umbilical vein. The umbilical cord begins to designate itself around the fifth week of gestation, replacing - from the functional point of view - the yolk sac, which guarantees the nutritional inputs in the early stages of embryonic development. [1a]

At the time of birth, the umbilical cord contains an exceptional richness. In fact, his blood is a valuable source of hematopoietic stem cells that can continuously produce red blood cells, white blood cells and platelets. Also present in the bone marrow and in the peripheral blood, hematopoietic stem cells are of vital importance in the treatment of multiple haematological, metabolic and immune diseases [2a]. Precisely for this reason it is very important to donate and store the umbilical cord blood.

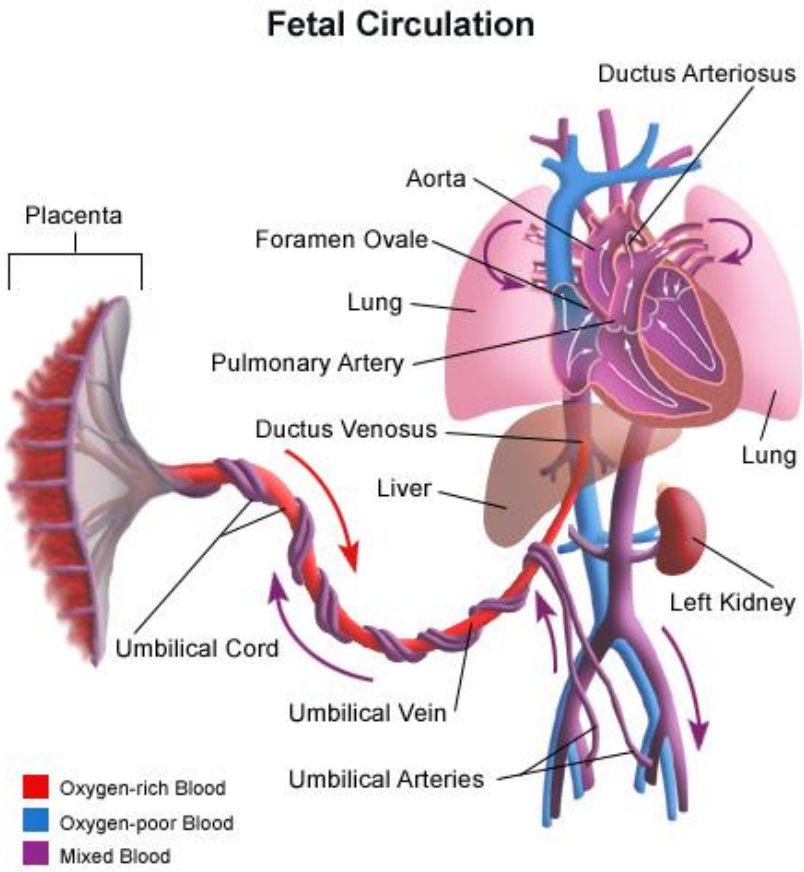

Figure 24. Fetal circulation

3.1.1 Cord blood bank

A biobank or bank for the preservation of the umbilical cord is a structure designed to conserve over time cord blood samples collected at the time of delivery. These samples, after their collection, are analyzed in the biobank receiving laboratories, which ensures that all the parameters of cellularity and vitality of the sample are within the norm, and that no condition exists for which conservation could be compromised (for example the presence of hepatitis B and C). After the sample has passed the analysis phase and has been declared suitable for cryopreservation, it is possible to proceed to the "freezing" phase of the sample.

In order to maintain the characteristics of the umbilical cord stem cells unchanged over time, the cord blood must be stored at a temperature of approximately -180 °C.

To reach such a temperature special containers are used with liquid nitrogen or in gas, able to keep this temperature constant for many years [3a].

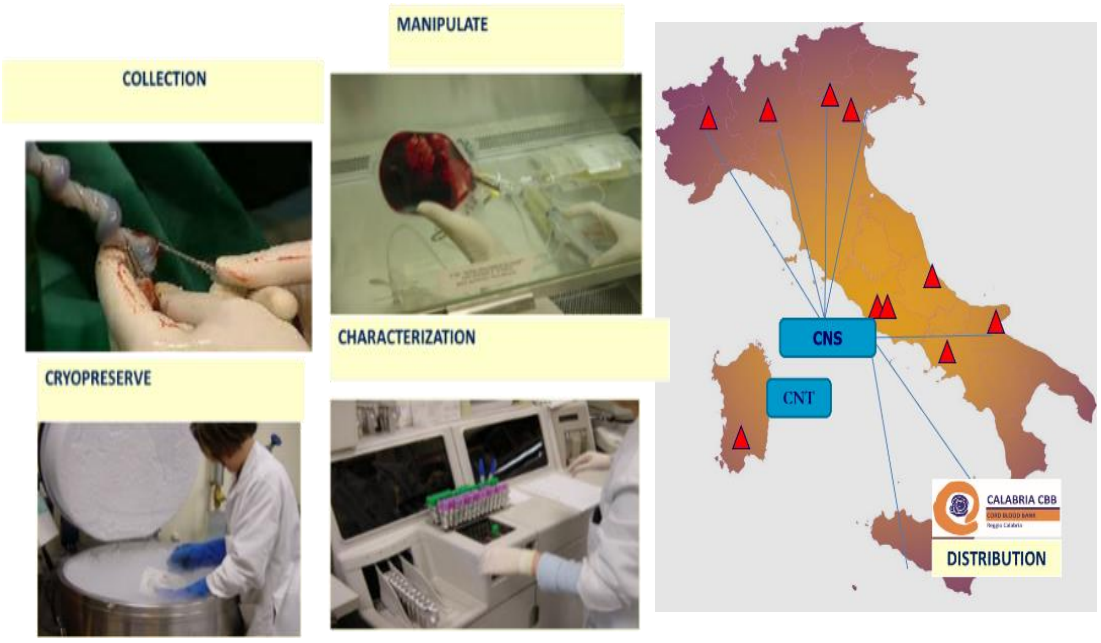

Figure 25. Scheme of Italian cord blood network

Based on the chosen donation formula, the sample taken will be kept in a public cryopreservation bank or in a private bank. Samples for allogeneic (heterologous) donation and for the dedicated donation are destined for public banks, while samples for autologous preservation are destined for private banks.

Public Banks in Italy are managed by the National Health Service and are the structures to which the collection centers refer to allocate the donated blood sample. There are nineteen and cover the entire national territory (Fig. 26).

Figure 26. Cord blood banks active in Italy.

The public banks are associated with about 300 accredited birth points, where mothers can give birth and be followed in the procedure by specialized personnel.

The transfusion law ("New discipline of transfusion activities and of the national production of blood products" L.219 / 2005) regulates donation, collection, storage and release for the transplantation of hematopoietic cells from cord blood. The donation is free, voluntary, without any burden for the donor. Public banks must possess internationally recognized quality requirements to ensure transparency and guarantees in the use of cells for therapies.

Private Banks can not be established on Italian territory, but as provided for by the Ministerial Decree of 18 November 2009 and the Regional State Agreement of 29 April 2010, parents have the possibility to export to autologous use, the sample of blood taken from foreign facilities. The export is authorized by the competent Autonomous Region or Province through the health management of the hospital where the birth takes place.

One of the most important Italian private banks abroad is called Sorgente which was founded in 1997 in Leipzig in Germany by a group of Italian biotechnological companies.

Calabria Cord Blood Bank. The Calabria region cordon bank, called Calabria Cord Blood Bank (Calabria CBB) was established with a resolution of the Calabria Region in May 2004 and has been officially active since January 2006. The CBB is based at the Transfusion Immunohematology Service of the Bianchi - Melacrino - Morelli Hospital of Reggio Calabria, and operates within the Regional Coordination Structure - Centro Regionale Sangue and the Regional Transplant Center. Calabria CBB is equipped with personnel with qualified experience in manipulation and conservation of stem cells.

It is part of the 19 banks active in Italy, which are coordinated by the National Blood Center (CNS) in collaboration with the National Transplant Center (CNT); it is authorized by the CNS and the CNT to enter the data of its bank units in the database of the Italian Bone Marrow Donor Registry (IBMDR), to which all the Transplant Centers in the world can be selected to select and request a patient's appropriate cordon unit oncoematologico.

Once the birth has occurred, when the cord has already been cut, the cord blood is collected. The drawn cordon unit is sent, together with the personal data, to the signed consent and the withdrawals, carried out at the time of delivery, at the Regional Bank of cord cells.

The staff of Calabria CBB sends a fax, within 24/48 hours of delivery, to the Collection Center where the cord was collected communicating whether the same was or was not. Subsequently the gynecological and obstetric staff of the Collection Center will communicate the outcome of the donation to the new mother. Moreover, about 2 months after the birth, the mother will receive a letter sent by the staff of Calabria CBB in which the outcome of the donation is communicated.

From the year 2006 to 2015 in the CBB, 8749 cordonal units were collected, of which 992 were banked and of these 23 were released for transplantation. Most units have been used for conditions such as Acute myeloid leukemia and acute lymphoblastic leukemia. Transplants have occurred in Italy, in Europe and in the USA. Younger patients are aged between 8 months and 2 years; the largest patient is 65 years of age.

Donation for research purposes. When the cord unit is collected, the mother signs the consent of the umbilical cord blood donation for both clinical and research purposes.

Only about 30% of the units collected are valid for conservation and possible use, but no donation is still discarded, in fact the remaining 70% remains the heritage of the National Health Service and is used for the preparation of drugs such as, for example, the platelet gel to treat burns or eye drops to treat traumas of the cornea and conjunctiva or can be used for scientific research.

That said, it is inappropriate to speak of "waste" referring to cord blood, even in the absence of a suitability for transplantation use.

3.1.2 Drugs crossing the placental barrier

It is well documented that many substances, even toxic substances, can cross the placenta and distribute in the fetus. The identification and quantification of substances in umbilical blood are challenging due to the low concentrations in which these are typically present in biological matrices. Many studies report damage in children caused by anesthesia such as respiratory depression, poor fetal positioning and increased fetal heart rate vulnerability.

The placental barrier is constituted by the chorionic villi which are formations located at the level of gaps in which the maternal blood circulates; these villi contain fetal capillaries. In order for substances to pass from maternal blood to fetal blood, they must cross not only the epithelium of the villi, but also the endothelium of the capillaries. The possibility of being able to cross this barrier depends on the time of pregnancy: in the first period is limited, but gradually increase because the fetus needs more nourishment and therefore the exchanges between maternal and fetal blood are more accentuated, thus favoring the passage of other substances, including drugs. The placental barrier is not as selective as the blood-brain barrier, even if at the placental level there are metabolic processes that prevent the passage of some drugs from the mother to the fetus.

The concentration of a drug in the fetus may be different from that of the mother depending on the characteristics of the drug itself. You can have drugs that reach the same concentration in the fetus and in the mother, while there are drugs that in the fetus reach a concentration lower than that of the mother.

There may be a need to administer a drug to the mother in order to have effects on the fetus:

• Antibiotics can be used to fight and prevent intrauterine infections;

• Narcotics antagonists (naloxone) when the mother makes use of narcotic substances;

• An enzyme inducer (phenobarbital) if hyperbilirubinemia is expected;

• Glucocorticoids to accelerate the maturation of the respiratory system and avoid respiratory syndrome.

The molecules cross the placental barrier according to the different known physiological mechanisms: passive diffusion, facilitated diffusion, active transport or endocytosis (as for the rubella virus, IgA, maternal proteins) [5a].

Guillaume Hoizey and his collaborators (2005) [75] have monitored Bupivacaine concentrations in human plasma: after administration of an epidural dose of 1.25 mg / kg, the drug concentration remains constant over time equal to about 250µg / ml. In 2014, Bolat and his collaborators evaluated the passage of Levobupivacaine and Bupivacaine into breast milk and plasma by measuring a concentration of 5.17 µg / ml and 4.79 µg / ml respectively in the two matrices.

In this section of thesis work, our attention was focused on the development of analytical techniques useful for the determination of anesthetic drugs in the cord blood. The main objective was to evaluate the possible modification of the therapeutic protocol currently in use in partoanalgesia, varying the concentrations of Bupivacaine (anesthetic in use) and the timing of administration in relation to the needs and characteristics of individual cases.

One of the key steps of the study was the optimization of a SPE extraction method to guarantee an optimal yield of the eluted product. The eluate samples were initially

analyzed by high performance liquid chromatography with diode array detector and subsequently by gaschromatography with mass detector.

3.1.3 Therapeutic protocols in analgesia

In Italy, during the practice of epidural in natural childbirth, a therapeutic protocol is respected, which can be summarized in the table 5.

Table *5. Therapeutic protocol for epidural anesthesia in natural childbirth.*

TRAVEL STAGE	**CERVICAL EXPANSION**	**INITIAL DOSE (ml)**		**NEXT DOSE (ml)**	
LATENT	< 2cm	ROPIVACAINE 0.1% o BUPIVACAINE 0.0625 % e FENTANYL 30mcg o SUFENTANIL 5mcg	10	ROPIVACAINE 0.1% or BUPIVACAINE 0.0625 % and FENTANYL 20mcg or SUFENTANIL 5mcg	15-20
ACTIVATE PRECOCE	> 2cm	ROPIVACAINE 0.15% o BUPIVACAINE 0.1 % e FENTANYL 20mcg o SUFENTANIL 5mcg	15-20	ROPIVACAINE 0.15% or BUPIVACAINE 0.1 % and FENTANYL 20mcg o SUFENTANIL 5mcg	15-20
				Continuous infusion ROPIVACAINE 0.075% or BUPIVACAINE 0.05% and FENTANEST 2mcg/ml o SUFENTANIL 0.5 mcg/ml	
ACTIVATE LATE	> 6 cm	ROPIVACAINE 0.15-0.2% o BUPIVACAINE 0.1-0.125 % e FENTANYL 20mcg o SUFENTANIL 5mcg	20	ROPIVACAINE 0.15-0.2% or BUPIVACAINE 0.1-0.125 %	10
EXPULSIVE PERIOD		LIDOCAINE 1%	5-10		

In our work, the cord blood samples were collected at the "Bianchi Melacrino Morelli" Hospital of Reggio Calabria; the therapeutic protocol used was the following:

- In case of subarachnoid anesthesia:
  - Hyperbaric Bupivacaine 5 mg/ml
  - Hyperbaric Bupivacaine 7.5 mg/ml
  - Chirocaine 5 mg/ml

- In case of epidural anesthesia for partoanalgesia:
  - Chirocaine 5 mg/ml in combination with Fentanest
- In case of general anesthesia, use:
  - Propofol (general intravenous anesthetic)
  - Nimbex (muscle relaxant).

3.1.4 Experimental

Bupivacaine hydrochloride monohydrate and Ropivacaine (> 98%) was obtained from Sigma Aldrich. HPLC-S grade water, acetonitrile of HPLC-S gradient grade quality and methanol of HPLC quality were acquired from Biosolve (Valkenswaard, The Netherlands). Water purified by reversed osmosis on a multi-laboratory scale was applied for all other purposes than preparing chromatographic eluents. Formic acid (analytical grade) was obtained from Merck (Darmstadt, Germany). Blood samples were supplied by the Calabria Cord Blood Bank of Reggio Calabria.

Samples extraction were made by C-18 silica cartridges.

The HPLC analysis was carried out using an Agilent 1100 Series chromatograph equipped with a Mod. G1312A binary pump, a DAD Mod. G1315B detector and a Mod. G1328B injection system. The chromatographic separation was performed on column C18 110A inverse phase Phenomenex GEMINI, 25.00 x 0.46 cm, packed with particles 5.00 µm. The solvents used have always been degassed by filtration with a Nylon membrane, 0.45 mm porosity, under vacuum.

Drug solutions in the concentration range of 0.002-10.0 µg/ml and real samples were analyzed by GC-MS for the processing of the chromatographic method. The GC/MS analyzes were performed with an Agilent instrument composed of a GC System 6890 N gas chromatograph and a mass spectrometer MSD 5973 N, using a capillary column DB-35MS (35% -difenylpolysiloxane, 1 = 20m, d = 0,18mm, of = 0.18 µm). The transposed gas used is helium with a flow of 1 ml / min. The ion source has an electronic impact (EI).

Sample preparation. Plasma sample (500 µL) was centrifugated at 3000 rpm for 10 min and the surnatant was purified by extraction procedure. At this aim, a solid phase extraction (SPE) method was optimized to recover bupivacaine from the plasma sample. 200 mg C-18 cartridges were activated with 2 mL of phosphate buffer (0.2M, pH=8) and then charged with the plasma samples. Plasma samples was diluted with 1500 µL of phosphate buffer (0.2M, pH=8).

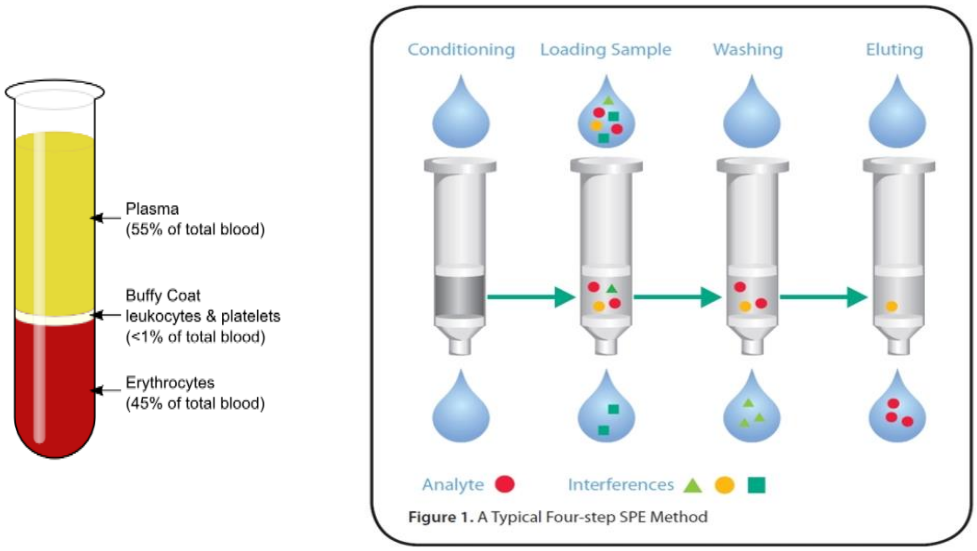

Figure 27 Blood sample preparation

The extraction capacity of the selected SPE cartridges for the determination of the studied compounds was monitored by HPLC.

3.1.5 Results and Discussion

HPLC method. Five solutions of Bupivacaine in the concentration range of 0.002-10.0 µg/ml were analyzed by HPLC by selecting the chromatographic method. Several attempts have been made varying the concentration and the polarity of the solvents chosen as the mobile phase, and also varying the flow rate from 0.5 ml/min to 1 ml/min. The samples were analyzed under different conditions and using different mobile phases consisting of different solvent mixtures:

• Acetonitrile: Phosphate buffer pH 8.0. (90/10, v / v)

• Acetonitrile: Water pH 3.2 (90/10, v / v); (60/40, v / v)

• Methanol: Phosphate buffer pH 8.0 (90/10, v / v); (70/30, v / v)

• Propanol: Water pH 3.2 (60/40, v / v)

• Methanol: Water pH 3.2 (60/40, v / v)

The following chromatographic conditions was set:

• Isocratic mobile phase methanol: water at pH 3.2 (60/40, v / v),

• Flow 0.5 ml / min,

• Injection volume 5 µl.

• λ 210 nm

As shown in the chromatogram in Figure 28, Bupivacaine has a retention time of 16.245 min.

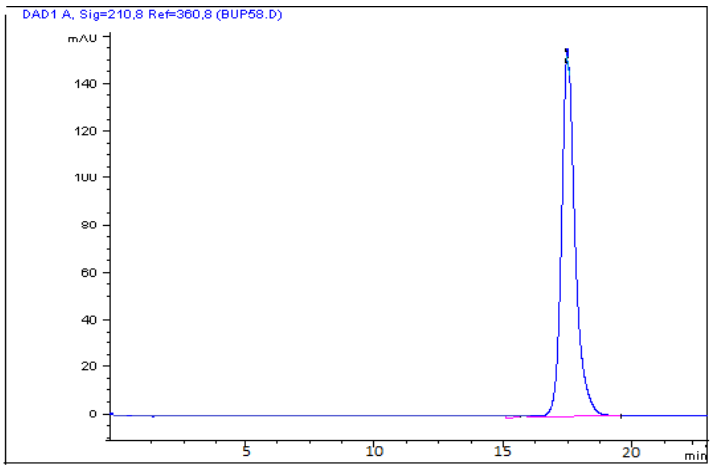

Figure 28. HPLC-DAD Chromatogram of Bupivacaine

Solid phase extraction. Several methods of extraction, both in liquid and solid phase, of cord blood plasma are reported in the literature. In the work of Lars I. Andersson (2000) [75] a solid-phase extraction method on C18-silica cartridge was developed to

extract Bupivacaine from human plasma. Columns C18 have been activated with 1 ml of hydrochloric acid (HCl) 1M, 2 ml methanol, 1 ml of water. Hans Onnerund, Fatma Bassiouny and Mohamed Abdel-Rehim [76] evaluated a further solid phase extraction technique for the determination of Bupivacaine and its human plasma metabolites. The total volume obtained from sample preparation was used for solid phase extraction with an automated procedure:

- Conditioning: 500µl of methanol and 500µl of buffer pH 8.0.
- Loading: 1 ml of drug
- Washing: buffer (pH 8.0) -methanol (1: 1, v / v) 1 ml.
- Elution: 1 ml of methanol.

In accordance with the techniques reported in the literature, a solid phase extraction strategy for Bupivacaine was optimized. Firstly, the ability of the cartridges to hold the drug was tested for the samples containing the drug only. Several SPE cartridges were used. The best results were obtained with SPE cartridges octadenyl silane (C18).

The extraction technique used was as follows:

• Conditioning: 2 ml of phosphate buffer pH 8.0

• Loading: 1 ml of bupivacaine water solution, 1 ml of phosphate buffer at pH 8.0

• Washing: 2 ml of water

• Elution: 2 ml of methanol.

Bupivacaine solutions at different concentrations in the range 5.0-30.0 g/ml were analyzed by HPLC.

Samples of cord blood, originating from natural delivery in the absence of analgesia, were then treated appropriately by centrifugation at 1300 rpm for 5 min and extraction. 100 µl of bupivacaine aqueous solution in the concentration range 1.0-150 µg/ml were added to the centrifuged plasma and the sample thus prepared was loaded into a cartridge as detailed below:

• Conditioning: 2 ml of phosphate buffer pH 8.0

• Loading: 500 µl of plasma, 100 µl of bupivacaine in water and 1.5 ml of phosphate buffer at pH 8.0 (Figure 29a)

• Washing: 2 ml of water (Figure 29b)

• Elution: 2 ml of methanol (Figure 29c).

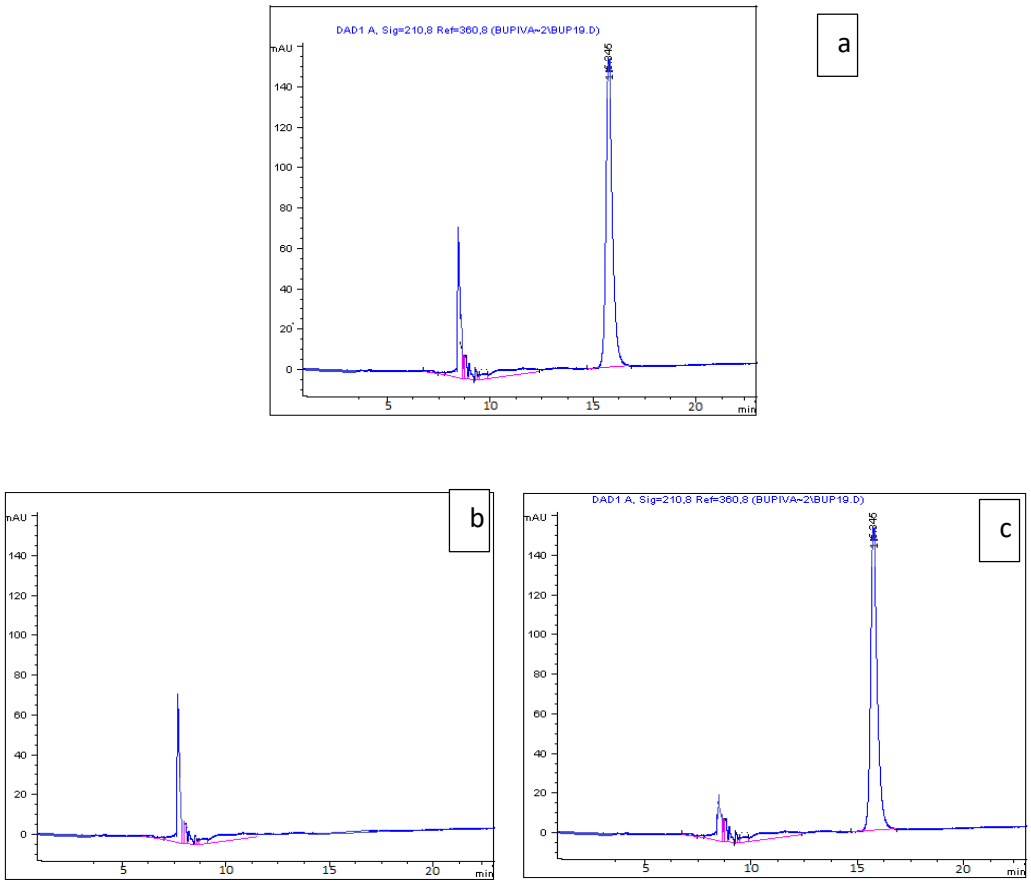

Figura 29 a-c Cromatograms of Pre-loading (a), washing (b) and elution (c) of Bupivacaine in SPE extraction

GC-MS method. Samples of bupivacaine in the range of 0.002-2.128 µg/ml were also assayed by GC/MS. The analyses were processed in splitless mode (splitless time = 1 min). GC/MS analysis was performed using the following chromatographic column temperature program:

• 70 °C for 2 minutes;

• Increase of 20 °C per minute up to 280 °C;

• 280 °C for 10 min.

Mass spectra were recorded in full-scan mode (total scan) as shown in Figure 30b. Mass fragmentation corresponding to the peak recorded for Bupivacaine at 12.62 min is shown in Figure 30a.

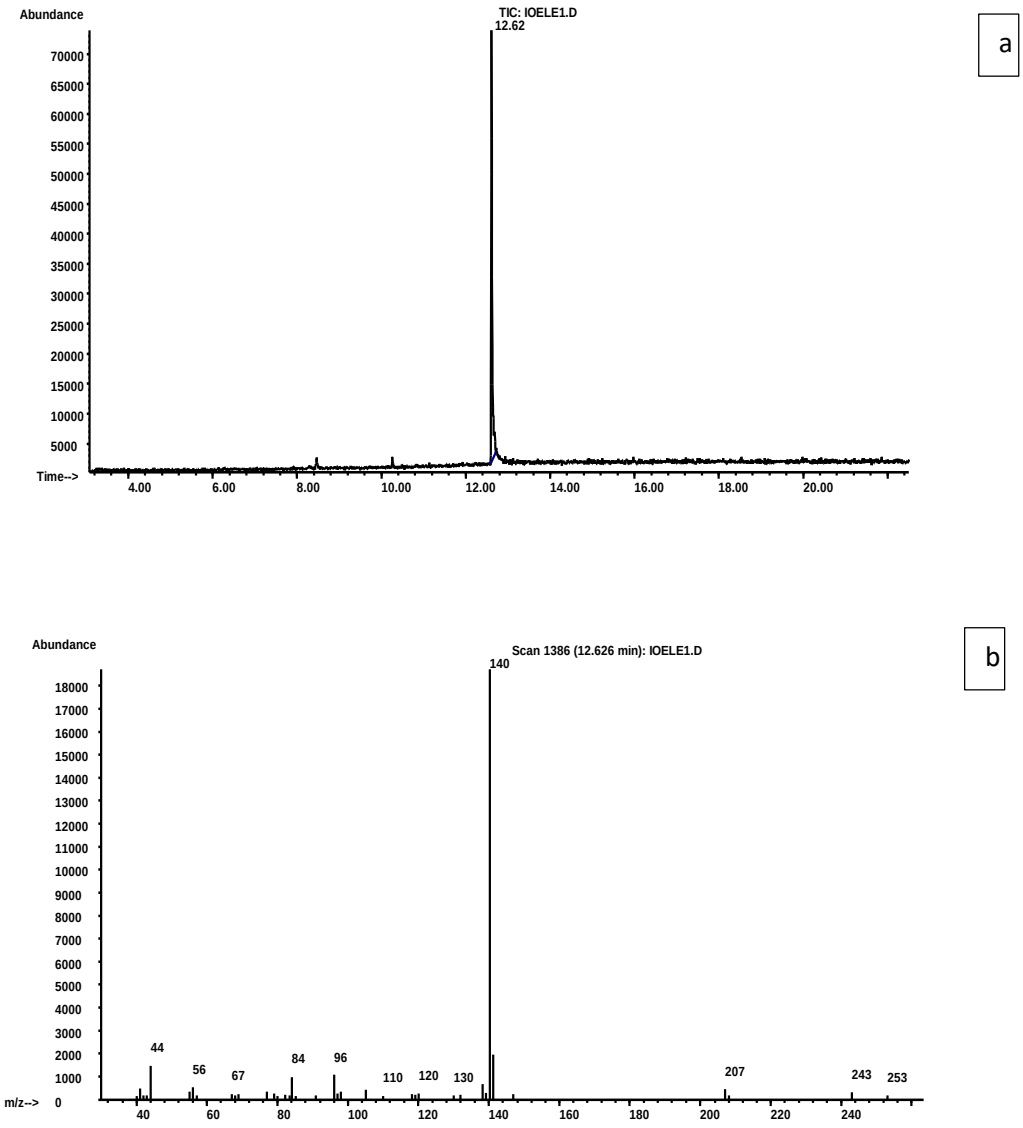

Figura 30 a-b. Chromatogram (a) and mass spectrum (b) of Bupivacaine

Limit of detection (LOD) was calculated to be 21.8 µg/ml.

Cromatographic conditions were further optimized as follow:

• Increase of 20 °C per minute up to 250 °C;

• 250 °C for 10 minutes.

Mass spectra were recorded in SIM mode ("selected ion monitoring"). In SIM mode the scan affects not the entire mass range considered, but only some characteristic ions of the analyte to be determined, as shown in Figure 31.

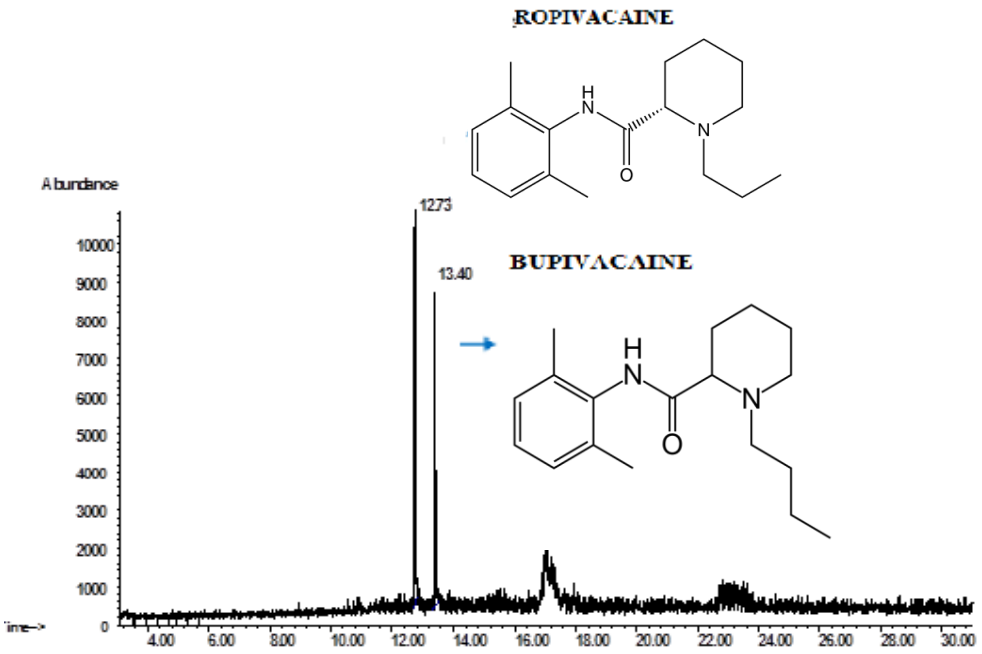

Figure 31. GC-MS Spectra of mixture of Bupivacaine (200 µg/ml) and Ropivacaine (212 µg/ml).

In these conditions, the most abundant ions were monitored, in particular the ion m/z = 126 (mass/charge ratio) for Ropivacaine used as internal standard in the concentration of 0.5 µg/ml and m/z = 140 for Bupivacaine (Figure 32).

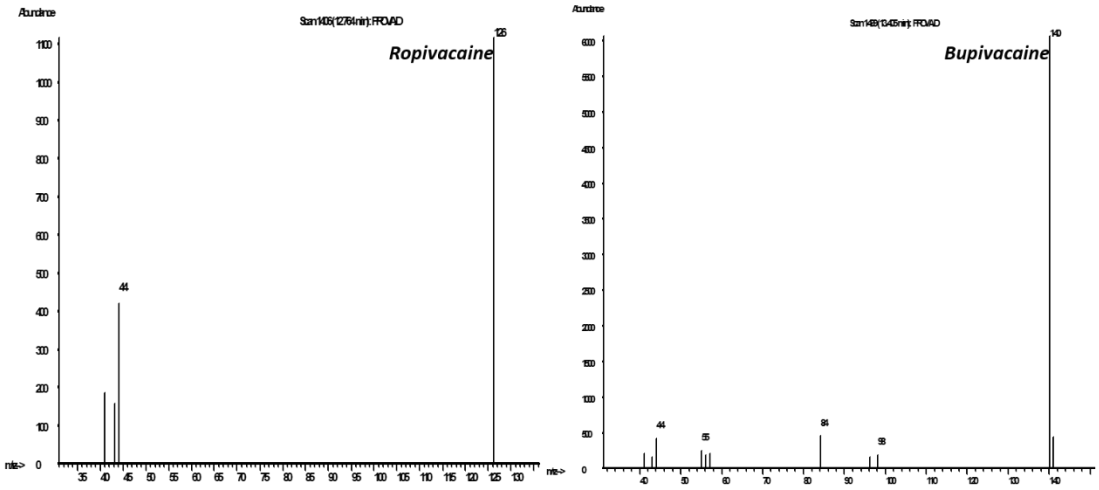

Figure 32. Mass spectrum of Ropivacaine and Bupivacaine.

Plasma samples spiked with the drugs were assayed by GC/MS after extraction procedure. 100 µl of Ropivacaine standards in concentration of 0.5 µg/ml were added to the sample, while the concentration of Bupivacaine was varied in the range 0.002-21.8 µg / ml.

The detection limit of the instrument was calculated to be 50 ng/ml for Bupivacaine.

The same chromatographic method was also applied to monitore the concentration of other two analgesic drugs used in therapeutic protocols: fentanyl and sufentanil. The mass spectra of two analytes were shown in fig. 33.

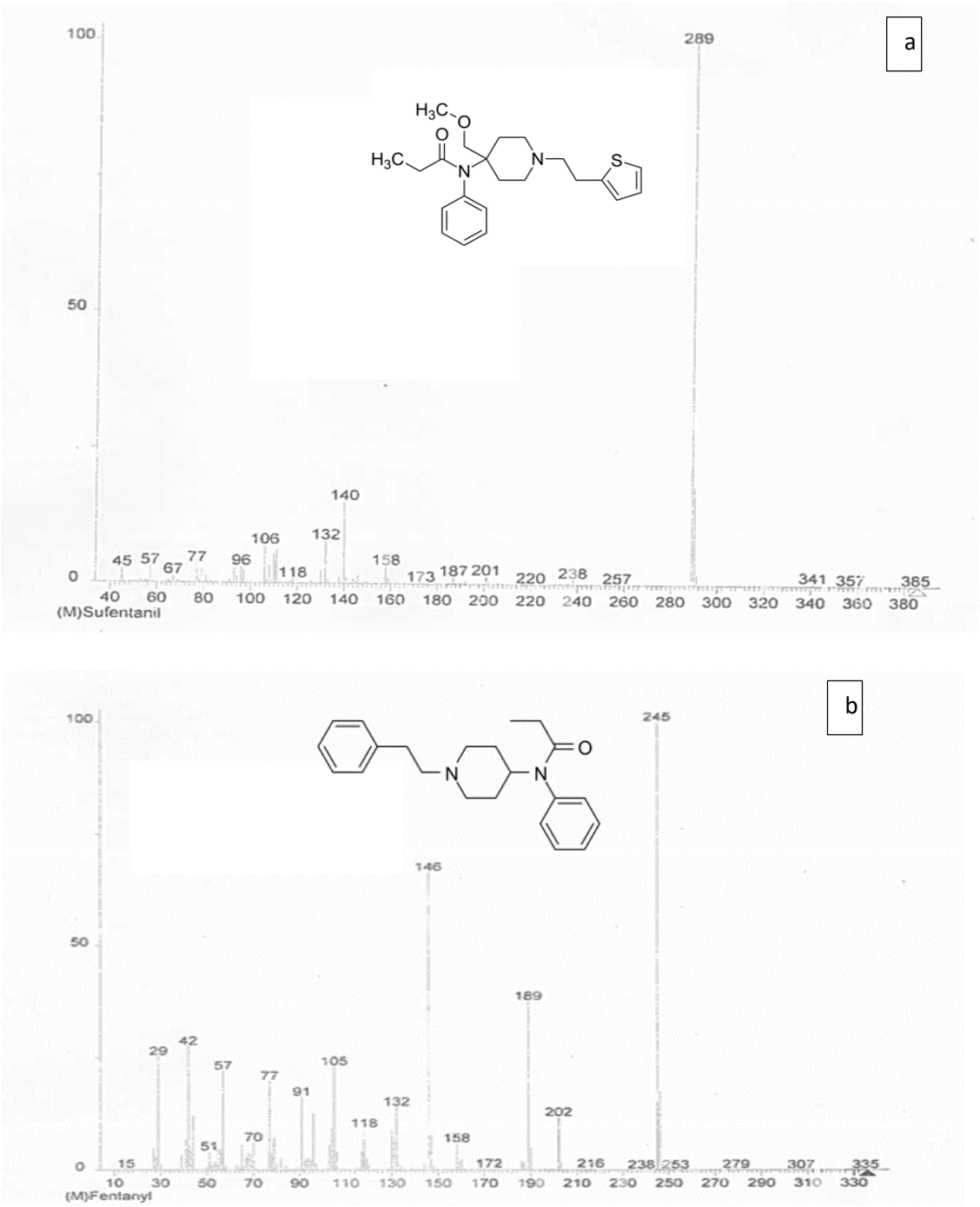

Figure 33. Mass spectrum of Sufentanil (a) and Fentanyl (b).

100 µl of Fentanyl and Sufentanil standards in concentration of 50 µg/ml were added to the plasma sample.

In the following pictures there are preliminary analysis on blood samples both in full scan and sim scan. In particular, the ratio m/z= 289 for sufentanil and m/z=245 for fentanyl, were considered.

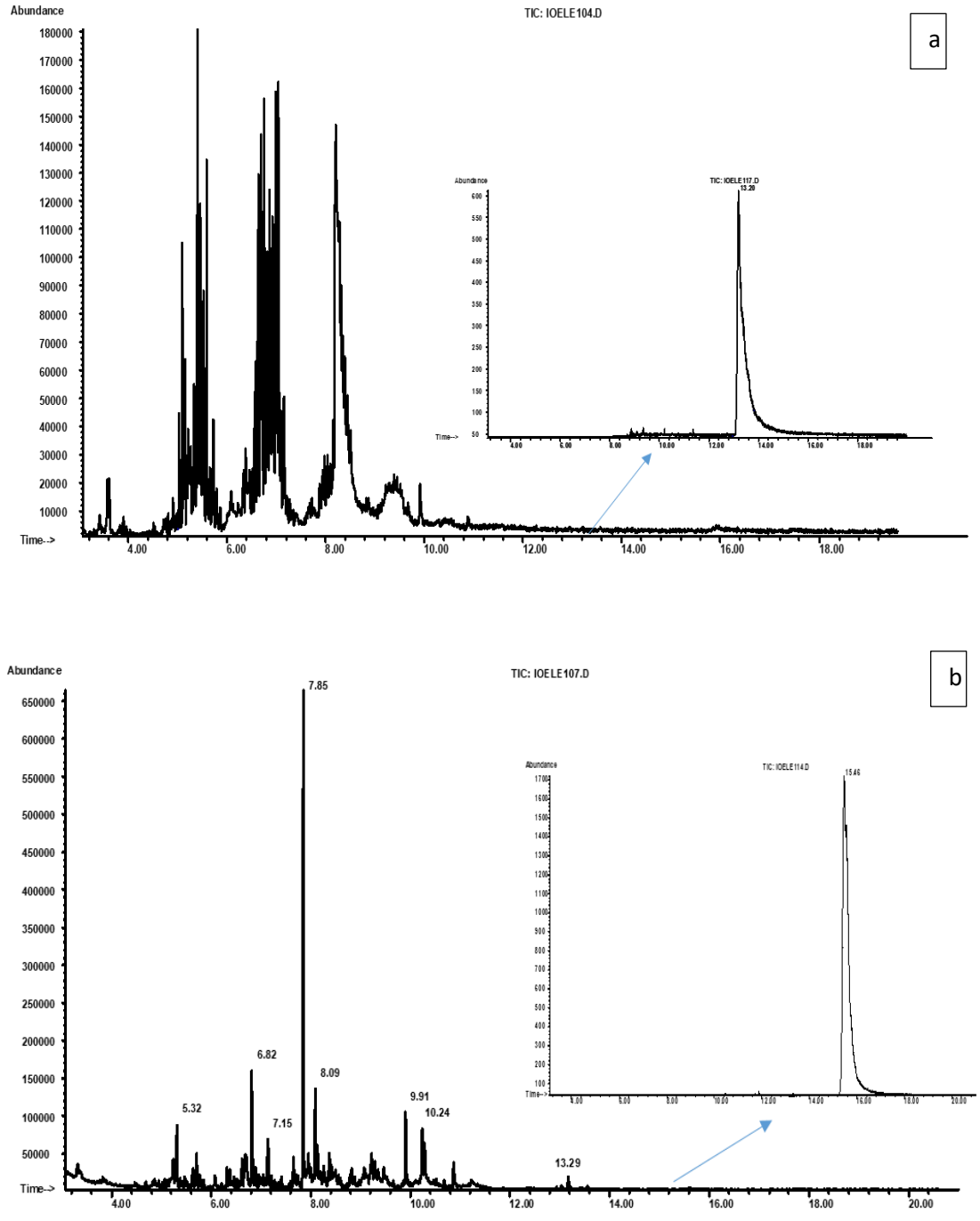

Figure. 34 Premilinary analysis of Sufentanil (a) and Fentanyl (b) on human blood sample.

The elaborated method was then applied to real samples. Figure 35 shows a chromatogram of a cord blond sample from mother subjected to analgesic treatment (Bupivacaine 0.1%) during active phase of labor. Bupivacaine was detected in a very low concentration, demonstrating so the health safety for the children when using the analgesia during labor.

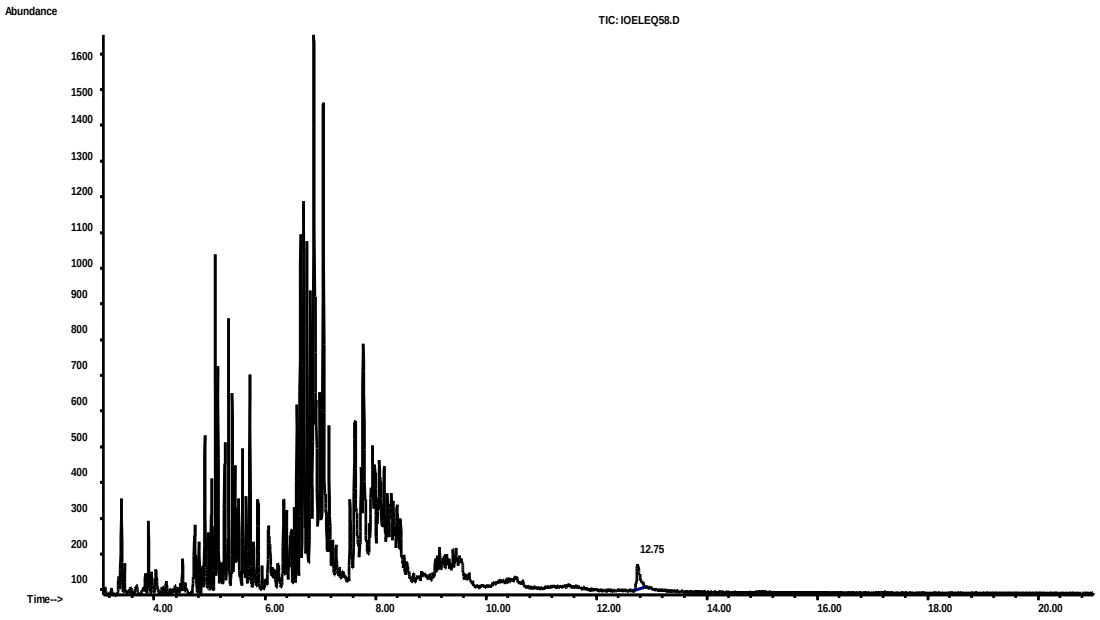

Figure 35. Analysis on real cord blood samples.

In this period, we have collected a large number of real samples in order to detect the bupivacaine concentration in the blood in different conditions during a natural labor.

Samples containing other drugs used in the therapeutic protocol in partoanalgesia, as fentanyl and sufentanil, will be also tested with the same chromatographic technique, in order to verify the safety of these analgesic drugs.

ANALYSIS OF BIOLOGICAL MATRICES

3.2 Bioanalytical assay for quantification of lorlatinib in mouse plasma

The following work has been developed at the University of Utrecht, the Netherlands under the supervision of prof. Sparidans.

The anaplastic lymphoma kinase (ALK) protein, encoded by the ALK gene, represents a clinical target in adult cancers in which the ALK domain is fused to an array of amino-terminal partners, such as the echinoderm microtubule-associated protein-like 4 (EML4) [78]in non -small cell lung cancer (NSCLC) [79] or nucleophosmin (NPM)[80]in anaplastic large cell lymphoma (ALCL). Its structure is similar to other receptor tyrosine kinases with an extracellular domain, a transmembrane segment and a cytoplasmatic receptor segment [81]. Subsequently more mutations of the ALK gene were described in many cancers such as inflammatory myofibroblastic tumors, diffuse large B cell lymphoma, colon cancer, renal cell carcinoma, breast carcinoma, esophageal cancer, and neuroblastoma [82].

The EML4-ALK oncogene was first described in 2007 when in a subset (7%) of Japanese patients was noted the fusion of ALK with the partner gene-echinoderm microtubule-associated protein-like 4 (EML4) [83,84]. Since EML4-ALK was recognized as an attractive drug target, a relevant number of ALK inhibitors have been developed and several are now approved for use in patients with NSCLC harboring ALK fusions. In order to support clinical studies, it is also necessary to develop bio-analytical assays that are able to monitor the concentration of these drugs in different biological matrices.

Liquid chromatography-tandem mass spectrometer assays of crizotinib [85], as the first generation of ALK inhibitor, and of ceritinib [86], as the second generation of ALK inhibitors, were already described for mouse and human plasma [87-89].

Since second generation of ALK inhibitors can cause tumor relapse and brain metastases [90], an alternative second-generation of ALK inhibitors are currently in

development, each affecting different crizotinib-resistance ALK target mutations [91]. Lorlatinib (PF-06463922) (fig.36) is an orally available ATP-competitive selective inhibitor of ALK and ROS1 and it belongs to the third generation of ALK inhibitors.

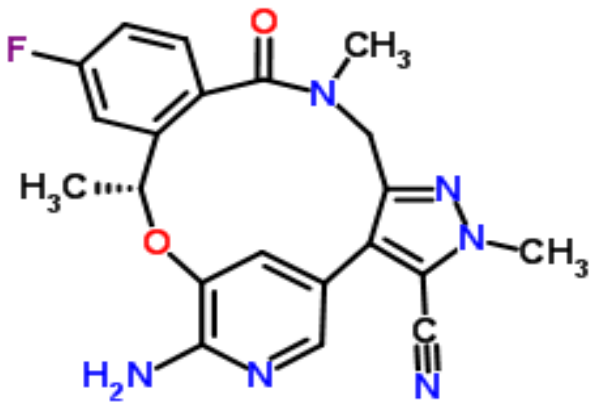

Figure 36. Chemical strucuture of Lorlatinib

It was reported that it has an excellent activity against both EML4-ALK as well as mutant EML4-ALK resistant forms identified in patients treated with crizotinib [92,93]. The oral availability and pharmacokinetic-pharmacodynamics of lorlatinib was studied in preclinical lung cancer. Plasma concentration of lorlatinib was determined by an LC-MS/MS method after protein precipitation of plasma samples and a naïve-pooled pharmacokinetic analysis was used to determine pharmacokinetic parameters of lorlatinib in mice [94–96]. Further, a preclinical study of lorlatinib demonstrated an increased potency against acquired NSCLC- ALK resistance mutations and was proven to be active in crizotinib resistant both in vitro and xenograft models [97-99].

Currently, lorlatinib is in phase 1/2 clinical trials for treatment of ALK-driven cancer [100]. The most interesting evidence was that a patient, after enrolling in this trial, was resensitizied to crizotinib after the patient failed the lorlatinib treatment, indicating that retreatment under molecular guidance can be an excellent clinical approach. In spite of this clinical evidence, in literature there are no significant tracks

about lorlatinib's metabolites and no validated bio-analytical assays were described yet for this drug.

In this work a fast and sensitive bio-analytical assay for mouse plasma was set up using LC-MS/MS. This method uses a simple protein precipitation step followed by LC-MS/MS analysis and it could be used for application in both human and mouse plasma.

3.2.1 Experimental

Lorlatinib (> 99.9%) was obtained from TargetMol (Boston, USA) and rucaparib (phosphate salt,>98.5%) from Sequoia Research Products (Pangbourne, UK). LC–MS grade water, acetonitrile of HPLC-S gradient grade quality and methanol of HPLC quality and were acquired from Biosolve (Valkenswaard, The Netherlands). Water purified by reversed osmosis on a multi-laboratory scale was applied for all other purposes than preparing chromatographic eluents. Formic acid (analytical grade) was obtained from Merck (Darmstadt, Germany). Lithium-heparinized plasma (pooled from humans and mice) and plasma of six single mice was obtained from Sera Laboratories (Haywards Heath, West Sussex, UK).

The Shimadzu (Kyoto, Japan) chromatographic system was build up from a DGU-14A degasser, two LC10-ADvp-µ pumps, a Sil-HTc autosampler and a CTO-10Avp column oven. Prepared samples were injected (5 µL) on a Varian Polaris C18-A (50×2.0 mm, 3 µm, Varian, Middelburg, The Netherlands), protected by an Agilent Polaris C18-A

Chromsep guard cartridge (10×2.0 mm, 3 µm, Agilent, Santa Clara, USA). The auto injector rack was maintained at 4 °C and the column oven at 40 °C. For the binary gradient, 0.1% (v/v) formic acid in water (A) and methanol (B) were mixed to obtain a total flow rate of 0.5 mL/min. After injection, 20% B was increased linearly to 45% in 1.2 min followed by flushing with 100% B for 0.3 min and equilibration of the column at the initial 20% B for 1.5 min until starting the following injection. The eluate was transferred to the electrospray nebulizer from 0.6 until 2.5 min after injection by switching the MS inlet valve. A TSQ Quantum Discovery Max quadrupole mass

spectrometer (Thermo Fisher Scientific, San Jose, CA, USA) was used for ionization, ion separation and detection. The Thermo Fisher Xcalibur software (Version 2.0.7 SP1) was used for data collection and control of the mass spectrometer.

Positive electrospray ionization was optimized by introducing 0.5 mL/min of a mixture of methanol and 0.1% v/v formic acid in water (50/50, v/v) and mixing the solvent mixture with 5 µg/mL lorlatinib at 5 µL/min. Settings with the highest response were used for monitoring both compounds: 4000 V spray voltage; 400 °C capillary temperature; nitrogen gas settings (arbitrary units) were 60 for sheath, 8 for ion sweep and 10 for the auxiliary gas; the skimmer voltage was set off (0 V); the argon collision gas pressure in SRM mode was 1.5 mTorr. The tube lens off-set was 113 V for lorlatinib and 92 V for rucaparib.

Lorlatinib was monitored at m/z 407.1→121, 180.1, 200.1 and 228.1 at respectively −41, −23, −26 and −23 V collision energies and rucaparib at m/z 324→293 at −17 V collision energy, all with 0.1 s dwell times. Both separating quadrupoles were set at m/z 0.7 mass resolution.

Calibration standards and quality control samples. Stock solutions were prepared in methanol at 250,000 ng/mL for calibration and at 500,000 ng/mL lorlatinib solution for quality control (QCs) samples. The highest calibration solution at 2000 ng/mL was made by diluting the 250,000 ng/mL stock solution in blank mouse plasma; it was stored in polypropylene tubes at −30 °C until further use. Additional calibration solutions were produced by diluting the highest calibration solution to 1000; 200; 100; 20; 10 and 2 ng/mL with blank mouse plasma. The 500,000 ng/mL lorlatinib stock solution was used to produce QC samples at 1500 (high), 75 (medium), 5 (low) and 2 (lower limit of quantitation, LLOQ) ng/ml by serial dilution with blank mouse plasma. QCs were also stored at −30 °C until further use.

Sample preparation. 10 µL of plasma was pipetted into a 1.5-ml polypropylene (PP) reaction tube. After addition of 20 µL of 200 ng/mL IS solution, 200 ng/ml rucaparib in acetonitrile, proteins were precipitated by vortex mixing vigorously for approximately 5 s. Centrifugation at 12000×g for 5 min at 10 °C resulted in a clear supernatant of which 20 µL was transferred to a 1.5 mL vial with a 250 µL glass micro-

insert. The vial was closed after addition of 100 µL water and placed in the autosampler for injectionof 5 µL of the final mixture.

Bioanalytical method validation. International guidelines EMA [101] and FDA [102] were used to obtain validation procedures for this bioanalytical assay. All calibration samples were pretreated in duplicate for each daily calibration. The calibration curve was constructed using weighted ($1/x^2$; x is the concentration of analyte) linear regression and data were calculated from the peak area of the analyte relative to the IS. Analytical performance (within- and between-day) was calculated after six-fold analysis of each QC in three analytical runs on separate days for all four QC samples (total: n=18 per QC). In addition, dilution integrity was tested on one day (n=6) at 4000 ng/ml lorlatinib after 5- fold dilution of 10 µL of mouse plasma with human plasma.

Individual mouse plasma samples (n=6) were investigated for the selectivity of the assay. Each sample was analyzed as double blank (no lorlatinib, no IS), blank (no lorlatinib, with IS) and LLOQ spiked (2 ng/ (2 ng/mL; n=6) were 1.80 ± 0.19 ng/mL showing the allowance of the tested LLOQ level.

The extraction recovery of the protein precipitation was determined at each QC level (high, medium, low) by comparing processed samples (n=4) with equivalent solutions of lorlatinib in blank plasma extracts. For assessment of the (absolute) matrix effect, an experiment was conducted in which lorlatinib and IS were both infused (5 µg/mL, 5 µL/min) post-column and mixed with the eluate during chromatographic runs, in which diluted blank extracts (n=6) of individual plasma samples were injected on the column, without using the divert valve. Further, the relative matrix effect for lorlatinib and rucaparib was determined by comparing the responses in an extracted plasma sample of six individual donors to reference solutions at high and low QC levels.

The plasma stability of lorlatinib was investigated for QC-high and -low samples stored in separate portions (10 µL; n=4). These portions in polypropylene tubes were exposed to three different conditions in three separate experiments: room temperature for 6 h, three freezethaw cycles (thawing at room temperature and

freezing again at−30 °C for at least 12 h) and−30 °C for two months. For autosampler stability, an analytical run was re-injected after additional storage of the diluted extracts at 4 °C for 24 h. Finally, stability in methanolic stock solutions was investigated after 6 h exposure to ambient temperature and after 30weeks storage at −30 °C (n=3) by comparison to freshly prepared stocks. LC–MS/MS analysis was used after sufficient dilution of the stock solutions with 25% (v/v) methanol and adding IS.

Pharmacokinetics in mice. A pharmacokinetic pilot study in wild type female mice (FVB/NRj genetic background) receiving 10 mg/kg lorlatinib orally (n=7) was conducted. Lorlatinib was dissolved in dimethyl sulfoxide (50 mg/mL), followed by 2.5-fold dilution with polysorbate 80/ethanol (1:1, v/v), and then 20-fold with 5% glucose in water to yield a drug working solution of 1 mg/mL, prepared freshly on each day of experiment. Mice were housed and handled according to institutional guidelines complying with Dutch legislation and treated similar to earlier reported protocols [103]. Shortly, mice were 10 to 14 weeks of age and housed in a temperature-controlled environment with a 12-h light/12-h dark cycle.

Animals received a standard diet and acidified water ad libitum and were fasted for 3 h before lorlatinib was administered by gavage into the stomach, using a blunt-ended needle. At 0.5, 1, 2, 4, and 8 h after administration, blood was collected from the tail vein in heparinized capillary tubes (Sarstedt, Germany). Mice were anesthetized with isoflurane after 24 h and a final blood sample was acquired by cardiac puncture. The pilot study was followed by similar studies in male mice for 8 h (n=5, sampling at 0.25, 0.5, 1, 2, 4, and 8 h) and 2 h (n=6, sampling at 0.125, 0.25, 0.25, 1, and 2 h). Plasma was obtained by centrifugation at 9000×g for 6 min at 4 °C and stored at −30 °C until analysis. The mouse plasma samples from t=0.5–8 h were diluted 5times with human lithium heparin plasma.

Incurred samples reanalysis was conducted for 20 of the diluted female mouse samples.The following pharmacokinetic parameters were assessed in female mice: maximum plasma concentration (Cmax), time to reach maximum plasma concentration (tmax), terminal half-life (t1/2) calculated from C8 and C24, area under

the plasma concentration-time curve until 2 h, 8 h, 24 h, and until infinity (AUC0→2, AUC0→8,AUC0→24 and AUC0→∞)calculated using the trapezoidal rule and extrapolation from 24 h to infinity. Finally, apparent clearance (Cl/F), apparent volume of distribution (Vd/F) and absorption rate (ka) were computed using the first order one-compartment model. For male mice, Cmax, tmax, AUC0→2, and AUC0→8 were calculated. These parameters were compared to female results by a two-sided unpaired heteroscedastic Student's t-test after dose correction using the measured drug concentration in the administered working solutions for the three different studies.

3.2.2 Results and Discussion

The plasma samples were prepared by protein precipitation usually used for the development of the bioanalytical kinase inhibitor assay [104]. Compared to solid or liquid phase extraction, this procedure is easier because the use of acetonitrile as a precipitating agent greatly reduces the sample dilution of the already small sample. Rucaparib was chosen as the internal standard because it demonstrated greater accuracy than dabrafenib or AT7519 used during the preliminary validation phase of the method. Initially, a procedure already present in the literature for the quantification of rucaparib was followed [105]. Afterwards, after having optimized the chromatographic conditions by varying the ratio of the solvents (acetontrile and methanol) the quantity of formic acid and evaluating the shape of the chromatograms, positive mode for ESI–MS/MS was selected atm/z 407.1 for lorlatinib and m/z 324.1 for rucaparib. Furthermore, the sum of the four most abundant dissociation products was measured for lorlatinib (m/z 121; 180.1; 200.1; 228.1) to improve instrument sensitivity. A product spectrum of lorlatinib is shown in Fig. 37.

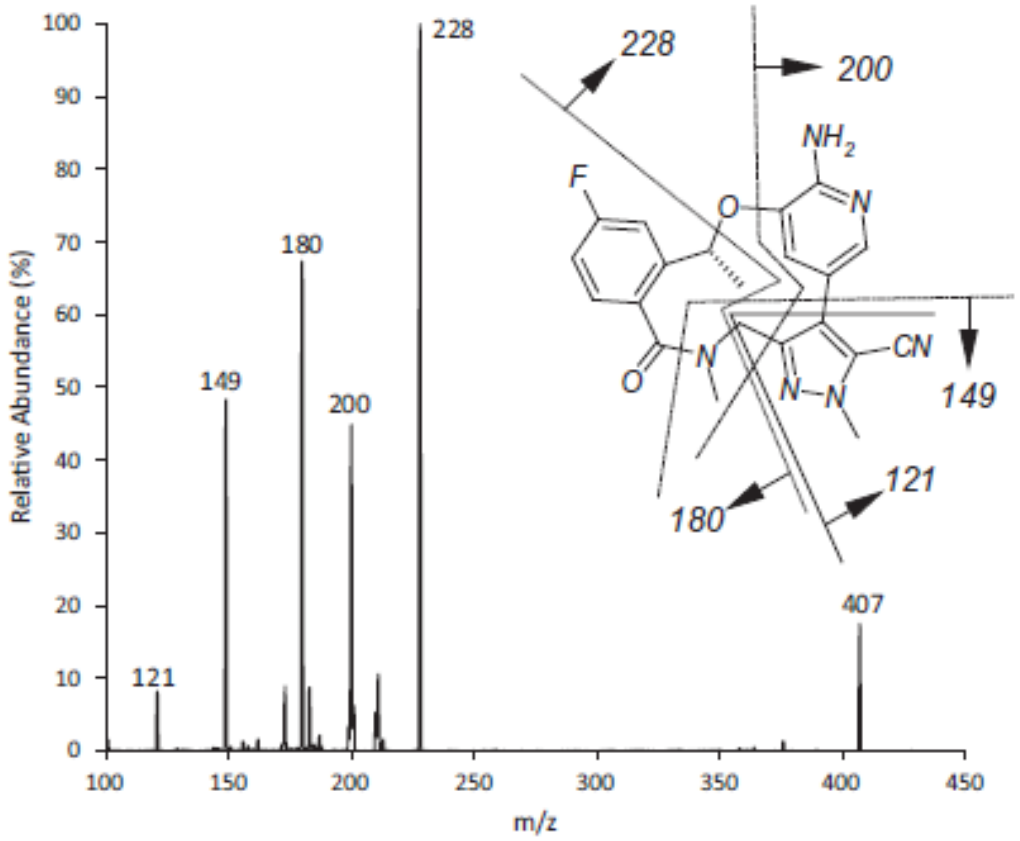

Figure 37. Chemical structure and product spectrum formed by collision induced dissociation of the protonated molecule of lorlatinib, m/z 407.1@−25 V.

A laboratory scheme based on international guidelines, published by the EMA [101] and FDA [102] was used for the validation procedures.

On the basis of a previous pharmacokinetic and pharmacodynamic (PKPD) study of lorlatinib in mouse [95,96], a 2–2000 ng/mL range was investigated during validation According to accepted guidelines [101,102]. In Fig. 38 there are representative chromatograms of analyte and IS in mouse plasma.

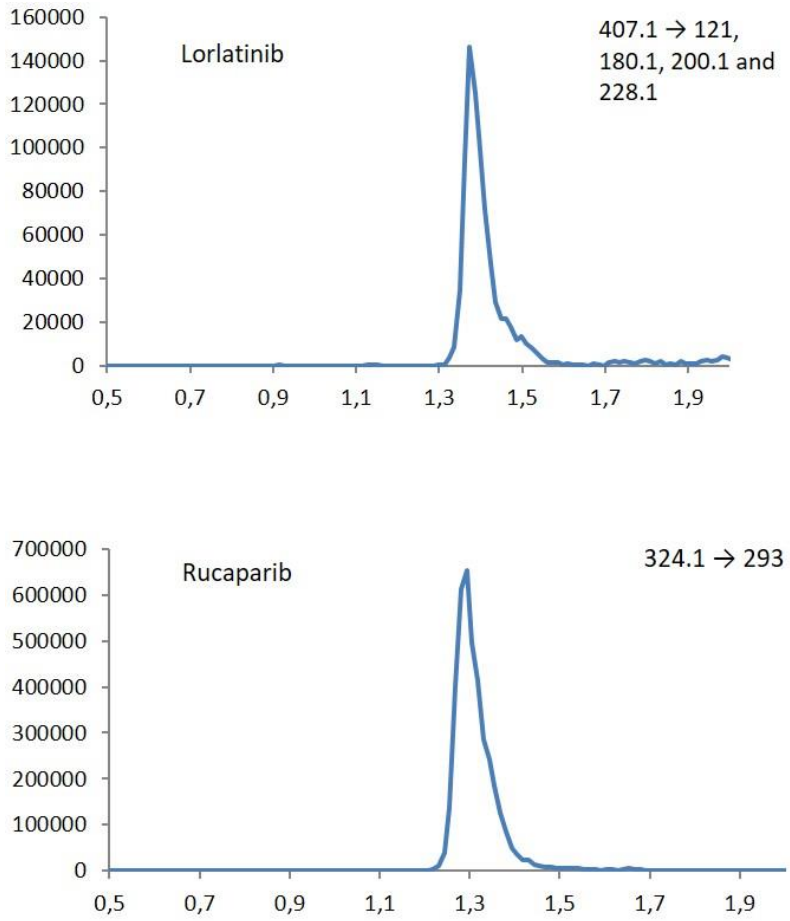

Figure 38. Chromatograms of rucaparib (IS) lorlatinib in mouse plasma. Concentration of internal standard is 200 ng/ml, while lorlatinib concentration is 20 ng/ml.

Calibration curves were built (n=8), with an average coefficient of determination (R^2) of 0.993 ± 0.002 (n=8) and the the linear function was described by *Y=0.0111(±0.0025) ×X+0.0016(±0.0017)* for lorlatinib (mean ± SD) where Y is the ratio of the analyte and IS response and X the concentration in ng/mL.

Table 6 shows Assay performance data of the assay in mouse plasma. According to EMA [101] and FDA [102] rules, precisions and accuracies of three analytical runs were within±15% for high, medium and low QCs and within±20% for LLOQ. To test dilution integrity at 4000 ng/mL (n=6) precision results 4.3% and accuracy 96.8 as suggesting international guidelines.

Table 6. Assay performance data of lorlatinib resulting from four validations (QC, n=18 each) samples in 3 analytical runs (n=6).

Level (ng/ml)	Within-day precision[%]	Between-day precision[%]	Accuracy[%]
1500	10.4	12.2	99.0
75	8.0	12.0	109.5
5	9.0	10.0	113.3
2	11.6	15.0	108.8

Selectivity was in line with international rules because blank lorlatinib responses were all<20% of the LLOQ [101] and blank IS responses were all<1% of the regular response. Concentrations calculated at the LLOQ spiked samples (2 ng/mL; n=6) were 1.80 ± 0.19 ng/mL showing the allowance of the tested LLOQ level [102].

The values of recoveries (n=4) ,115.8 ± 9.2%, 118.9 ± 4.9% and 117.9 ± 3.1% at the respectively QC-high, -medium and -low levels, were high because protein precipitation lead to a volume reduction. The absolute matrix effect, tested by infusion experiments, was no relevant in each individual mouse plasma analyzed in time range from 1 to 1.5 min. In the same way, the relative matrix effect (IS normalized matrix factor, n=6) respects guidelines's rules (92.2 ± 9.9% and 88.4 ± 6.4% at the high and low QC levels) and above all the standard variations of these IS-normalized MF calculated from the 6 lots of matrix were within±15%.

The stability parameters of lorlatinib in lithium heparin mouse plasma are listed in Table 7. The results obtained demonstrates that lorlatinib, according to EMA and FDA guidelines can be considered stable in methanolic stocks.

Table 7. Stability data (recovery (%); ± SD; n=4) of lorlatinib in mouse lithium heparin plasma

Storage conditions	QC-high	QC-low
3 freeze-thaw cycles	106.2±8.8	98.9±10.2
6 h at ambient temperature	99.0±4.9	87.1±7.9
2 months at -30°C	99.0±4.5	98.2±11.1

Pharmacokinetics in mice. In conclusion, pharmacokinetic pharmacokinetic plots for seven female mice are shown in Fig. 39 and parameters were calculated and collected in table 8.

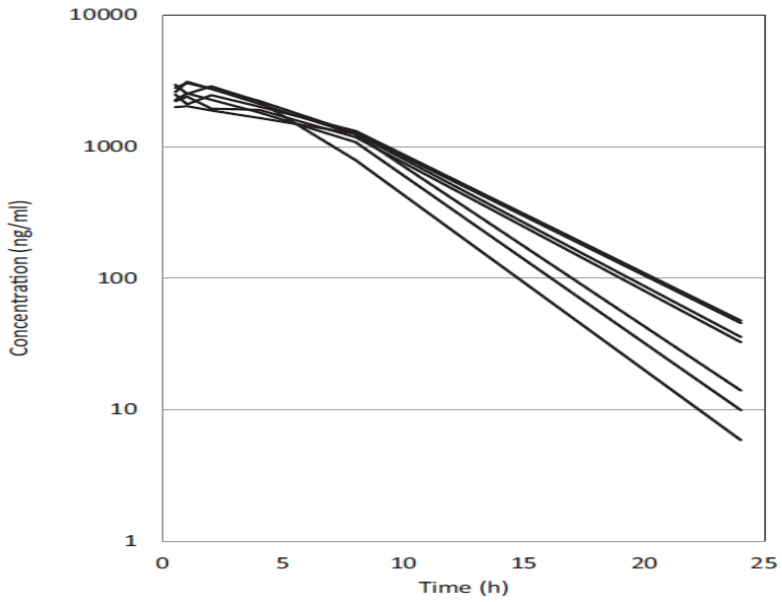

Figure 39. Pharmacokinetic plots of lorlatinib in plasma after administration of 10 mg/kg orally to female FVB/NRj mice (n=7).

Table 8. Pharmacokinetic parameters of lorlatinib in plasma after administration of 10 mg/kg

PHARMACOKINETIC PARAMETERS	
t_{max} *(h)*	0.86 ± 0.24
C_{max} *(ng/ml)*	2651 ± 398
$t_{1/2}$*(h)*	2.9 ± 0.5
$AUC_{0\rightarrow 24}$ ($ng \cdot h \cdot ml^{-1}$)	24,534 ± 2123
$AUC_{0\rightarrow \infty}$($ng \cdot h \cdot ml^{-1}$)	24,656 ± 2173
Cl/F ($ml \cdot h^{-1} \cdot kg^{-1}$)	408 ± 35
Vd/F (ml/kg)	1670 ± 233
ka (h^{-1})	0.44 ± 0.11

Compared to a previous oral study in implanted female athymic nu/nu mice [95], some parameters such as Cl/F Vd/F and ka are respectively 3–4 times lower, 3–6 times smaller 3–9 times slower in the present study and the reason of these differences could be associated with mouse strain, drug formulation, fasting state, lab-specific microflora, and commercial chew, either alone or in combination. Comparison between male and female mice is shown in Table 9. There is only a small difference so we can affirm that lorlatinib oral pharmacokinetics is not affected by gender's mice.

Table 9. Comparison of pharmacokinetic data of male and female mice after dose correction using the measured drug concentration in the administered working solutions.

Pk parameters	**Male**	**Female (n=7)**	**P**
Cmax	2272 ± 351 (n=11)	2637 ± 396	0.07
tmax	0.91 ± 0.58 (n=11)	0.86 ± 0.24	0.8
$AUC_{0\rightarrow 2}$	3922 ± 685 (n=11)	2 4320 ± 612	0.22
$AUC_{0\rightarrow 8}$	12,948 ± 5423 (n=5)	14,965 ± 1531	0.038

4. ANALYSIS OF PHARMACEUTICAL MATRICES

4.1 A new generation of dihydropyridines: photodegradation and photostabilization strategies.

1,4-dihydropyridines (DHPs) (Fig.40) are calcium antagonist drugs, able to interact with the calcium channels present on the myocardium and on the vascular smooth muscle, therefore they are used in the treatment of disorders and diseases of the cardiovascular system, such as the angina pectoris, hypertension and cardiac arrhythmias. Thanks to their abilty to cross the blood-brain barrier, they can also be used to reduce brain blood pressure. However, they prefer calcium channels located in the arterial smooth muscle, for which they mainly exert a vasodilatory action and are particularly indicated in the treatment of arterial hypertension [105]. At the same time, they present reduction of side effects, as headache, excessive hypotension, edema and tachycardia.

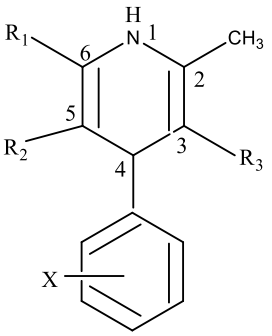

Compounds	R_1	R_2	R_3	X
Amlodipine	$CH_2O(CH_2)_2NH_2$	$CO_2CH_2CH_3$	CO_2CH_3	2-Cl
Felodipine	CH_3	$CO_2CH_2CH_3$	CO_2CH_3	2,3-Cl_2
Nicardipine	CH_3	$CO(CH)_2$-N-CH_3 H_2C-C_6H_5	CO_2CH_3	3-NO_2
Nifedipine	CH_3	CO_2CH_3	CO_2CH_3	2-NO_2
Nimodipine	CH_3	$CO_2CH_2CH_2OCH_3$	$CO_2CH(CH_3)_2$	3-NO_2
Nisoldipine	CH_3	$CO_2CH_2CH(CH_3)_2$	CO_2CH_3	2-NO_2

Figure 40. Dihydropyrdines compounds.

Studies on photodegradation of DHP antihypertensive, have begun for many years but the number of publications on this topic has increased over time, demonstrating a great deal of interest by a good number of researchers.

The DHP drugs exhibit high sensitivity to light, undergoing a photo degradation process consisting, in most of the cases, in the oxidation of the dihydropyridine ring to pyridine derivative, as shown in fig. 41[106, 107].

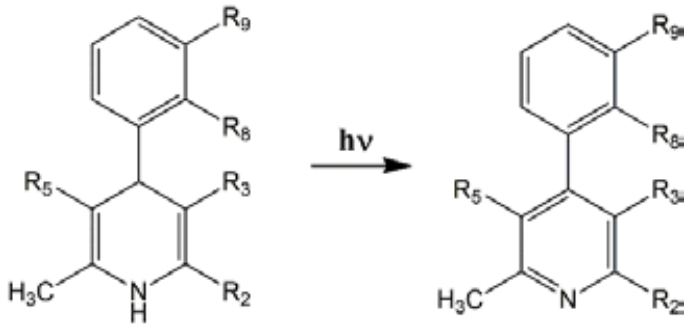

Figure 41. Photodegradation of DHP to pyridine derivative

In a limited number of DHPs, a more complex degradation has been demonstrated with the formation of secondary photoproducts. These molecular changes lead to loss of therapeutic effect or in some cases to toxic effects.

Large part of the research carried out in our research laboratories has been focused on the study of the photodegradation process of DHPs and on the definition of photostabilization systems.

The simultaneous determination of several DHPs and respective photoproducts was defined through a classical least squares (CLS) model built on the UV spectral data. A procedure for selecting the more useful wavelength ranges to use in calibration was also proposed. The good accuracy of the procedure was demonstrated by the recovery values over 97% [108]. Light sensitivity of eleven DHPs was correlated against a series of molecular descriptors through a quantitative structure-property relationships (QSPR) model. The photodegradation rates, calculated from the spectral data collected throughout stressing photo degradation experiments, were combined with the values of the molecular descriptors by Partial Least Squares (PLS)

analysis. The variables fitting the PLS model were selected and the resulting QSPR model was validated. The model was applied to other DHPs, showing good agreement between predicted and measured photodegradation rates [109].

Actually, it is mandatory for the pharmaceutical industry to conduct photoreactivity studies on drugs in formulation and packaging processes [110]. An overall stress testing for the new drugs is detailed in the rules ICH (International Conference on Harmonization), adopted since 1997 by the European Community, the United States and Japan. In particular, second part Q1B "Photostability testing of new drug substances and products" is an integral part of the overall stress testing [111].

To investigate this topic, photostability of eleven DHPs was monitored in spiked plasma samples exposed to laboratory light. The screening procedure was performed by analyzing the samples by LC-MS-MS. Nifedipine and nisoldipine were reduced by 75% in just 2 h. In a manner similar to in vitro reactions, the pyridine analogue resulted as the main degradation product, referred also as the first metabolite in the metabolic pathway. Lercanidipine and nicardipine showed further ester hydrolysis after this first oxidation reaction. Several additional minor degradation products were found for the other drugs [112].

One of the most relevant limit in the use of DHPs in solution is represented by their high photo-lability, reason for which almost all DHPs are dispensed in solid formulations, usually tablets, where the stability is significantly high [114, 115].

Several studies have been proposed or have been undertaken to define new formulations or to design other technological systems able of providing valid photoprotection for these drugs. At present, only few specialties are marketed in solution form, packaged in amber glass containers or other completely opaque materials.

The photoprotective effect of a series of containers in different glassy or polymeric matrices was investigated with regard to four DHPs in solution, felodipine, lercanidipine, nimodipine, nifedipine [116]. These results sound very interesting to design liquid dosage forms of DHPs as an alternative to the solid forms. Another approach increasing the photostability of the DHP specialties is the addition of light

absorbing excipients, usually presenting absorption spectra similar to those of the drugs and, as confirming literature, the degradation rate constant of a methanol solution of nisoldipine decreased as concentration of β-carotene increased, assessing the role of this excipient as photoprotective agent [117].

Over the last few years, great interest aroused the supramolecular matrices, which are able to incorporate a high number of drugs through non-covalent bonds, even if they are difficult soluble in other systems. The most famous of these complex matrices are the "self-assembled" structures, of which the liposomes are the most representative, and the "host-guest systems", among which the most famous "hosts" are the cyclodextrins (CD) [118, 119]. Some of most used DHPs are entrapped in CD or liposomes or appropriate combination of these matrices, into which drugs remained stable and pharmacologically active after irradation test. [120-123].

According to many studies reported in literature, surfactants was tested as means to improve aqueous solubility. Subsequently, the drugs solubilized by surfactants were introduced into different containers (quartz, blue and amber PET) to test their photoprotective power through the use of a parameter $t_{0,1}$ defined as the time necessary to degrade about 10% of the drug. The experiments were monitored by UV-vis spectrometry and spectral data processed by multivariate analysis, useful for evaluating the kinetics of the photodegradation process and for monitoring the concentration of drugs and photoproducts, drawing at the same time their spectra. [124]

The aim of this section of my thesis was the evaluation of new strategies to realize light-stable liquid formulations of novel DHPs.

4.1.1 Synthesis of new dihydropyridines

As part of a collaboration started some time ago, at the Department of Pharmaceutical Chemistry of Hacettepe University in Ankara, Turkey, a series of new DHP derivatives able to block the 1.2 cavity of L-type and T-type calcium channels have been synthesized. In these series of compounds, the modification of an ester portion promotes the blocking affinity of the Land T channels, and also allows the development of DHP with a selectivity of 30 times greater for the T-type channels than the L-type.

Voltage-dependent calcium channels are important regulators of calcium flow in a variety of cell types. They offer the possibility of carrying out an electrical activity in a cell, which in turn activates a wide range of intracellular events, from neurotransmitter and hormone release to gene expression, to the contraction of smooth and cardiac muscle. Calcium channels can be broadly classified into high voltage (HVA) and low voltage (LVA) channels. Among the HVA class, the calcium channel of type L cavity 1.2 (Cav1.2) has been particularly well characterized. It is a heteromeric protein consisting of a pore that forms an α1 subunit that gathers a α2δ, β and γ subunit to form a functional channel. Cav. 1.2 is important for both brain and heart function and can be both inhibited and activated by DHP, and some compounds are used clinically to treat cardiovascular disease. In contrast, LVA calcium channels of type T are formed by a single α1 subunit and show a small unit conductance, a low probability of openness and activate resting membrane neuronal potentials. They are poorly characterized from the pharmacological point of view.

There are several inhibitors of T-type calcium channels, including small organic molecules such as mibefradil, etosuccimide and some DHPs, but generally these compounds also block other types of ion channels. Because the abnormal activity of the T-type channel has been associated with conditions such as epilepsy and pain, the identification of selective T-channel inhibitors is of utmost importance. Previous studies have shown that the best substituent in the C-4 position of DHP is phenyl

because toxicity has been demonstrated in the animal with the presence of heteroaromatic rings. In addition, ester groups in positions C-3 and C-5 have shown to be important for both modulations of activity and tissue selectivity. Finally, a study conducted by Goldmann and Stoltefuss indicates that at most one ester group must be in cis position with respect to the double binding of DHPs to allow the hydrogen bond to the receptor site [125].

In the present study a one-pot microwave method was applied for the synthesis of dihydropyridine derivatives indicated as compounds M1-M5. These compounds were obtained by a modified Hantzsch reaction between 4,4-dimethyl-1,3-cyclohexanedione, 5-nitrosalicylaldehyde, alkylacetacetate and ammoniumacetate in methanol according to the following scheme:

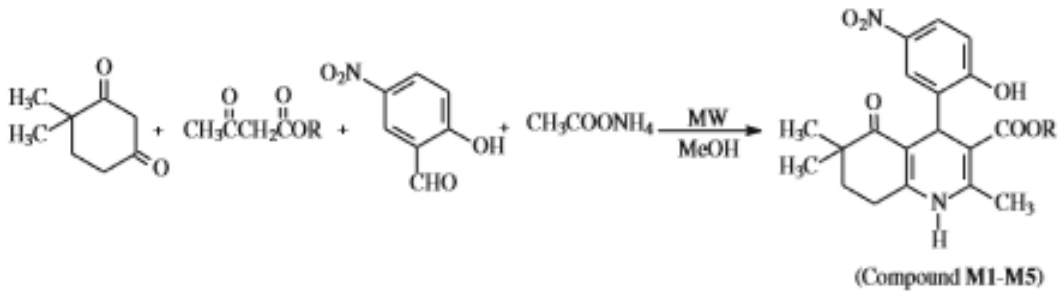

Compound	R	Melting point (°C)	Molecular weight
M1	CH_3	200-202	386
M2	C_2H_5	208-210	400
M3	**$CH_2C_6H_5$**	**185-187**	**462**
M4	$CH_2CH(CH_3)_2$	170-171	428
M5	$C(CH_3)_3$	198-200	428

Figure 42. Scheme of synthesis of M1-M5 compounds.

In the M1-M5 series, the increase in the size of the R group or the introduction of a ring structure (compound M3) in this locus resulted in a significant increase in receptor affinity and thus in the blocking of the canal. [126] For this reasons, our

attention was focalized on the M3 compound. The solutions of this drug candidate were exposed to light and the photodegradation process was monitored by MCR method applied on spectral data.

Stabilization of the liquid formulations was tested by preparing the drug-cyclodextrin complex, or adding surfactants to the aqueous solutions and then putting these solutions in polyethylene terephthalate containers.

Thanks to their ambivalent structure consisting in a lipholic part and in a hydrophilic part, surfactants are substances able to lower the surface tension of a liquid, facilitating the wettability of the surfaces or the miscibility between different liquids. The effect of surfactants on the various properties of dispersed solutions / systems is related to their aggregation status [127]. Some effects will be related to the unimeric state, ie with the number of molecules positioned at the interface, others with micellar status.

Surfactants can be classified according to the ionic properties of the hydrophilic polar head in:

• Anionic,

• Cationic,

• Neutral,

• Amphionics (zwitterionici);

In our work, the attention was focused on the polysorbates, in particular Tween 20, for the known application both in food and pharmaceutical fields.

All the stabilization strategies were also applied to the solution of nimodipine, to compare the photodegradation process of this well-known DHP with the new synthesized compounds.

4.1.2 Experimental

M3 was synthesized by the research staff of the Department of Pharmaceutical Chemistry of Hacettepe University, 06100, Ankara, Turkey; Tween20, nimodipine, methyl-β-cyclodextrin (mβC), hydroxypropyl-β-cyclodextrin (hpβC), methyl-cyclodextrin (mC) were purchased from Sigma-Aldrich (Germany); Ethanol, Methanol, Isopropanol were purchased by J.T. Baker (Holland).

Drug-cyclodextrin complex preparation. The drug-cyclodextrin complex was prepared by optimization of a method previously used by our research group [128]. Several ratio drug: cyclodextrin and different cyclodextrins were tested to evaluate the amount and the type of cyclodextrin to use. The best inclusion complex percentage was calculated by preparing the complex in the ratio 1: 1, as described below, using the β-cyclodextrin (βC):

• 49 mg of βC 5×10^{-4} M are solubilized in 100 ml of EtOH;

• At 2 ml of this solution 2 mg of drug are added, ratio 1: 1;

• 10 ml of Britton-Robinson pH 6.57 (0.04 M of phosphoric acid, 0.04 M of acetic acid, 0.04 M of boric acid and 0.2 M of NaOH) were then added;

• the solution was stirred (120 rpm for 24 hours at 37°C) in a closed glass flask;

• the solution was filtered (0.45 μm filter) and stored for 24 hours at a temperature of 4 °C and finally used for analysis.

The complexes containing other type of cyclodextrin were prepared in the same way by varying the cyclodextrin amount according their molecular weigth, as follow:

• 132 mg of methyl-βC(mβC) 5×10^{-4} M in 100 ml of EtOH;

• 73 mg of 2-Hydroxy-propyl-βC (HpβC) 5×10^{-4} M in 100 ml of EtOH.

Drug-Tween20 solution preparation. Through various tests varying the amount of Tween20, the ratio 1: 5 was chosen to guarantee a good solubilization. The drug-Tween20 complex was prepared as described below:

• 9 mg M3 2 × 10^{-3} M were solubilized in 1 ml of EtOH (10%);

• 0.12 g of Tween20 were added;

• The whole was brought to volume 10 ml with water;

• The solution was stirred (120 rpm for 24 hours at 37 °C) in a closed glass flask;

• The solution was filtered (0.45 µm filter), left to rest for about an hour and then used for analysis.

Photodegradation test. The photodegradation experiments were conducted in accordance with the ICH guidelines, using the controlled irradiation chamber, Suntest CPS + (Heraeus, Milan, Italy). In the present work, the samples were irradiated in a range of wavelengths (λ) between 300 and 800 nm, interposing a quartz filter.

The sonication of the samples was carried out in an ultrasonic bath Ultrasonic Cleaner CP104 (eia S.A. International, France).

Photodegradation experiments were monitored by UV-vis spectrometry and spectral data processed using the multivariate analysis technique, useful for evaluating the kinetics of the photodegradation process and for monitoring the concentration of drugs and photoproducts, drawing at the same time their spectra [124].

The UV spectra of the samples, placed in quartz cuvettes with a thickness of 10 mm, were recorded by a Perkin-Elmer Lambda 40P Spectrophotometer, under the following conditions: λ range 200-450 nm, scan rate 1 nm s^{-1}; time response 1 s; spectral band 1 nm. The UV software Winlab 2.79.01 (Perkin-Elmer) was used for the acquisition and processing of spectra. All chemometric procedures were performed with the Matlab® program (Mathwork Inc., version 7).

4.1.3 Result and Discussion

Photodegradation studies of DHP solution. Due to the low solubility of M3 in water, the photodegradation process of this compound was firstly performed in ethanol at a concentration of 5 × 10^{-4} M, in aquartz cuvette. The absorbance spectra, reported

in figure 43, of the alcohol solution of M3 (20 µg/ml) were recorded from 200 to 400 nm during the photodegradation experiment up to 7 hours at the following exposure times: 1-3-5-10-15-20-25-30-35-40-45-50-55-60-70-80-90-100-110-120-130-140-150-160-170-180-190-200-230-260-300-350-420 minutes. The data were elaborated by the multivariate approach MCR, as above described (figure 43).

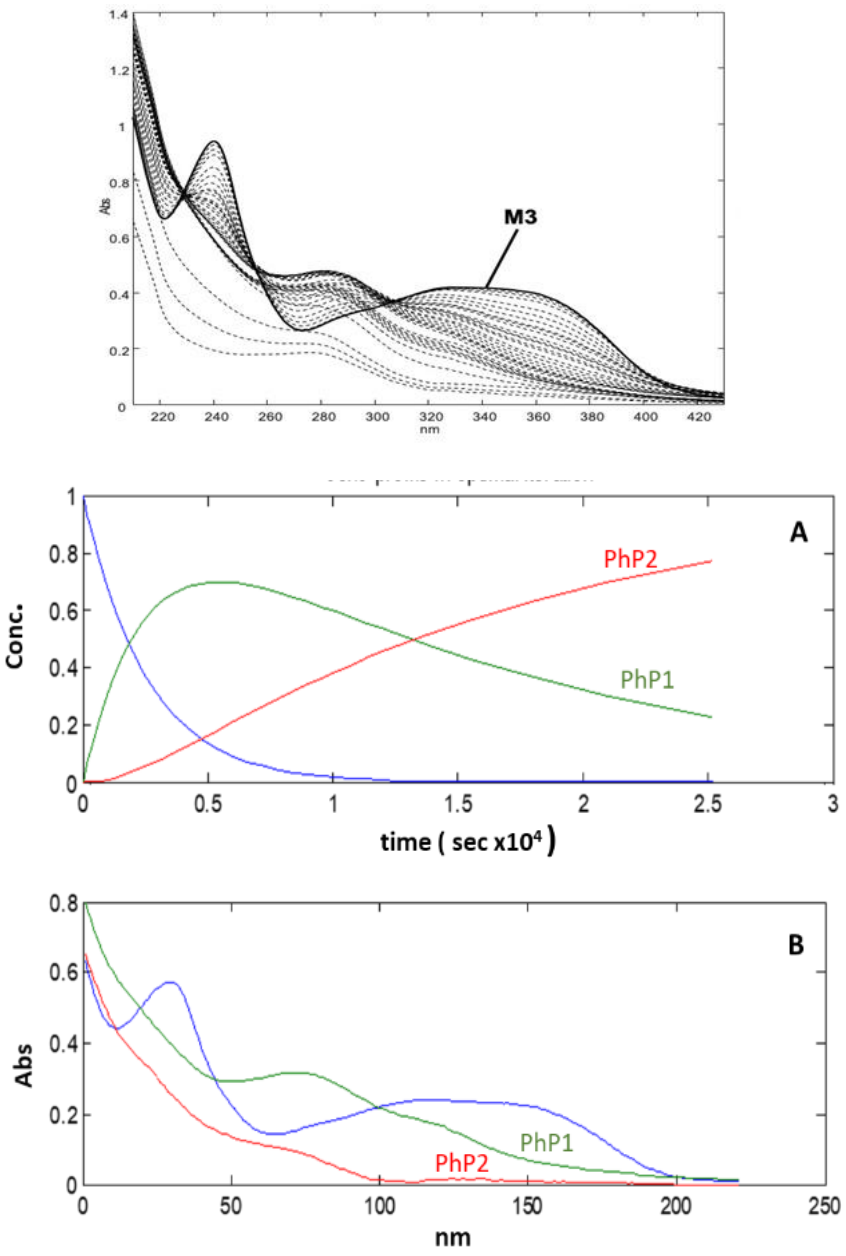

*Figure 43. UV spectra of the solution of M3 in EtOH (20 µg / ml) during irradiation test and concentration profiles (**A**) and spectral (**B**) of the photoproducts by MCR processing.*

The elaboration of the data showed the formation of a photoproduct (PhP 1) in a large quantity and a second product (PhP 2) in a smaller amount. The degradation process followed a first order kinetics, described by the equation:

$$\log [\% M3] = - k1 \cdot t + 2$$

where%M3 indicates the percentage of residual drug, k1 is the rate of photodegradation speed, t is the time (expressed in minutes) and 2 is the logarithm of the initial concentration (100%). The parameter $t_{0.1}$ (time needed to determine 10% of degradation) was chosen as a criterion for comparing the behavior assumed by the samples tested during the degradation process. This parameter is adopted by convention because a drug can no longer be used when its purity falls below 90%. The relative standard deviation values of all points fall within the range: 1.92-6.01%.

The analyzed sample was found to be not very stable already in the first 10 minutes of exposure, confirmed by the immediate appearance of the photoproduct (PhP 1). This product, reached its maximum value at about 20 minutes, but subsequently accompanied by a progressive decrease. The second photoproduct was detected, unlike PhP1, after about 5 minutes. The complete degradation of M3 was observed after 10 minutes.

Nimodipine (NIM, figure 44) in ethanol solution, used as reference standard, was subdued to forced irradiation test. Figure 45 shows the absorbance spectra recorded at the same intervals reported above.

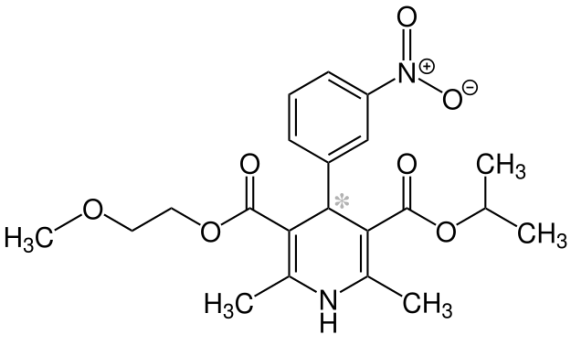

Figure 44. Nimodipine

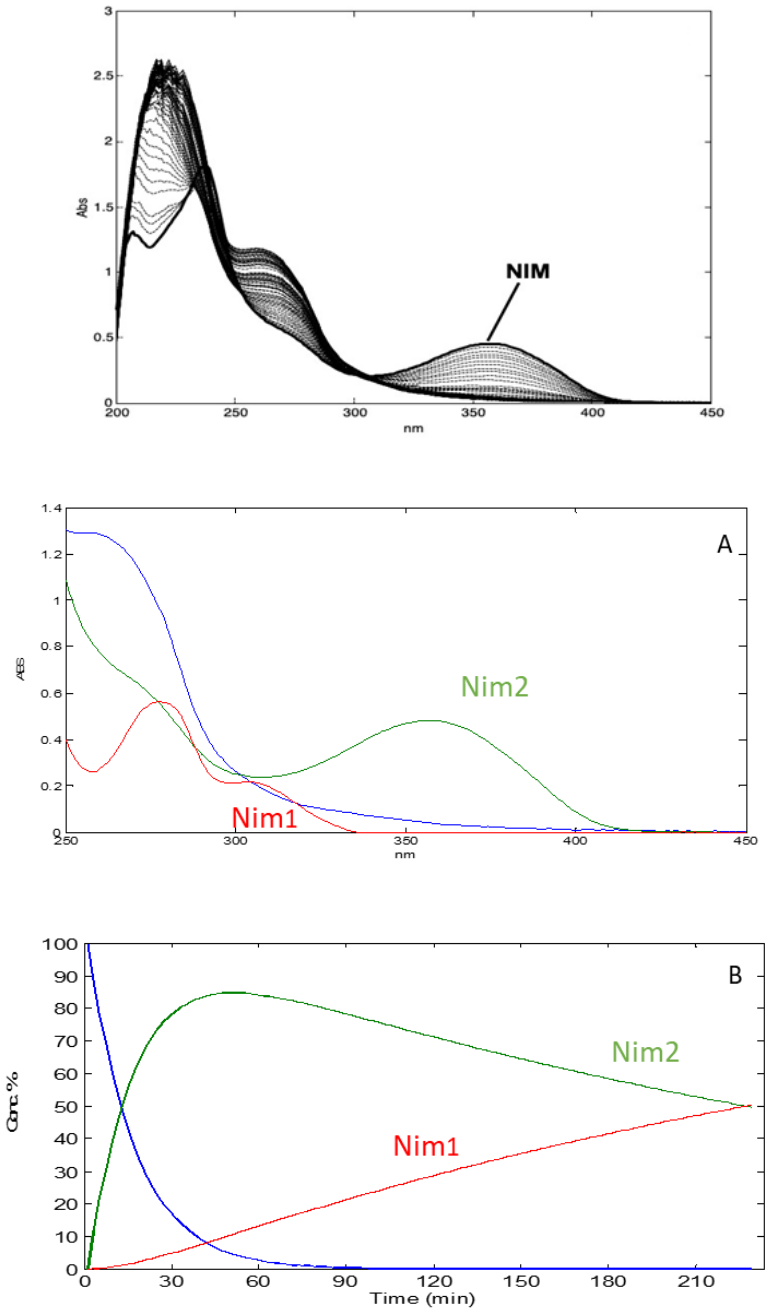

*Figure 45. UV spectra of the solution of NIM in EtOH (80 µg / ml) during irradiation test and concentration profiles (**A**) and spectral (**B**) of the photoproducts after MCR processing.*

MCR analyis revealed a formation of two photoproducts, in particular Nim1 is more aboundant than Nim2 and also we can observe the complete degradation of the drug in less than 1 hour.

Photodegradation studies of DHPs in cyclodextrin complex. The difficulty in the realization of a liquid formulation is due mainly to the low drug solubility in water. For this reason, the proposed strategies consisted firstly in the preparation of a water soluble complex by using cyclodextrins.

According to the study reported in literature [124], hydroalcoholic solutions of drug-cyclodextrin with a concentration of 20 µg/ml was prepared. The complex formation was tested in several M3-CD ratios and with 3 different CDs: βC, mβC and 2-HpβC.

The best results were provided by the 1: 1 ratio using 2-HpβC, as shown in Figure 46.

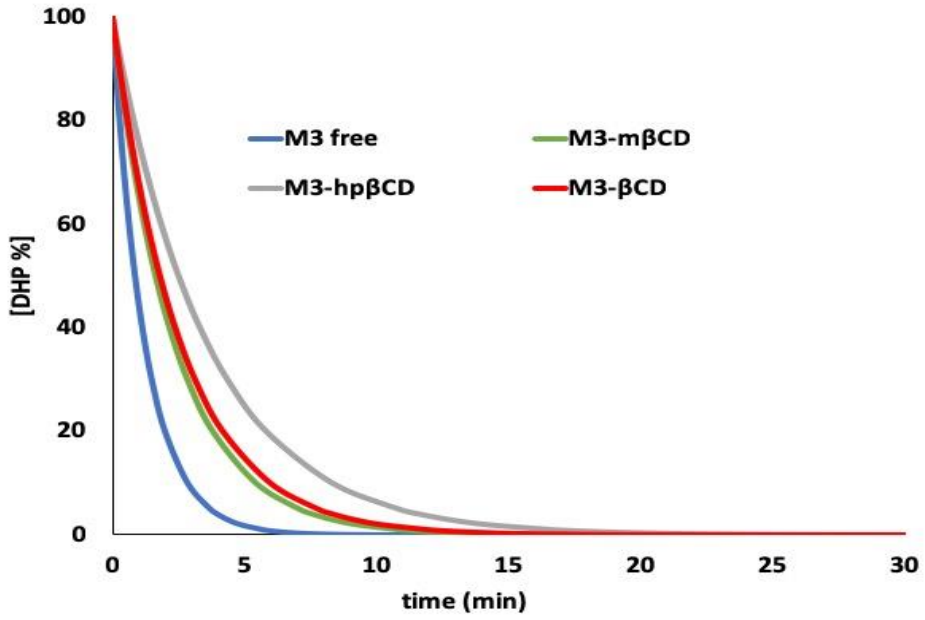

Figure 46. Degradation profile of M3-CD complex in ethanolic solution.

Table 10 shows the degradation kinetics of the drug in an ethanolic solution and included in the different cyclodextrins. Although the drug-cyclodextrin inclusion complex is formed, this photoprotection system did not provide the desired results both in terms of solubility and stability of the drug subjected to irradiation stress.

Table 10. Kinetic parameters of M3 in ethanolic solution and in the various cyclodextrins.

Samples	% Entrapment efficiency	K (x 10^{-3})	$t_{0.1}$ (min)	R^2
M3 free	-	0.351	2.36	0.992
M3-mβCD	15.9	0.184	4.53	0.992
M3-hpβCD	29.7	0.120	6.95	0.988
M3-βCD	18.3	0.167	4.98	0.985

Photodegradation studies of DHP in surfactant solution. Another approach proposed to increase the solubility of drugs, consists in the use of surfactants, amphiphilic substances able to perform the phenomenon called "micellar solubilization". The micelles, characterized by a hydrophilic outer wall and an internal hydrophobic, adsorb slightly soluble or insoluble compounds on the external wall or incorporate it into the inner core, with consequent increase in their solubility. The surfactant used is Tween20, already used in food field.

A solution of M3 was prepared with the Tween 20 in a ratio of 1: 5, as indicated above in the preparation of the drug -Tween 20 solution, and subdued to forced degradation in Suntest CPS+. The spectrophotometric analysis of the sample in quartz cuvette was performed at the following time intervals: 30-60-90-120-150-180-210 minutes.

The use of surfactant increased the solubility but also the light stability of both M3 and NIM, as evidenced by the degradation profile compared with the degradation of drugs solution, in figure 47.

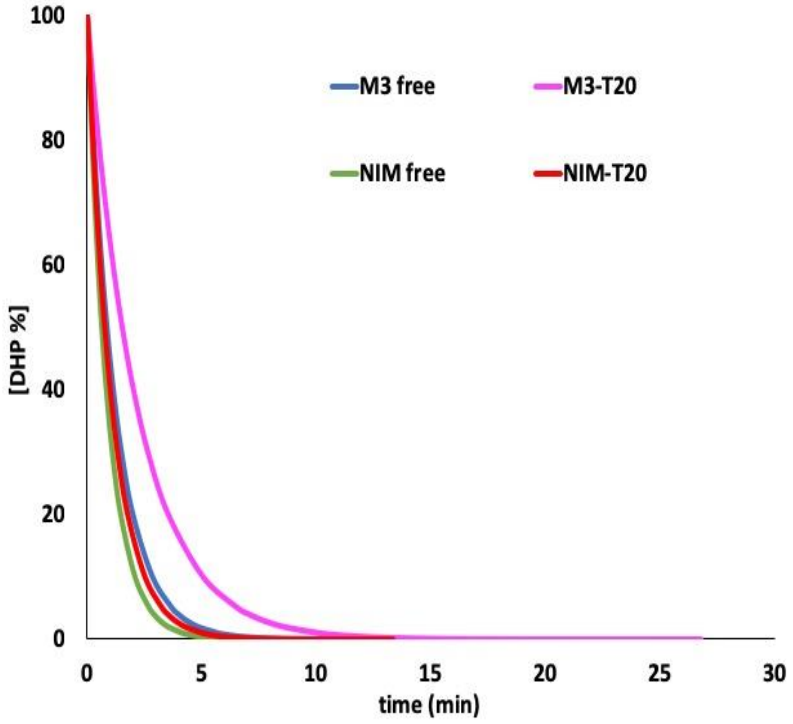

Figure 47 Photodegradation of M3 and NIM in ethanol and surfactant solutions.

Photodegradation studies of DHP in different containers. In a previous work [117], a significant photoprotection for DHPs was obtained with the use of polyethylene terephthalate (PET) containers. The best result was achieved for the felodipine solution in transparent blue PET 0.6 mm thick, reaching almost complete stabilization for up to 6 hours under irradiation stress.

On the contrary, glass containers, also colored, did not provide satisfactory photoprotection of the drugs, however showing values of t0.1 under 24 min. These results may be a good opportunity to design a new pharmaceutical packaging for DHPs in liquid dosage form.

Several containers were so tested: quartz; glass; amber glass; blue PET; amber-colored PET. Photodegradation studies were performed on M3 and on Nimodipine, both in ethanol and surfactant solutions. Figures 48 and 49 show the photodegradation profiles of drug concentration versus time for the surfactant complex in different containers.

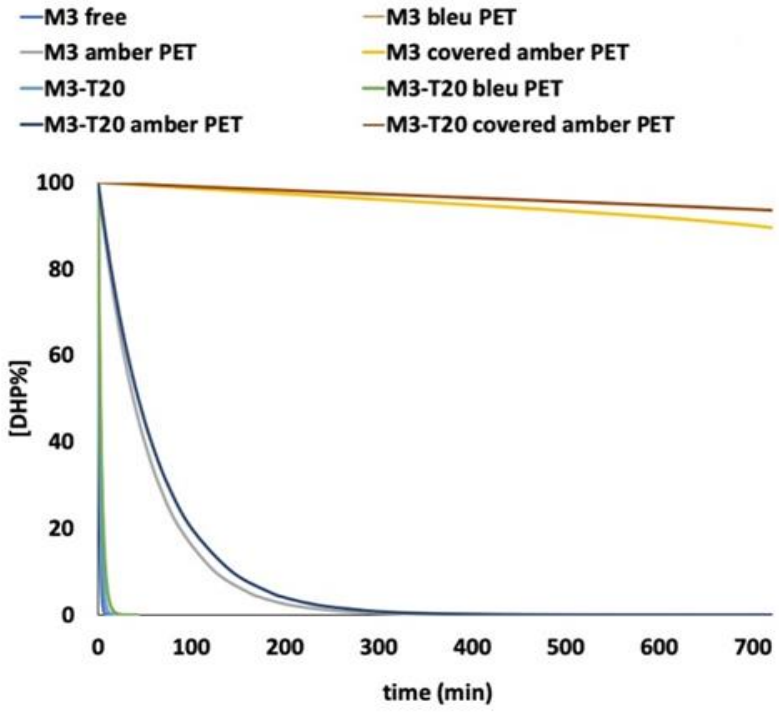

Figure 48. Comparison of photodegradation profile of M3 (in ethanolic solution and in surfactant solution) in different containers.

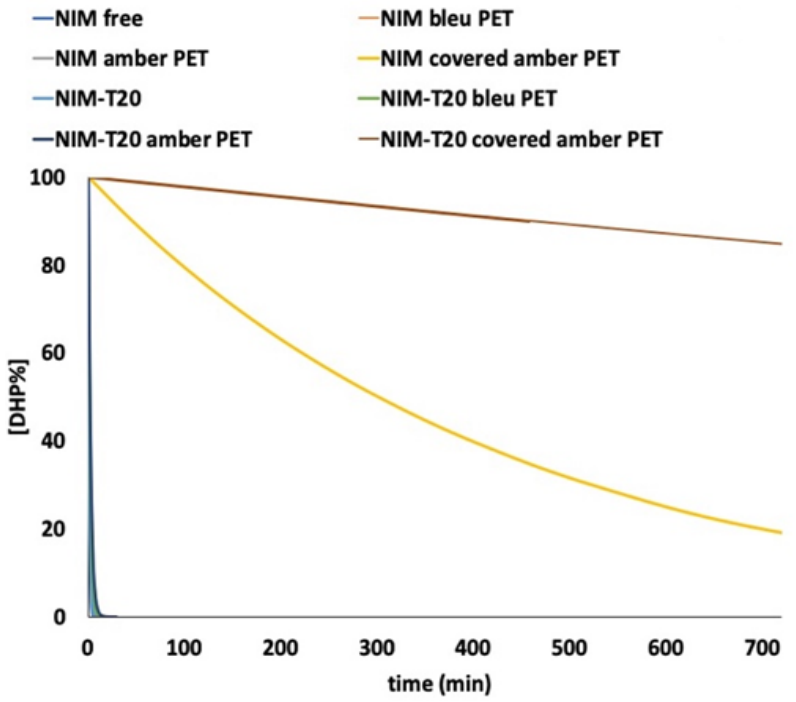

Figure 49. Comparison of photodegradation profile of NIM (in ethanolic solution and in surfactant solution) in different containers

Table 11 shows the degradation kinetics parameters calculated for the different samples exposed to light.

Table 11. Degradation kinetic parameters calculated for M3 and NIM formulations.

Sample	Container	k (x 10^{-3})	$t_{0.1}$ (min)	R^2
M3 free	quartz	0.351	2.36	0.992
	blue PET	0.132	6.31	0.999
	amber PET	0.008	104.17	0.999
	covered amber PET	-	-	-
M3-T20	quartz	0.198	4.21	0.969
	blue PET	0.125	6.67	0.999
	amber PET	0.007	115.02	0.996
	covered amber PET	-	-	-
NIM free	quartz	0.481	1.73	0.999
	blue PET	0.291	2.86	0.996
	amber PET	0.184	4.53	0.999
	covered amber PET	0.066	45.76	0.989
NIM-T20	quartz	0.397	1.91	0.992
	blue PET	0.241	3.45	0.991
	amber PET	0.181	4.60	0.991
	covered amber PET	0.006	457.58	0.987

The best results were obtained by preparing the surfactant solutions in the amber coated container, showing a degradation percentage of the drug lower than 5%. The proposed system is promising for the development of DHP liquid formulations and could be extended to other photosensitive drugs.

CONCLUSIONS

The doctoral course in "TRASLATIONAL MEDICINE" has a multidisciplinary approach based on biochemical and genetic or analytical and organic chemistry knowledge, which allows to create a professional profile able to develop innovative therapies or to design new molecules to be transferred in the diagnostic and clinical-therapeutic field.

During my three years of PhD, my studies have been focused in the application of advanced analytical techniques and data processing for the analytical study of complex biological and food matrices.

The application of chemometric techniques on the IR spectrum of breast milk has proved to be very effective in tracing even minimal variations in the composition and characteristics of the human milk, being able to exploit the non-specific information stored in the infrared digital impression. In this case, the processing of ATR-FTIR spectral fingerprints by PCA and PLS regression procedures was able to detect fraudolent addition of water or cow's milk. In particular, the PLS-DA technique was essential to recognize pure breast milk from the adulterated milk. A further definition of four PLS1 models, allowed to determine the amount of specific adulterants.

The research on food matrices has been extended to a series of edible oils aims to verify their photostability under forced light irradiation. Analysis by UV-vis spectroscopy, FTIR-ATR and HPLC-DAD showed quantitative and qualitative changes of the major fatty acids.

The research has been focused to linseed oil, for its great importance as a functional food. Also in this case, UV spectroscopy and HPLC revealed significant changes in the concentration of fatty acids, reduced to 35% after 48 hours of light exposure. The amount of lignans, other important nutraceutic components, showed significant stability. Photoprotection of the linseed oil was studied by testing amber glass containers and addition of ascorbyl palmitate as an antioxidant, obtaining impressive results. These results could be a huge stimulus to increase the shelf life of linseed oil

or other edible oils by the adoption of an appropriate formulation associated with accurate physical protection.

The studies on the food matrices have demonstrated that the combined use of chemometrics with IR spectral analysis has both great economic and practical advantages, as it requires reduced execution times and no sample pretreatment. The results obtained by an accurate validation process on sets of external samples have shown an excellent predictive power, and could be applied on several matrices to identify any change due to different causes.

The monitoring of drugs in biological fluids represents another important topic of my thesis work. A very interesting work was the determination of the anesthetic bupivacaine in the cord blood. Determination of the drug was defined by means of an SPE extraction method followed by HPLC and Gc-MS analysis. This study will proceed with the analysis of a large number of real samples, in order to evaluate the safety of anesthetics administered during natural birth and so modulate the therapeutic protocol currently used in partoanalgesia.

A very important experience during the three-year PhD was the period spent at the Utrecht University. In this occasion I participated in the study of a bioanalytical assay of lorlatinib, a first third-generation ALK inhibitor. Plasma preparation and optimization of chromatografic conditions have been the most diffucult steps of the work being the first completely reported validated assay for this compound. A procedure LC-MS/MS method was defined able to measure the pharmacokinetic properties of the drug in mice.

The research activity on pharmaceutical matrices aimed to verify the stability in aqueous solution and underlight of a newly synthesized 1,4dihydropyridine (M3), due the well-known poor solubility and photolability of this class of drugs. A series of surfactants, such as tweens, was used to promote water solubility showing good results through the use of the nonionic surfactant Tween20. Subsequently, the photostability of the complex M3-Tween 20 was studied by using different containers: quartz, blue PET, amber PET, coated dark glass. The best photoprotection was guaranteed by the amber PET and the dark coated glass container. So, the

combined use of surfactants and new containers represented an interesting strategy to be applied to photolabile and mainly lipophilic drugs.

All the research work done during the three years of PhD has allowed to test and apply promising and useful analytical techniques for the analysis of various complex matrices. The results obtained have demonstrated that the pharmaceutical analysis is a valid support for the different areas of translational medicine and can be applied in qualitative and quantitative analysis of food, pharmaceutical and biological matrices, in determination of drugs or contaminants, in improving the pharmacological behaviour of new synthetized drugs, in optimizing the technical characteristics of new drug formulations.

REFERENCES

[1] K.S.R. Raju, I. Taneja, S.P. Singh, Wahajuddin, Utility of noninvasive biomatrices in pharmacokinetic studies, *Biomedical Chromatography*, 27(**2013**) 1354-1366.

[2] H. Rowe, T. Baker, T.W. Hale, Maternal Medication, Drug Use, and Breastfeeding, *Child and Adolescent Psychiatric Clinics of North Americ*a, 24 (**2015**) 1-20.

[3] C.E. Briere, J. McGrath, X. Cong, R. Cusson, An integrative review of factors thatinfluence breastfeeding duration for premature infants after NICU hospitalization,
J. Obstet. Gynecol. Neonatal Nurs., 43 (**2014**) 272-281.

[4] M.G. Parker, A.L. Patel, Using quality improvement to increase human milk usefor preterm infants, *Semin. Perinatol*. 41 (**2017**) 175-186.

[5] L.R. Kair, V.J. Flaherman, Donor milk or formula: a qualitative study of postpartummothers of healthy newborns*, J. Hum. Lact.* 33 (**2017**) 710-716.

[6] M. St-Onge, S. Chaudhry, G. Koren, Donated breast milk stored in banks versus breast milk purchased online, *Can. Fam. Physician* 61 (**2015**) 143e146.

[7] S.R. Geraghty, K.A. McNamara, C.E. Dillon, J.S. Hogan, J.J. Kwiek, S.A. Keim, Buying human milk via the Internet: just a click away, *Breastfeed. Med*. 8 (**2013**) 474-478.

[8] J.H. Kim, S. Unger, C. Nutr Gastroenterol, Human milk banking*, Paediatr*. *ChildHealth* 15 (**2010**) 595-598.

[9] S.A. Keim, M.M. Kulkarni, K. McNamara, S.R. Geraghty, R.M. Billock, R. Ronau,J.S. Hogan, J.J. Kwiek, Cow's milk contamination of human milk purchased viathe Internet, *Pediatrics* 135 (**2015**) 1157-1162.

[10] E.E. Ziegler, Adverse effects of Cow's milk in infants, issues in complementary feeding, *Karger* (**2007**) 185-199.

[11] S. Basnet, M. Schneider, A. Gazit, G. Mander, A. Doctor, Fresh Goat's milk for infants: myths and realitiesea review, *Pediatrics* 125 (**2010**) 973-977.

[12] D. Doron, K. Hershkop, E. Granot, Nutritional deficits resulting from an almond-based infant diet, *Clin. Nutr.* 20 (**2001**) 259-261.

[13]] E.E. Ziegler, Consumption of cow's milk as a cause of iron deficiency in infants and toddlers, *Nutr. Rev.* 69 (**2011**) S37-S42.

[14] L. Christie, R.J. Hine, J.G. Parker, W. Burks, Food allergies in children affect nutrient intake and growth, *J. Am. Diet. Assoc.* 102 (**2002**) 1648-1651.

[15] M.H.K. Ho, W.H.S. Wong, C. Chang, Clinical spectrum of food allergies: a comprehensive review, *Reviews in allergy & immunology*, (**2014**).

[16] Ariadni Geballa-Koukoulaa, Irene Panderia, Konstantinos Zervasa, Khalil Geballa-Koukoulasb, Eirini Kavvalouc, Eirini Panteri-Petratoud, Panagiota Vournae, Dimitra Gennimataf, A porous graphitized carbon LC-ESI/MS method for the quantitation of metronidazole and fluconazole in breast milk and human plasma, *Journal of Chromatography B* 1084 (**2018**) 175–184

[17] R.W. Sparidans, S. van Hoppe, J.J. Rood, A.H. Schinkel, J.H. Schellens, J.H. Beijnen, Liquid chromatography-tandem mass spectrometric assay for the tyrosine kinase inhibitor afatinib in mouse plasma using salting-out liquid-liquid extraction, *J. Chromatogr. B Analyt. Technol. Biomed. Life Sci.* 1012–1013 (**2016**)118–123.

[18] Michele De Luca, Giuseppina Ioele, Claudia Spatari,Gaetano Ragno. Photodegradation of 1,4-dihydropyridine antihypertensive drugs:an updated review. *International Journal of Pharmacy and Pharmaceutical Sciences.* 10(1), (**2017**) 8-18.

[19] De Luca, M., Ioele, G., Risoli, A., & Ragno, G. Improvement of multivariate calibration techniques applied to 1-to-N component mixtures through an optimized experimental design. *Microchemical Journal*, 83(1) (**2006**), 24–34.

[20] Geladi, P., & Kowalski, B. R. Partial least square regression: A tutorial. *Analytica Chimica Acta*, 185, (**1986**)1–17.

[21] De Luca, M., Ioele, G., Spatari, C., & Ragno, G. Optimization of wavelength range and data interval in chemometric analysis of complex pharmaceutical mixtures. *Journal of Pharmaceutical Analysis*, 6(1), (**2016**) 64-69.

[22] Palabiyik, I. M., Göker, E., Çağlayan, M. G., & Onur, F. Multivariate optimization model in a partial least squares-1 method for simultaneous determination of dorzolamide hydrochloride and timolol maleate in eye drops. *Current Pharmaceutical Analysis*, 9(4), (**2013**) 404-412.

[23] Galvão, R. K. H., Araujo, M. C. U., José, G. E., Pontes, M. J. C., Silva, E. C., & Saldanha, T. C. B. A method for calibration and validation subset partitioning. *Talanta*, 67(4), (**2005**)736–740.

[24] Amodio, M. L., Derossi, A., Mastrandrea, L., Martínez Hernández, G. B., & Colelli, G. The use of multivariate analysis as a method for obtaining a more reliable shelf-life estimation of fresh-cut produce: A study on pineapple. *Acta Horticulturae*, 1141, (**2016**)131-136

[25] De Luca, M., Restuccia, D., Clodoveo, M. L., Puoci, F., & Ragno, G. Chemometric analysis for discrimination of extra virgin olive oils from whole and stoned olive pastes. Food Chemistry, 202, (**2016**)432–437.

[26] Carbonaro, M., & Nucara, A. Secondary structure of food proteins by Fourier transform spectroscopy in the mid-infrared region. *Amino Acids*, 38(3), (**2010**)679-690.

[27] Ye, M. P., Zhou, R., Shi, Y. R., Chen, H. C., & Du, Y. Effects of heating on the secondary structure of proteins in milk powders using mid-infrared spectroscopy. *Journal of Dairy Science*, 100(1), (**2017**)89–95.

[28] Zhou, Q., Sun, S.-Q., Yu, L., Xu, C.-H., Noda, I., & Zhang, X.-R. Sequential changes of main components in different kinds of milk powders using two-dimensional infrared correlation analysis. *Journal of Molecular Structure*, 799(1–3), (**2006**)77–84.

[29] Bassbasi, M., De Luca, M., Souhassou, S., Hirri, A., Berkani, M., Kzaiber, F., Oussama, A. Determination of Milk Adulteration by Sucrose Using FT-MIR Spectroscopy and Chemometrics *Methods. Agricultural Science Research Journal*, 11(4), (**2014**)175–180.

[30] Kasemsumran, S., Thanapase, W., & Kiatsoonthon, A. Feasibility of Near-Infrared Spectroscopy to Detect and to Quantify Adulterants in Cow Milk. *Analytical Sciences*, 23(7), (**2007**)907–910.

[31] De Luca, M., Ioele, G., & Ragno, G. Cumulative area pre-processing (CAP): A new treatment of UV data for the analysis of complex pharmaceutical mixtures. *Journal of Pharmaceutical and Biomedical Analysis,* 90, (**2014**)45–51.

[32] Iñón, F. A., Garrigues, J. M., Garrigues, S., Molina-Díaz, A., & De La Guardia, M. Selection of calibration set samples in determination of olive oil acidity by partial least squares-attenuated total reflectance-Fourier transform infrared spectroscopy. *Analytica Chimica Acta*, 489(1), (**2003**)59–75.

[33] W.Terouzi,M.DeLuca,A.BollicA.OussamaaM.PatumidG.IoelebG.Ragno,A discriminant method for classification of Moroccan olive varieties by using direct FT-IR analysis of the mesocarp section, *Vibrational Spectroscopy*, 56(2), (**2011**)123-128.

[34] De Luca, M., Restuccia, D., Clodoveo, M. L., Puoci, F., & Ragno, G. Chemometric analysis for discrimination of extra virgin olive oils from whole and stoned olive pastes. *Food Chemistry*, 202, (**2016**)432-437.

[35] Oguz, U., & Banu, O. Prediction of various chemical parameters of olive oils with Fourier transform infrared spectroscopy. *LWT - Food Science and Technology*,63, (**2015**)978-984

[36] Akhtar, S., Khalid, N., Ahmed, I., Shahzad, A., & Suleria, H. A. R. Physicochemical characteristics, functional properties, and nutritional benefits of peanut oil: A review. *Critical Reviews in Food Science and Nutrition*, 54, (**2014**)1562-1575.

[37] Chang, A. S., Sreedharan, A., & Schneider, K. R. Peanut and peanut products: A food safety perspective. *Food Control*, 32, (**2013**)296-303.

[38] Ruijie, L., Qingzhe, J., Huang, J., Liu, Y., Wang, X., Mao, W., et al. Photodegradation of Aflatoxin B1 in peanut oil. *European Food Research and Technology*,232, (**2011**). 843-849.

[39] Juarez, M. D., Osawa, C. C., Acuna, M. E., Samman, N., & Gonçalves, L. A. G.

Degradation in soybean oil, sunflower oil and partially hydrogenated fats afterfood frying, monitored by conventional and unconventional methods. *Food Control*, 22, (**2011**)1920-1927.

[40] Wenle, Z., Na, L., Yuyan, F., Shujun, S., Tao, L., & Bing, L. A unique quantitative method of acid value of edible oils and studying the impact of heating on edible oils by UVeVis spectrometry. *Food Chemistry*, 185, (**2015**)326-332.

[41] Guillen, M. D., & Uriarte, P. S. Monitoring by 1H nuclear magnetic resonanceof the changes in the composition of virgin linseed oil heated at frying temperature. Comparison with the evolution of other edible oils. *Food Control*,28, (**2012**)59-68.

[42] Goicoechea, E., & Guillen, M. D. Oxidation products of corn oil at room temperature. *Processing and Impact on Active Components in Food*, 29, (**2015**). 243-249.

[43] International Conference on Harmonization. (**2003**). ICH Q1, Stability testing of new drug substances and products. Geneva: IFPMA.

[44] Wise, B. M., Ricker, N. L., Veltkamp, D. F., & Kowalski, B. R. A theoretical basis for the use of principal component models for monitoring multivariate processes. *Process Control and Quality*, 1, (**1990**) 41-51.

[45] Siong, F. S., & Woei, T. An automated approach for analysis of Fourier Transform Infrared (FTIR) spectra of edible oils. *Talanta*, 88, (**2012**)537-543.

[46] Bassbasi, M., De Luca, M., Ioele, G., Oussama, A., & Ragno, G. Prediction of the geographical origin of butters by partial least square discriminant analysis (PLSDA) applied to infrared spectroscopy (FTIR) data. *Journal of Food Composition and Analysis*, 33, (**2014**) 210-215.

[47] Ioele, G., De Luca, M., Oliverio, F., & Ragno, G. Prediction of photosensitivity of 1,4-dihydropyridine antihypertensives by quantitative structure-property relationship. *Talanta*, 79, (**2009**)1418-1424.

[48] Guarrasi V, Mangione MR, Sanfratello V, et al (**2010**) Quantification of underivatized fatty 350 acids from vegetable oils by HPLC with UV

detection. *J Chromatogr Sci* 48:663–668. 351 doi: 10.1093/chromsci/48.8.663

[49] Rodríguez Y, Christophe AB (**2005**) Long-chain ω6 polyunsaturated fatty acids in erythrocyte phospholipids are associated with insulin resistance in non-obese type 2 diabetics. *Clin Chim Acta* 354:195–199. doi: 10.1016/j.cccn.2004.11.018

[50] Endo J, Arita M (**2016**) Cardioprotective mechanism of omega-3 polyunsaturated fatty acids*. J. Cardiol.* 67:22–27

[51] O'Connell TD, Block RC, Huang SP, Shearer GC (**2017**) ω3-Polyunsaturated fatty acids for heart failure: Effects of dose on efficacy and novel signaling through free fatty acid receptor 4. *J. Mol. Cell. Cardiol.* 103:74–92

[52] Funari SS, Barceló F, Escribá P V. (**2003**) Effects of oleic acid and its congeners, elaidic and stearic acids, on the structural properties of phosphatidylethanolamine membranes. *J Lipid Res* 44:567–575. doi: 10.1194/jlr.M200356-JLR200

[53] Dixon RA (**2004**) Phytoestrogens*. Annu Rev Plant Biol* 55:225–261. doi: 333 10.1146/annurev.arplant.55.031903.141729

[54] Westcott ND, Muir AD (**2003**) Flax seed lignan in disease prevention and health promotion. *Phytochem Rev* 2:401–417. doi: 0.1023/B:PHYT.0000046174.97809.b6

[55] Attoumbré J, Mahamane Laoualy AB, Bienaimé C, et al (**2011**) Investigation of lignan accumulation in developing Linum usitatissimum seeds by immunolocalization and HPLC. *Phytochem Lett* 4:194–198. doi: 10.1016/j.phytol.2011.03.004

[56] Bravi E, Perretti G, Marconi O, et al (**2011**) Secoisolariciresinol diglucoside determination in flaxseed (Linum usitatissimum L.) oil and application to a shelf life study. *Food Chem* 126:1553–1558. doi: 10.1016/j.foodchem.2010.11.169

[57] Touré A, Xueming X (**2010**) Flaxseed lignans: Source, biosynthesis, metabolism, antioxidant activity, Bio-active components, and health

benefits. *Compr Rev Food Sci Food Saf* 9:261–269. doi: 10.1111/j.1541-4337.2009.00105.x

[58] Herchi W, Arráez-Román D, Trabelsi H, et al (**2014**) Phenolic Compounds in Flaxseed: a Review of Their Properties and Analytical Methods. An Overview of the Last Decade. *J Oleo Sci* 63:7–14. doi: 10.5650/jos.ess13135

[59] De Goede J, Geleijnse JM, Boer JMA, et al (**2010**) Marine (n-3) fatty acids, fish consumption, and the 10-year risk of fatal and nonfatal coronary heart disease in a large population of Dutch adults with low fish intake. J Nutr 140:1023–1028. doi: 10.3945/jn.109.119271

[60] Destaillats F (**2011**) Formulating functional foods with long-chain polyunsaturated fatty acids: Challenges and opportunities. *Eur. J. Lipid Sci. Technol*. 113:1293–1295

[61] Frankel EN (**1996**) Antioxidants in lipid foods and their impact on food quality. In: *Food Chemistry*. Elsevier, pp 51–55

[62] Ragno G, Risoli A, Ioele G, De Luca M (**2006a**) Photo- and thermal-stability studies on benzimidazole anthelmintics by HPLC and GC-MS. *Chem Pharm Bull* 54: doi: 10.1248/cpb.54.802

[63] Gonçalves RP, Março PH, Valderrama P (**2014**) Thermal edible oil evaluation by UV-Vis spectroscopy and chemometrics. *Food Chem* 163:83–86. doi:10.1016/j.foodchem.2014.04.109

[64] Sherazi STH, Talpur MY, Mahesar SA, et al (**2009**) Main fatty acid classes in vegetable oils by SB-ATR-Fourier transform infrared (FTIR) spectroscopy. *Talanta* 80:600–606. doi: 10.1016/j.talanta.2009.07.030

[65] Spatari C, De Luca M, Ioele G, Ragno G (**2017**) A critical evaluation of the analytical techniques in the photodegradation monitoring of edible oils. *LWT - Food Sci Technol* 76 : doi: 10.1016/j.lwt.2016.10.055

[66] Zeb A, Murkovic M (**2013**) Determination of thermal oxidation and oxidation products of β-400 carotene in corn oil triacylglycerols. *Food Res Int* 50:534–544. doi:401 10.1016/j.foodres.2011.02.039

[67] ICH (**1996**) Q1B Guideline Photostability Testing of New Drug Substances and Products Comments for its Application. Fed Regist 62

[68] Ragno G, Risoli A, Loele G, et al (**2006b**) Photostabilization of 1,4-dihydropyridine antihypertensives by incorporation into β-cyclodextrin and liposomes. *J Nanosci Nanotechnol* 6: doi: 10.1166/jnn.2006.407

[69] Michotte D, Rogez H, Chirinos R, et al (**2011**) Linseed oil stabilisation with pure natural phenolic compounds. *Food Chem* 129:1228–1231. doi: 10.1016/j.foodchem.2011.05.108

[70] Montedoro G, Servili M, B Aldioli M, Miniati E (**1992**) Simple and Hydrolyzable Phenolic Compounds in Virgin Olive Oil. 1. Their Extraction, Separation, and Quantitative and Semiquantitative Evaluation by HPLC. *J Agric Food Chem* 40:1571–1576. doi: 10.1021/jf00021a019

[71] Chen B, Mcclements DJ, Decker EA (**2011**) Minor components in food oils: A critical review of their roles on lipid oxidation chemistry in bulk oils and emulsions. *Crit. Rev. Food Sci. Nutr*. 51:901–916

[72] Gerstenmeyer E, Reimer S, Berghofer E, et al (**2013**) Effect of thermal heating on somelignans in flax seeds, sesame seeds and rye. *Food Chem* 138:1847–1855. doi:10.1016/j.foodchem.2012.11.117

[73] Gargouri B, Zribi A, Bouaziz M (**2015**) Effect of containers on the quality of Chemlali olive oil during storage. *J Food Sci Technol* 52:1948–1959. doi: 10.1007/s13197-014-1273-2

[74] Cort WM (**1974**) Antioxidant activity of tocopherols, ascorbyl palmitate, and ascorbic acid and their mode of action. *J Am Oil Chem Soc* 51:321–325. doi: 10.1007/BF02633006

[75] Guillaume Hoizey et al. “Sensitive bioassay of bupivacaine in human plasma by liquid-chromatography-ion trap mass spectometry”. *Journal of Pharmaceutical and Biomedical Analysis* 39 (**2005**) 587-592.

[76] Lars I. Andersson “Efficient sample pre-concentration of bupivacaine from human plasma by solid-phase extraction on moleculary imprinted polymers” *The Analyst comunication* ;125(9): (**2000**) 1515-7.

[77] Hans Onnerund, Fatma Bassiouny and Mohamed Abdel-Rehim “Chromatographic Behavior of Bupivacaine and Five of uts Major Metabolites in Human Plasma, Utilizing Solid-Phase Extraxtion and

Capillary Gas Chromatography" *Journal of Chromatographic Science*, Vol. 48, (**2010**).

[78] K. Rikova, A. Guo, Q. Zeng, A. Possemato, J. Yu, H. Haack, J. Nardone, K. Lee, C. Reeves, Y. Li, Y. Hu, Z. Tan, M. Stokes, L. Sullivan, J. Mitchell, R. Wetzel, J. MacNeill, J.M. Ren, J. Yuan, C.E. Bakalarski, J. Villen, J.M. Kornhauser, B. Smith, D. Li, X. Zhou, S.P. Gygi, T.L. Gu, R.D. Polakiewicz, J. Rush, M.J. Comb, Global Survey of Phosphotyrosine Signaling Identifies Oncogenic Kinases in Lung Cancer, *Cell*. 131 (**2007**) 1190–1203. doi:10.1016/j.cell.2007.11.025.

[79] M. Soda, Y.L. Choi, M. Enomoto, S. Takada, Y. Yamashita, S. Ishikawa, S. Fujiwara, H. Watanabe, K. Kurashina, H. Hatanaka, M. Bando, S. Ohno, Y. Ishikawa, H. Aburatani, T. Niki, Y. Sohara, Y. Sugiyama, H. Mano, Identification of the transforming EML4 – ALK fusion gene in non-small-cell lung cancer, *Nature.* 448 (**2007**) 561–6. doi:10.1038/nature05945.

[80] M.M. Awad, A.T. Shaw, ALK inhibitors in non-small cell lung cancer: Crizotinib and beyond, *Clin. Adv. Hematol. Oncol.* 12 (**2014**) 429–439. doi:10.1158%2F2159-8290.CD-13-0846

[81] S.W. Morris, M.N. Kirstein, M.B. Valentine, K.G. Dittmer, D.N. Shapiro, D.L. Saltman, A.T. Look, Fusion of a kinase gene, ALK, to a nucleolar protein gene, NPM, in non-Hodgkin's lymphoma., *Science*. 263 (**1994**) 1281–4. doi:10.1126/science.8122112

[82] J. Duyster, R.Y. Bai, S.W. Morris, Translocations involving anaplastic lymphoma kinase (ALK), *Oncogene*. 20 (**2001**) 5623–5637. doi:10.1038/sj.onc.1204594.

[83] B. Hallberg, R.H. Palmer, Mechanistic insight into ALK receptor tyrosine kinase in human cancer biology., *Nat. Rev. Cancer*. 13 (**2013**) 685–700. doi:10.1038/nrc3580

[84] K. Kinoshita, Y. Ono, T. Emura, K. Asoh, N. Furuichi, T. Ito, H. Kawada, S. Tanaka, K. Morikami, T. Tsukaguchi, H. Sakamoto, T. Tsukuda, N. Oikawa, Discovery of novel tetracyclic compounds as anaplastic lymphoma kinase inhibitors., *Bioorg. Med. Chem. Lett.* 21 (**2011**) 3788–3793. doi:10.1016/j.bmcl.2011.04.020.

[85] Z. Song, Y. Yang, Z. Liu, X. Peng, J. Guo, X. Yang, K. Wu, J. Ai, J. Ding, M. Geng, A. Zhang, Discovery of novel 2,4-diarylaminopyrimidine analogues (DAAPalogues) showing potent inhibitory activities against both wild-type and mutant ALK kinases, *J. Med. Chem.* 58 (**2015**) 197–211. doi:10.1021/jm5005144.

[86] S.-H.I. Ou, E.L. Kwak, C. Siwak-Tapp, J. Dy, K. Bergethon, J.W. Clark, D.R. Camidge, B.J. Solomon, R.G. Maki, Y.-J. Bang, D.-W. Kim, J. Christensen, W. Tan, K.D. Wilner, R. Salgia, A.J. Iafrate, Activity of Crizotinib (PF02341066), a Dual Mesenchymal-Epithelial Transition (MET) and Anaplastic Lymphoma Kinase (ALK) Inhibitor, in a Non-small Cell Lung Cancer *Patient with De Novo MET Amplification*, (**2011**). doi:10.1097/JTO.0b013e31821528d3.

[87] L. Friboulet, N. Li, R. Katayama, C.C. Lee, J.F. Gainor, A.S. Crystal, P.Y. Michellys, M.M. Awad, N. Yanagitani, S. Kim, A.M.C. Pferdekamper, J. Li, S. Kasibhatla, F. Sun, X. Sun, S. Hua, P. McNamara, S. Mahmood, E.L. Lockerman, N. Fujita, M. Nishio, J.L. Harris, A.T. Shaw, J.A. Engelman, The ALK inhibitor ceritinib overcomes crizotinib resistance in non-small cell lung cancer, *Cancer Discov.* 4 (**2014**) 662–673. doi:10.1158/2159-8290.CD-13-0846.

[88] R.W. Sparidans, S.C. Tang, L.N. Nguyen, A.H. Schinkel, J.H.M. Schellens, J.H. Beijnen, Liquid chromatography-tandem mass spectrometric assay for the ALK inhibitor crizotinib in mouse plasma, *J. Chromatogr. B Anal. Technol. Biomed. Life Sci.* 905 (**2012**) 150–154. doi:10.1016/j.jchromb.2012.08.021.

[89] M.S. Roberts, D.C. Turner, A. Broniscer, C.F. Stewart, Determination of crizotinib in human and mouse plasma by liquid chromatography electrospray ionization–tandem mass spectrometry (LC-ESI–MS/MS), *J. Chromatogr. B.* 960 (**2014**) 151–157. doi:10.1016/j.jchromb.2014.04.035.

[90] O. Heudi, D. Vogel, Y.Y. Lau, F. Picard, O. Kretz, Liquid chromatography tandem mass spectrometry method for the quantitative analysis of ceritinib in human plasma and its application to pharmacokinetic studies, *Anal. Bioanal. Chem.* (**2014**) 7389–7396. doi:10.1007/s00216-014-8125-9.

[91] M. Qian, B. Zhu, X. Wang, M. Liebman, Drug resistance in ALK-positiveNon-small cell lungcancer patients, *Semin. Cell Dev. Biol.* (**2016**). doi:10.1016/j.semcdb.2016.09.016

[92] I.B. Muller, A.J. De Langen, R.J. Honeywell, E. Giovannetti, G.J. Peters, Overcoming crizotinib resistance in ALK-rearranged NSCLC with the second-generation ALK-inhibitor ceritinib, *Expert Rev. Anticancer Ther.* 16 (**2016**) 147–157. doi:10.1586/14737140.2016.1131612.

[93] Q. Huang, T.W. Johnson, S. Bailey, A. Brooun, K.D. Bunker, B.J. Burke, M.R. Collins, A.S. Cook, J.J. Cui, K.N. Dack, J.G. Deal, Y.L. Deng, D. Dinh, L.D. Engstrom, M. He, J. Hoffman, R.L. Hoffman, P.S. Johnson, R.S. Kania, H. Lam, J.L. Lam, P.T. Le, Q. Li, L. Lingardo, W. Liu, M.W. Lu, M. McTigue, C.L. Palmer, P.F. Richardson, N.W. Sach, H. Shen, T. Smeal, G.L. Smith, A.E. Stewart, S. Timofeevski, K. Tsaparikos, H. Wang, H. Zhu, J. Zhu, H.Y. Zou, M.P. Edwards, Design of potent and selective inhibitors to overcome clinical anaplastic lymphoma kinase mutations resistant to crizotinib, *J. Med. Chem.* 57 (**2014**) 1170–1187. doi:10.1021/jm401805h.

[94] T.W. Johnson, P.F. Richardson, S. Bailey, A. Brooun, B.J. Burke, M.R. Collins, J.J. Cui, J.G. Deal, Y.-L. Deng, D. Dinh, L.D. Engstrom, M. He, J. Hoffman, R.L. Hoffman, Q. Huang, R.S. Kania, J.C. Kath, H. Lam, J.L. Lam, P.T. Le, L. Lingardo, W. Liu, M. McTigue, C.L. Palmer, N.W. Sach, T. Smeal, G.L. Smith, A.E. Stewart, S. Timofeevski, H. Zhu, J. Zhu, H.Y. Zou, M.P. Edwards, Discovery of (10R)-7-Amino-12-fluoro-2,10,16-trimethyl-15-oxo-10,15,16,17-tetrahydro-2H-8,4-(metheno)pyrazolo[4,3-][2,5,11]-enzoxadiazacyclotetradecine-3-carbonitrile (PF-06463922), a Macrocyclic Inhibitor of Anaplastic Lymphoma Kinase (ALK) and c-ros O, *J. Med. Chem. 57* (**2014**) 4720–4744. doi:10.1021/jm500261q.

[95] S. Yamazaki, J.L. Lam, H.Y. Zou, H. Wang, T. Smeal, P. Vicini, Translational Pharmacokinetic-Pharmacodynamic Modeling for an Orally Available Novel Inhibitor of Anaplastic Lymphoma Kinase and c-Ros Oncogene 1, *J. Pharmacol. Exp. Ther. J Pharmacol Exp Ther Dyn. Metab. Oncol. Res. Unit. 351* (**2014**) 67–76. doi:10.1124/jpet.114.217141.

[96] S. Yamazaki, J.L. Lam, H.Y. Zou, H. Wang, T. Smeal, P. Vicini, Mechanistic understanding of translational pharmacokinetic-pharmacodynamic relationships in nonclinical tumor models: A case study of orally available novel inhibitors of anaplastic lymphoma kinase, *Drug Metab. Dispos. 43* (**2015**) 54–62. doi:10.1124/dmd.114.061143.

[97] H.Y. Zou, L. Friboulet, D.P. Kodack, L.D. Engstrom, Q. Li, M. West, R.W. Tang, H. Wang, K. Tsaparikos, J. Wang, S. Timofeevski, R. Katayama, D.M. Dinh, H. Lam, J.L. Lam, S. Yamazaki, W. Hu, B. Patel, D. Bezwada, R.L. Frias, E. Lifshits, S. Mahmood, J.F. Gainor, T. Affolter, P.B. Lappin, H. Gukasyan, N. Lee, S. Deng, R.K. Jain, T.W. Johnson, A.T. Shaw, V.R. Fantin, T. Smeal, PF-06463922, an ALK/ROS1 Inhibitor, Overcomes Resistance to First and Second Generation ALK Inhibitors in Preclinical Models, *Cancer Cell. 28* (**2015**) 70–81. doi:10.1016/j.ccell.2015.05.010.

[98] E.R. Tucker, L.S. Danielson, P. Innocenti, L. Chesler, Tackling crizotinib resistance: The pathway from drug discovery to the pediatric clinic, *Cancer Res. 75* (**2015**) 2770–2774. doi:10.1158/0008-5472.CAN-14-3817.

[99] N.R. Infarinato, J.H. Park, K. Krytska, H.T. Ryles, R. Sano, K.M. Szigety, Y. Li, H.Y. Zou, N. V. Lee, T. Smeal, M.A. Lemmon, Y.P. Moss??, The ALK/ROS1 inhibitor PF-06463922 overcomes primary resistance to crizotinib in ALK-driven neuroblastoma, *Cancer Discov. 6* (**2016**) 96–107. doi:10.1158/2159-8290.CD-15-1056.

[100] U.S. National Institutes of Health, ClinicalTrials.gov, Clinicaltrials.gov. **2017**, https://clinicaltrials.gov/ct2/results?term=lorlatinib(accessed: 0.03.2017).

[101] E.M. Agency, European Medicines Agency, Reproduction. 2 (**2006**) 1–15. doi:10.1016/S0140-6736(10)60785-4.

[102] F. and D.A. FDA, Food and Drug Administration, Guidance for Industry: Bioanalyticalmethodvalidation.,**2001**. doi:http://www.labcompliance.de/documents/FDA/FDA-others/Laboratory/f-507-bioanalytical-4252fnl.pdf

[103] R.W. Sparidans, D. Iusuf, A.H. Schinkel, J.H. Schellens, J.H. Beijnen, Liquid chromatography-tandem mass spectrometric assay for the light sensitive

tyrosine kinase inhibitor axitinib in human plasma, *J. Chromatogr. B Anal. Technol. Biomed. Life Sci. 877* (**2009**) 4090–4096.

[104] J.J.M. Rood, J.H.M. Schellens, J.H. Beijnen, R.W. Sparidans, Recent developments in the chromatographic bioanalysis of approved kinase inhibitor drugs in oncology, *J. Pharm. Biomed. Anal. 130* (**2016**) 244–263. doi:10.1016/j.jpba.2016.06.037.

[105] R.W. Sparidans, S. Durmus, A.H. Schinkel, J.H. Schellens, J.H. Beijnen, Liquid chromatography-tandem mass spectrometric assay for the PARP inhibitor rucaparib in plasma, *J. Pharm. Biomed. Anal. 88* (**2014**) 626–629.

[106] Tratto da: G.L. Nicolosi - Trattato di ecocardiografia clinica.

[107] Maafi W, Maafi M. Modelling nifedipine photodegradation, photostability and actinometric properties. *Int J Pharm* (**2013**);456:153–64.

[108] Vetuschi C, Ragno G, Veronico M, Risoli A, Gianandrea A. Comparative evaluation of analytical methods for simultaneous determination of nisoldipine and its photodegradation products. *Anal Lett* (**2002**);35: 1327–39.

[109] Ragno G, Vetuschi C, Risoli A, Ioele G. Application of a classical least-squares regression method to the assay of 1,4-dihydropyridine antihypertensives and their photoproducts. *Talanta* (**2003**); 59:375–82.

[110] Ioele G, De Luca M, Oliverio F, Ragno G. Prediction of photosensitivity of 1,4-dihydropyridine antihypertensives by quantitative structure-property relationship. *Talanta* (**2009**);79: 1418–24.

[111] Tønnessen HH. Photostability of drugs and drug formulations. *CRC Press*; (**2010**). p. 435.

[112] ICH Q1B Guideline Photostability Testing of New Drug Substances and Products Comments for its Application. *Fed Regist*; (**1996**). p. 62.

[113] Baranda AB, Alonso RM, Jimenez RM, Weinmann W. Instability of calcium channel antagonists during sample preparation for LC–MS–MS analysis of serum samples. *Forensic Sci Int* (**2006**);156 :23–34.

[114] Gil-Agustí MT, Carda-Broch S, Ll Monferrer-Pons, Esteve-Romero JS. Photostability studies for micellar liquid chromatographic determination of

nifedipine in serum and urine samples. *Biomed Chromatogr* (**2006**); 20:154–60.

[115] De Filippis P, Bovina E, Da Ros L, Fiori J, Cavrini V. Photodegradation studies on lacidipine in solution: basic experiments with a cis-trans reversible photoequilibrium under UV-A radiation exposure. *J Pharm Biomed Anal* (**2002**);27: 803–12.

[116] Kawabe Y, Nakamura H, Hino E, Suzuki S. Photochemical stabilities of some dihydropyridine calcium-channel blockers in powdered pharmaceutical tablets. *J Pharm Biomed Anal* (**2008**);47:618–24.

[117] Michele De Luca, Giuseppina Ioele, Claudia Spatari, Gaetano Ragno Photostabilization studies of antihypertensive 1,4-dihydropyridines using polymeric containers, *International Journal of Pharmaceutics* (**2016**) 505(1).

[118] Mielcarek J, Grobelny P, Szamburska P. The effect of β-carotene on the photostability of nisoldipine. *Methods Find Exp Clin Pharmacol* (**2005**);27:167–71.

[119] Sharma S, Saraogi GK, Kumar V. Development of spectrophotometric methods for simultaneous determination of artesunate and curcumin in liposomal formulation. *Int J Appl Pharm* (**2015**); 7:18-21.

[120] Yunus YK, Vasanti S. Liposomes containing phytochemicals for cancer treatment-an update. *Int J Curr Pharm Res* (**2017**); 9:20-4.

[121] Jang DJ, Jeong EJ, Lee HM, Kim BC, Lim SJ, Kim CK. Improvement of bioavailability and photostability of amlodipine using redispersible dry emulsion. *Eur J Pharm Sci* (**2006**); 28:405–11.

[122] Narkhede MR, Kuchekar BS, Nehete JY. Ternary systems of HP β-cyclodextrin felodipine inclusion complexes: preparation, characterization and solubility studies. *Res J Pharm Technol* (**2011**); 4: 1809–15.

[123] Brito J, Pozo A, Garcia C, Nunez-Vergara L, Morales J, Gunther G, *et al.* Photodegradation of nimodipine and felodipine in microheterogeneous systems. *J Chil Chem Soc* (**2012**);57:1313–7.

[124] Ioele G, Gunduz MG, De Luca M, Simsek R, Safak C, Muzzalupo R, et al. Photodegradation studies of 1,4-dihydropyridine compounds by MCR analysis on UV spectral data. *Future Med Chem* (**2016**);8:107–15.

[125] M.Bechem S.Goldmann R.Gross, St.Hallermann S.Hebish J.Hutter, H.-P.Rounding, M.Schramm, J.Stoltefuss, A.Straub.A new type of Ca-channel modulation by a novel class of 1,4-DHPs, *Life Sci.* (**1997**);60(2):107-18.

[126] Chris Bladen & Miyase Gözde Gündüz & RahimeŞimşek & Cihat Şafak & Gerald W. Zamponi.Synthesis and Evaluation of 1,4-Dihydropyridine Derivatives with Calcium Channel Blocking Activity, *Pflugers Arch.* (**2014**) Jul;466(7):1355-63. doi: 10.1007/s00424-013-1376-z

[127] Vinarov et al. Micellar solubilization of poorly water-soluble drugs: effect of surfactant and solubilizate molecular structure, *Drug Dev. Ind. Pharm.* (**2018**) ;44(4):677-686. doi: 10.1080/03639045.2017.1408642.

[128] Ioele G, De Luca M, Ragno G. Photostability of barnidipine in combined cyclodextrin-in-liposome matrices. *Future Med Chem* (**2014**); 6:35-43.

Sitography

[1a] www.mypersonaltrainer.it

[2a] www.cordoneombelicale.it

[3a] www.cellulestaminalicordoneombelicale.it

[4a] www.centronazionalesangue.it

[5a] www.Medicinapertutti.it